A design study of a pressure damping inlet for parachute systems.

Pyle, Joanne

IRVIN-GQ

A Design Study of a Pressure Damping Inlet for Parachute Systems

MPhil Thesis by Joanne Pyle

Industrial supervisor Dr. Adrian Jones, Principal Engineer
Academic supervisor Dr. Ian Masters, Lecturer

University of Wales, Swansea and Irvin GQ Ltd

Research and work carried out 2001 - 2003

Declaration

This work has not previously been accepted in substance for any degree and is not being currently submitted in candidature for any degree.

Signed (candidate): _____

Date: 12/3/04

Statement 1

This thesis is the result of my own investigations, except where otherwise stated. Other sources are acknowledged by footnotes giving explicit references. A bibliography is appended.

Signed (candidate): _____

Date: 12/3/04

Statement 2

I hereby give consent for my thesis, if accepted, to be available for photocopying and for inter-library loan, and for title and summary to be made available to outside organisations.

Signed (candidate): _____

Date: 12/3/04

Acknowledgements

I would like to thank the following people and organisations that have helped me in the work undertaken in this thesis:

Dr. Ian Masters, my supervisor, for his guidance and encouragement.

Dr. Adrian Jones, Principal Engineer, Irvin GQ Ltd., for his help and support in the design and testing.

Mr. David Hirst, Engineering Director and everybody in R&D who helped me at Irvin GQ Ltd. in the design and analysis of the pressure damping inlet.

The Teaching Company Scheme (TCS) and Irvin GQ Ltd. for funding the study and making it possible for me to complete the project during my placement.

Mr. Clive Francis and everybody at the University of Wales, Swansea for making it possible for me to carry out the wind tunnel tests.

Summary

The Automatic Activation Device (AAD) is designed to automatically open a parachute at a predetermined height if the parachutist is unable to operate it first. It works by calculating the height and rate of descent from pressure readings taken from inside the parachute pack. Altitude errors have been recorded in tests of up to 650 feet due to input pressure noise. This would have a catastrophic effect on the parachutists safety if the AAD was set off too soon, or too late.

Work has been carried out investigating the possibility of including a pressure damping inlet to the AAD. This would include the use of static inlet porting, that takes an average of two pressure readings from around the body. Static inlet porting reduces the effects of changing body position and hence attenuates the low frequency noise. The actual effect of static porting was investigated, and an average attenuation of 45% was found by using static inlet porting.

Work has also been conducted investigating the concept of a choked pressure inlet that could be used to damp the pressure input seen by the transducer. Through a process of numerical and experimental data analysis, it was found that the choked pressure inlet alone could not damp the pressure adequately without excessive lag to the static pressure measured.

Further investigations analyse the effect of combining the choked pressure inlet with the static porting arrangement. It was found that the static inlet porting results in a 45% error reduction that may be used with a realistically specified choke assembly, to achieve an acceptable damped pressure reading. This configuration gives a maximum error of 300 feet, where the original descent data gives an altitude error of up to 650 feet. This is an improvement of 54%.

The configuration resulting from the numerical study was then verified in wind tunnel tests conducted at the University of Wales, Swansea. The configuration tested did not attenuate the pressure signal as expected. The Orthogonal Array Technique was then used to re-visit the design of the choke, and test different configurations in the wind

tunnel. The technique used was proven successful and resulted in an optimum choke configuration.

Wind tunnel verification trials were conducted on the final pressure damping inlet configuration. Analysis of the results shows that the configuration attenuates the pressure signal by an average of 49%. This will greatly improve the reliability of the Automatic Activation Device.

Notation

A	cross sectional area
C	capacitance
Cc	discharge constant
p	static pressure applied
P	pressure difference
Pa	Initial pressure
R	resistance
T	time
tc	time constant
v	velocity
V	voltage/volume of chamber
V_o	voltage out
ρ	mass density of the fluid
τ	time constant

Table of Contents

List of Figures

Chapter 1

Chapter 2

Chapter 3

Chapter 4

Chapter 5

Chapter 6

Chapter 7

List of Tables

Chapter 1 - Introduction

1.1 Introduction to the Pressure Damping Inlet

Irvin GQ Ltd specialise in the design, development and manufacture of safety and survival systems to international aerospace industries and military markets. The product range includes parachutes for emergency escape, tactical parachute systems for airborne and special forces, weapons delivery and aerial delivery, air-sea rescue harnesses and rescue stretchers and associated equipment.

The study of work contained in this thesis was undertaken as part of a TCS (Teaching Company Scheme) placement with Irvin GQ and the University of Wales Swansea. TCS is a government-funded scheme that enables business to access the skills and resources of the UK knowledge base for strategic advantage with high quality graduates working in companies on knowledge transfer projects.

The MOD Automatic Activation Device (AAD) developed at Irvin GQ Ltd calculates the height and derives the rate of descent of a parachutist by taking pressure readings throughout his descent. It can then automatically activate the main and/or reserve parachute at a preset altitude if the parachutist is unable to pull his own ripcord. The pressure transducer on the AAD reads an erratic inlet pressure, which is due to a combination of changing body position, flapping clothing and noise.

As part of the TCS project, a pressure damping inlet was designed and verified in conjunction with Irvin GQ and the University of Wales Swansea, and reported in this MPhil thesis.

1.2 Concept of the Choked Pressure Inlet

Work included a theoretical study into the concept of a choked pressure inlet. The choke concept was based on the theory that an erratic pressure passing through a small inlet, into a large volume would mechanically damp the reading reaching the pressure sensor in the AAD. An erratic and noisy airflow would decelerate through a long and narrow inlet, eliminating the abnormalities and peak pressures, so that the output pressure reading would be smooth.

A transfer function was required to predict the effectiveness of the choke, and laboratory tests were carried out recording the time taken for a set volume in vacuum to equalise through different choke assemblies with standard air pressure. It was found that the graphs from the experiment were similar to those exhibited by a capacitor discharging and may be modelled using a first order transfer function which models exponential decay (Figure 1.1).

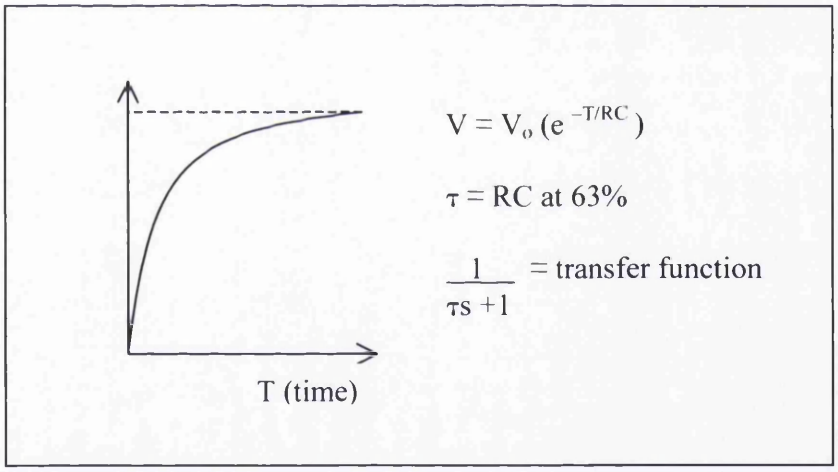

Figure 1.1: First order transfer function used for modelling exponential decay.

1.3 Static Inlet Porting

Previous parachute trials have shown that parachutists during freefall can incur large aerodynamic pressure variations around the circumference of their body and pack. The AAD measures pressure as some mixture between static pressure, dynamic pressure and wake pressure.

The velocity of a fluid in general varies from one point to another even in the direction of flow. Ref [1]. Newton's First Law states that a change of velocity must be associated with a force, and therefore it is to be expected that the pressure of the fluid also changes from point to point. Ref [2]. Swiss mathematician, Daniel Bernoulli proposed that in a flowing ideal fluid, the sum of the forces of the static pressure, due to the random motion of the atoms, plus the dynamic pressure, due to the motion of the fluid, is a Constant.

$$p + 1/2\ \rho v^2 = \text{constant} \qquad \text{[Equation 1.1]}$$

where **p** represents the static pressure applied to the fluid, the term $1/2\ \rho v^2$ is the kinetic pressure developed in the fluid, ρ is the mass-density of the fluid and **v** is its velocity. This expression is essentially a statement of the principle of the conservation of energy, applied to fluids in motion and the conclusion is that as the velocity of a fluid increases, its static pressure decreases and vice versa.

In almost all cases in which flow takes place round a solid body, the boundary layer separates from the surface at some point. Downstream of the separation position the flow is greatly disturbed by large scale eddies, and this region of eddying motion is known as the wake. As a result of the energy dissipated by the highly turbulent motion in the wake, the pressure there is reduced and the pressure drag on the body is increased.

The body attitude, shape and activity can all influence the pressure seen by the device, both statically and dynamically. When using an electronic pressure transducer to measure the pressure at one single point, these pressure variations make it difficult to establish the

---

[1] Massey BS, 1989, *Mechanics of Fluids*, 6th edition, London, Chapman & Hall
[2] Kempe, 2002, *Kempes Engineers Yearbook*, Kent, CMP Information Ltd

true pressure and hence altitude, of the parachutist at any given point during freefall. Ref [3].

Irvin GQ has developed a static averaging tube as shown in Figure 1.2. It has been tested with one end of the tube placed in a chamber at 3000ft and the other at ambient pressure. Pressure readings were taken at the AAD connection point and found to give a constant average pressure of the two areas. This concept reduces the large aerodynamic pressure variations monitored by the pressure transducer with static porting giving an averaged pressure around the parachutist and thus giving a realistic pressure/altitude.

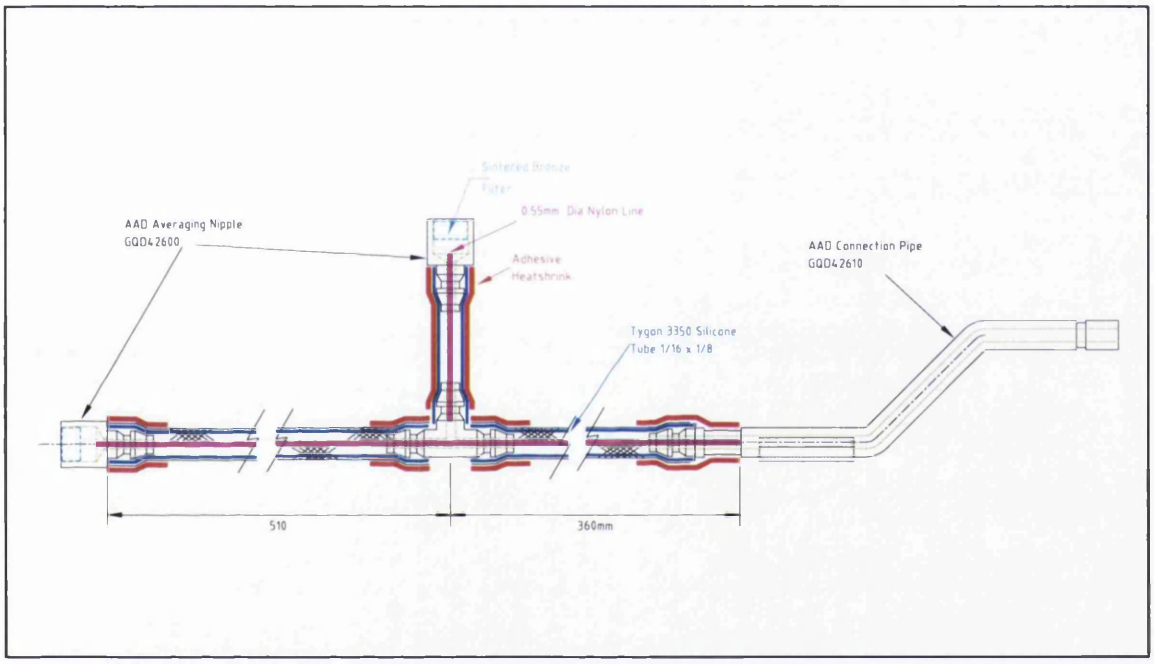

Figure 1.2: Construction of AAD Static Tube Assembly

GQ TR 01001 Issue 1 Ref [4] documents a programme of work carried out during wind tunnel trials, conducted on 14 April 2001 at the Sky Venture Wind Tunnel, Florida. Trials were carried out with and without the static port tube to establish the effect of the overall system. It quantifies and records the pressure, whilst the parachutist performs manoeuvres or holds specific body attitudes in order to establish what pressure fluctuations are seen by the sensor under these conditions.

---

[3] Knacke. TW, 1992, *Parachute Recovery Systems Design Manual*, Santa Barbara, Para Publishing
[4] Williams. PM, 2001, *Test Results for Wind Tunnel Trials Conducted on the MOD AAD with Static Inlet Porting*, GQ TR 01001, Irving GQ Ltd

The general conclusions reported in GQ TR 0101, state that the altitude-offset error was small (max 300ft to –400ft) in comparison with operational use. Although small, this error is most significant and must be taken into account when considering operating procedures. It should also be noted that these tests were only conducted at low speed (200ft/sec). Previous trials have shown that greater speeds will produce greater altitude errors. This would be due to a greater pressure differential between the front and back of the body (up to 800 ft) that increases with velocity. If the body is unstable, the pressure transducer may be reading a pressure that is alternating from high pressure at the leading edge of the body, to low pressure in the stagnation area of the trailing edge.

In general, the static porting tube reduced the pressure/altitude errors by up to 95%. It was therefore recommended that the Static porting tube be used to reduce these errors. It was also recommended that further studies were to be conducted to ascertain whether the static porting can be further advanced. This is the basis of this thesis: to investigate and design a choking device to further advance the static port tube.

1.4 Orthogonal Array Analysis

The orthogonal array technique was used to identify the final Pressure Inlet configuration in this thesis. Ref [5]. The technique was used to design an experiment that would help to analyse every factor involved in the choke assembly.

The purpose of any experiment is to assess the functionality of the given product or process. Ref[6]. The function may be affected and therefore possibly improved by any of the many characteristics it has. To optimise the design of a process the factors that have the greatest influence, and which produce the most consistent performance must be identified.

Orthogonal arrays are used in process optimisation methods such as the Taguchi Method. They help to reduce the experiment to a manageable size whilst allowing independent assessment of each of the factors. The use of these orthogonal arrays make it possible to measure an average characteristic for each combination of factors, with a limited number of experiments. A response table is constructed alongside the array that calculates the results and analyses the optimum levels for each factor.

---

[5] Gethin DT and Claypole TC, 2002, *Process Optimisation Module Notes*, University of Wales Swansea

[6] Roy RK, 2001, *Design of Experiments Using the Taguchi Approach: 16 Steps to Product and Process Improvement*, New York, John Wiley & Sons

1.5 Layout of Thesis

Following this introductory chapter, this thesis is presented in the following way:

Chapter 2 - Choked Damping

This chapter investigates the concept of a choked pressure inlet. It involves laboratory tests that helped produce a transfer function to mathematically model the device.

Chapter 3 - Distributed Static Port Venting

This chapter further investigates the results from a wind tunnel trial previously conducted at Irvin GQ, into the effects of static inlet porting.

Chapter 4 - Choked Static Port Venting

This chapter investigates combining the choke concept with the static porting inlet to achieve an ideal configuration.

Chapter 5 - Wind tunnel Verification

This chapter records initial wind tunnel tests carried out on the pressure damping inlet configuration that came as a result of the previous chapter. This configuration was not found to give adequate damping and it was decided to conduct an orthogonal array test to produce an ideal choke arrangement.

Chapter 6 - Orthogonal Array Testing

This chapter describes the experiment designed using the orthogonal array technique, and shows the analysis performed in order to identify the optimal Pressure Damping Inlet configuration.

Chapter 7 - Full System Verification

This chapter describes the final wind tunnel tests performed on the Pressure Damping Inlet that verified and confirmed its function and attenuation f the pressure signal.

Chapter 8 – Conclusions and Recommendations

This chapter is a conclusion to the work presented in this thesis, and recommendations for further work in the area.

Chapter 2 – Choked Damping

2.1 Introduction

Choked damping is a term developed during this study and refers to the attenuation of a noisy input pressure signal through a restricted narrow inlet.

An investigation was carried out to see if a choked pressure inlet could be used to damp the pressure input seen by the transducer without excessive lag to the static pressure measured.

Work has also been carried out to investigate the effect of static inlet porting (GQ TR 01001 Ref [4]), where an average of two pressure readings was taken from around the body. This reduces the effects of changing body position and hence attenuates the low frequency signals. However, for the purposes of this initial investigation, the effects of the choked pressure inlet shall be considered independently of static inlet porting.

Figure 2.1 shows the initial concept of the choke.

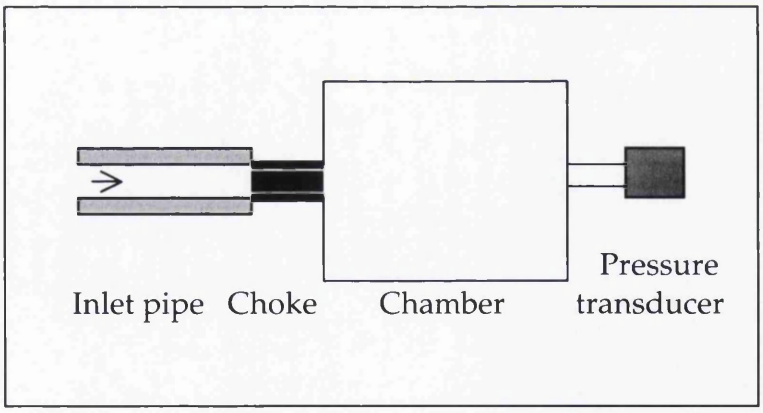

Figure 2.1: Initial concept of the choke

Work was carried out to establish the viability of the damping system and determine dimensional information such as choke effective diameter, chamber volume etc.

2.2 Method

A chamber was evacuated to 600mbar absolute, and the internal pressure was monitored over the time taken for it to equalise to atmospheric pressure through a hypodermic tube. It was envisaged that the system transfer function would be a function of volumes and diameters. Therefore the variables were identified as:

Volume of chamber:	1 pint bottle = 568 ml Water was added to vary the volume to: 400ml, 300ml, 200ml and 100ml.
Diameter of choke:	Hypodermic needles 0.15mm and 0.84mm bore.
Length of choke:	The needles were cut to length, 25mm and 10mm.

Due to the small diameters required by the design of the choke, care was taken in manufacture of the choke samples to prevent damaging the internal diameter of the needle. This was achieved by cutting the needle 2mm longer than the specified length and then filing the end down to the correct length.

The results were recorded by a PICO200 dual channel analogue to digital converter (ADC), and were transferred to an Excel spreadsheet to be analysed further.

The experiment was then repeated with a 0.07mm effective diameter choke, created by inserting a wire into the bore of the 0.84mm internal diameter hypodermic needle. This process increased the boundary surfaces in the choke.

2.3 Results

Four choke configurations were tested with five different chamber volumes resulting in a series of exponentially decaying graphs. The results were recorded as a change in pressure, in order that the final reading would equalise to zero. Figures 2.2 to 2.6 show the results obtained.

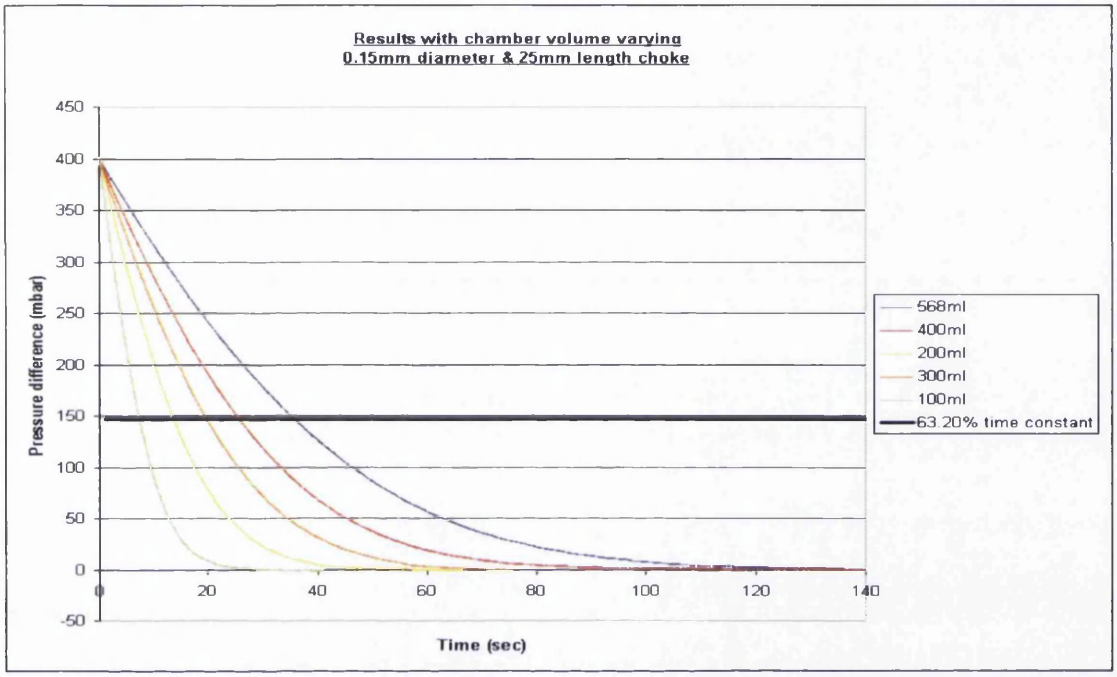

Figure 2.2: Results showing the time taken for the evacuated chamber to equalise through a 0.15mm diameter x 25mm choke with varying chamber volumes.

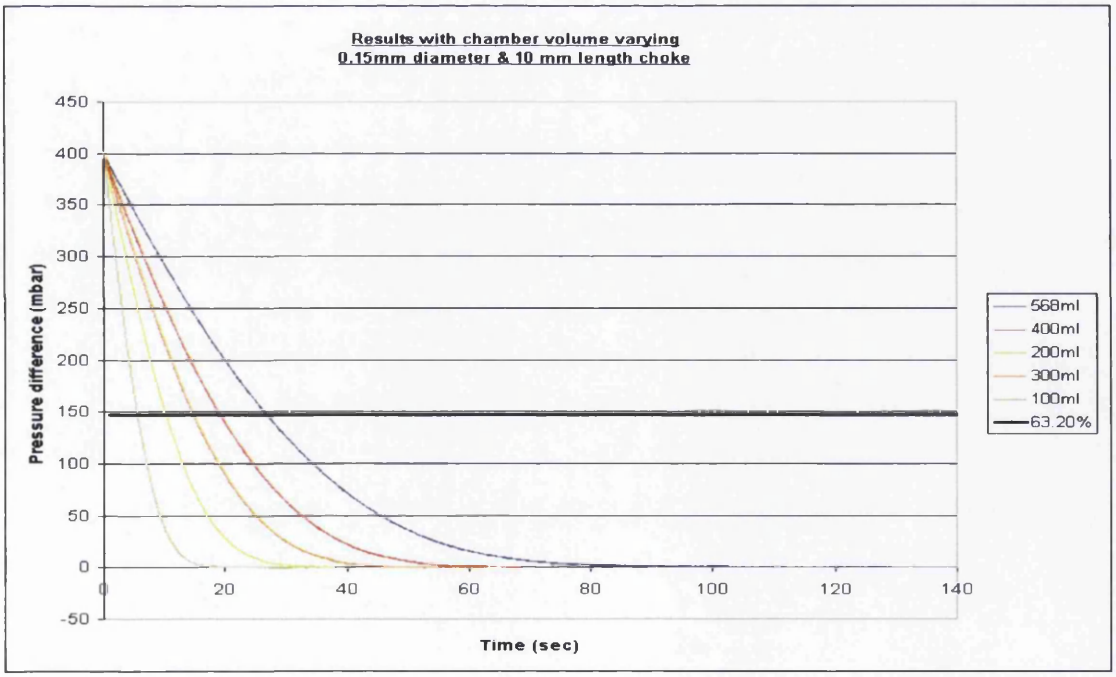

Figure 2.3: Results showing the time taken for the evacuated chamber to equalise through a 0.15mm diameter x 10mm choke with varying chamber volumes.

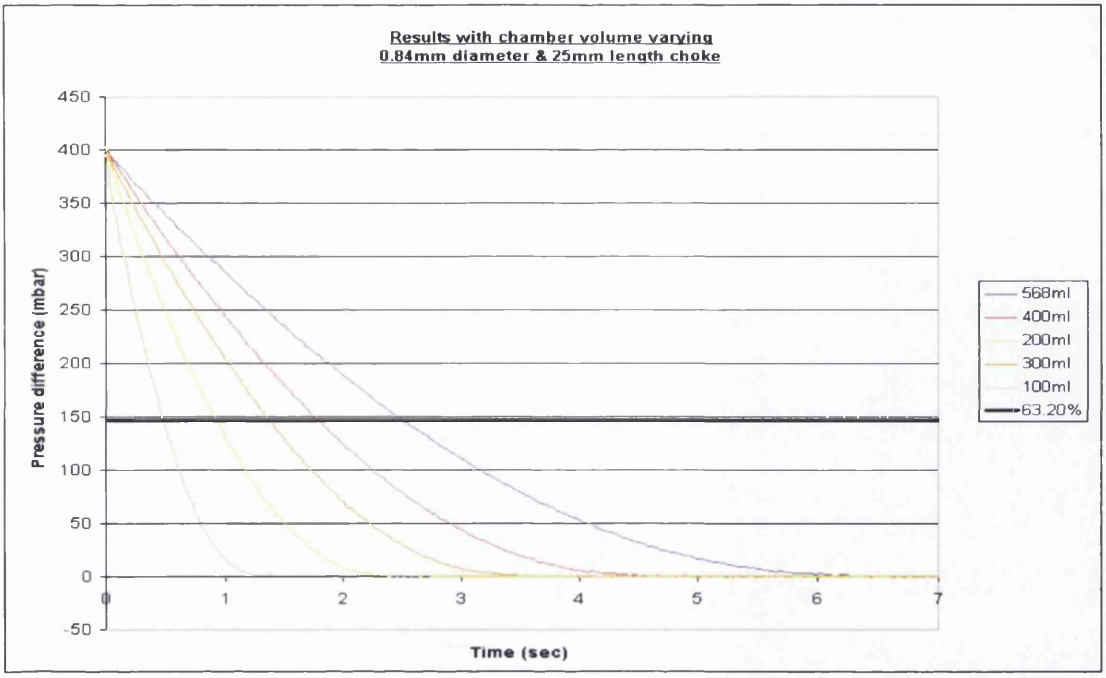

Figure 2.4: Results showing the time taken for the evacuated chamber to equalise through a 0.84mm diameter x 25mm choke with varying chamber volumes.

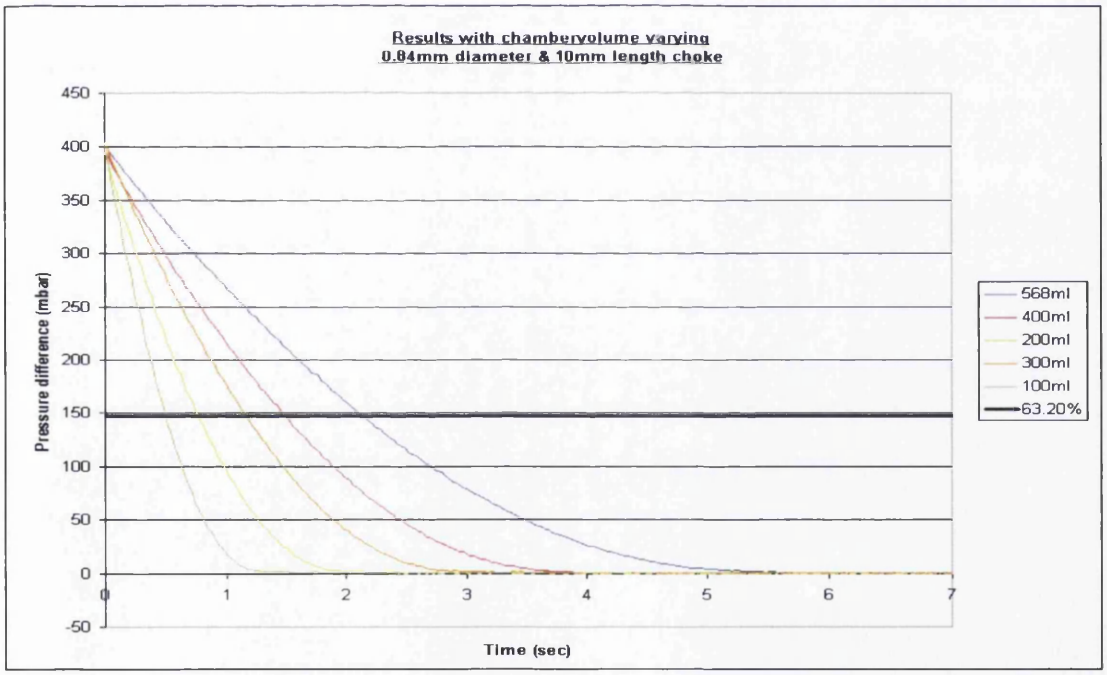

Figure 2.5: Results showing the time taken for the evacuated chamber to equalise through a 0.84mm diameter x 10mm choke with varying chamber volumes.

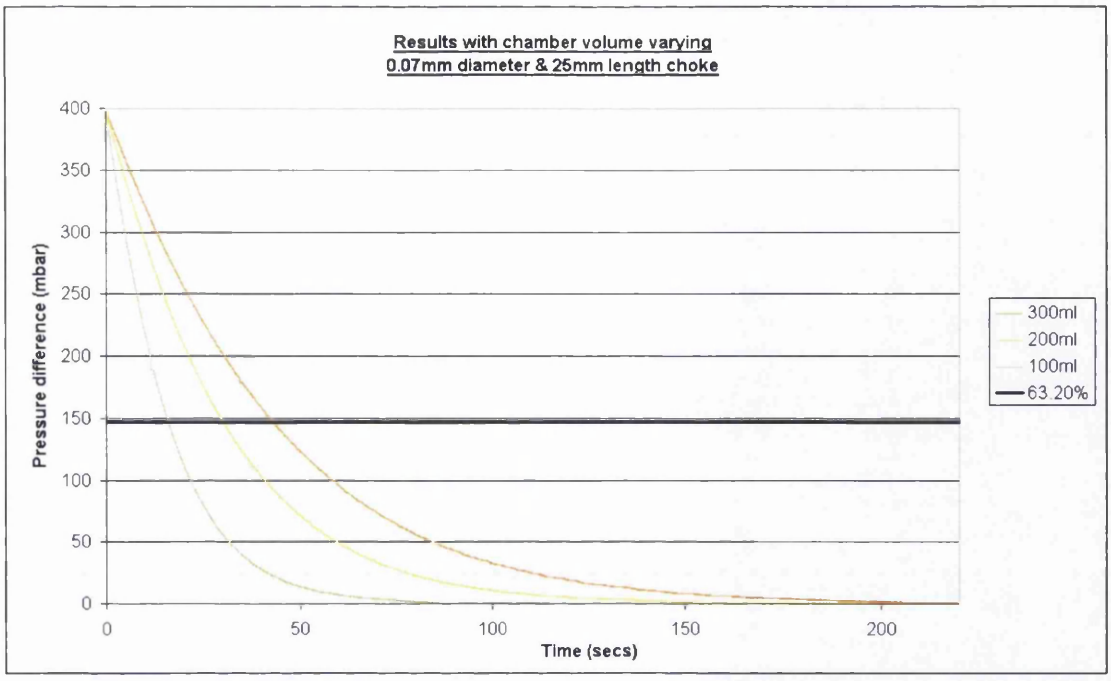

Figure 2.6: Results showing the time taken for the pressurised chamber to equalise through a 0.07mm diameter x 25mm choke with varying chamber volumes.

The graphs show an exponential decay as the chamber equalises through the choked inlet. As the volume increases, the time to equalise also increases.

2.4 Calculations

It was noted that the graphs were similar to that exhibited by a capacitor discharging. The first order transfer function which models exponential decay yields an equation that describes the decay traces seen above.

The equation is shown below where the time constant, tc, is taken off the graphs when the trace has achieved 63.2% of equalisation.

$$P = Pa \times e^{\frac{-t}{A.Cc}} \qquad \text{Equation [2.1]}$$

where: $Cc = \frac{tc}{V.A}$

and P = Pressure difference

Pa = Initial pressure

t = time

A = Cross sectional area of choke

V = Volume of chamber

Cc = Discharge constant

tc = Time constant

The time constant is taken at 63.2% due to:

$P = Pa \times e^{-t/tc}$ where: t = time, and tc = time constant.

When t = tc: $P = Pa \times e^{-1}$

$= 0.368\ Pa$

Therefore the graph reaches one time constant at (1–0.368=0.632), 63.2% of the initial pressure difference.

The time constants, obtained from the graphs in Figure 2.2 – 2.5, were plotted against the volumes for each choke configuration. This relationship was assumed to be linear over the area of interest and was used to produce an equation that predicts the time constants for smaller volumes. See Figure 2.7 and Table 2.1 for equations obtained.

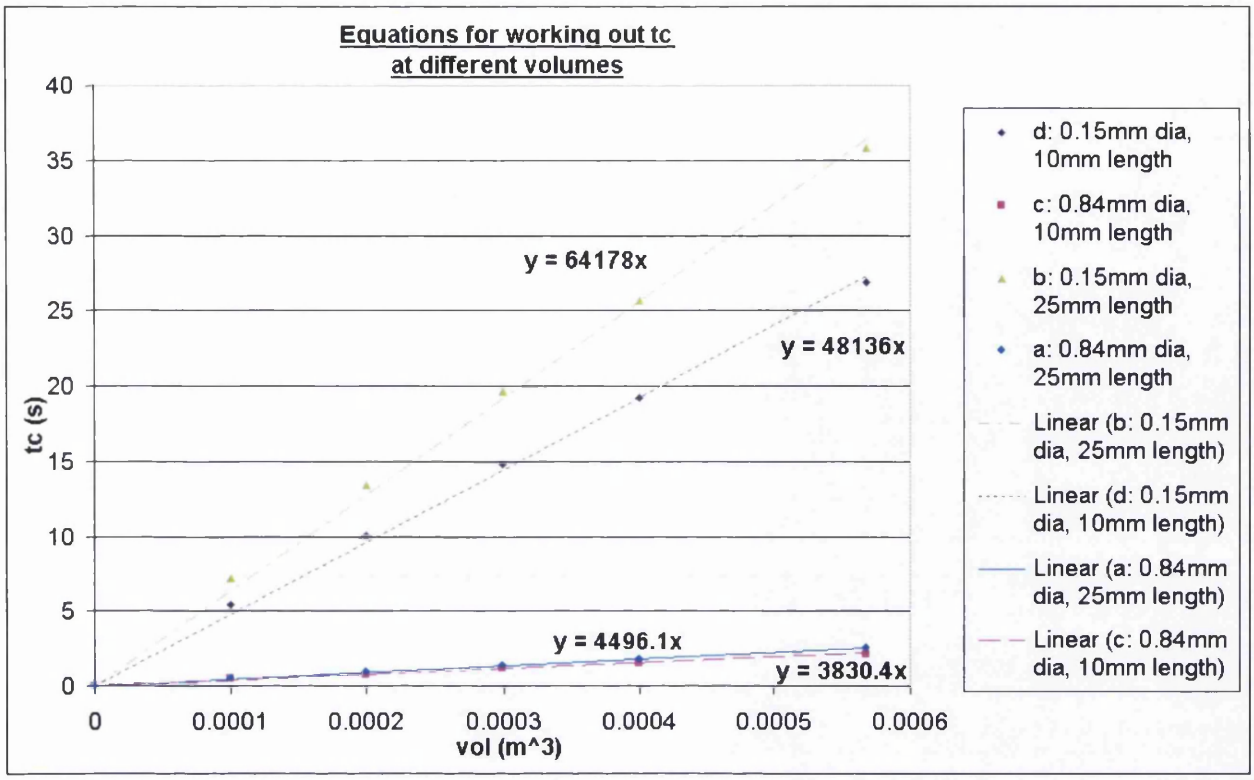

Figure 2.7: Graphs and equations used for working out the time constant at smaller volumes.

Diameter of choke	Length of choke	Time constant equation
0.15mm	10mm	tc = 48136 V
0.84mm	10mm	tc = 3830.4 V
0.15mm	25mm	tc = 64178 V
0.84mm	25mm	tc = 4496.1 V

Table 2.1: Time constant equations taken from graph

The time constants obtained were then fed back into Equation [2.1], and the equation used to analyse typical descents. This established which choke would be most advantageous. Figure 2.8 shows the worst case, un-damped, trace of a descent, against the calculated damped traces using a 10 and 20ml chamber volume. It shows that the choked pressure inlet would attenuate the pressure signal.

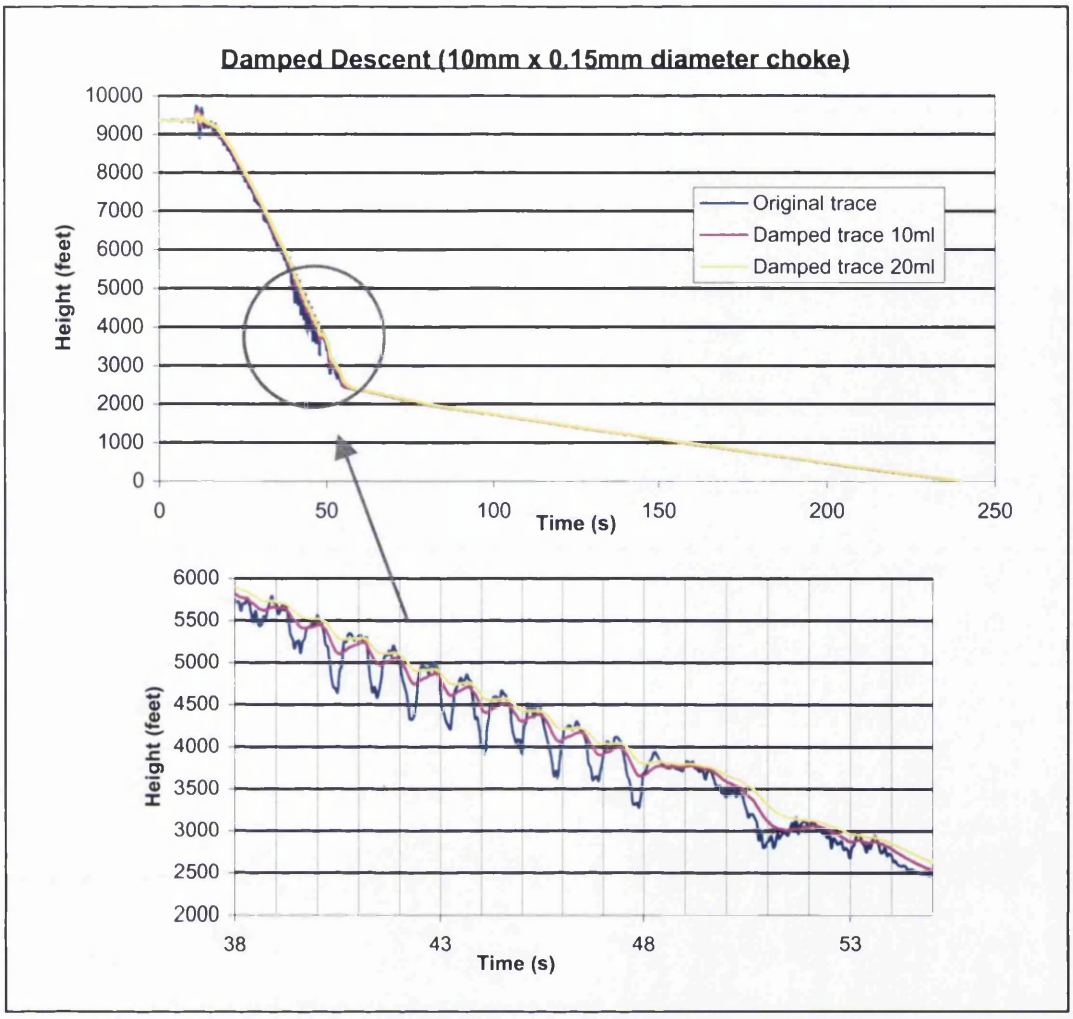

Figure 2.8: Pressure trace of a parachutist descent from an aircraft starting at 9363 feet and two damped traces (predicted).

It was found that the 0.84mm diameter choke had little effect on the pressure variations, however the 0.15mm diameter choke gave a considerably damped output when used with a 20ml chamber (Figure 2.8). However, the 20ml chamber is impractical for the AAD and work was continued to find a smaller choke and chamber arrangement.

The experiment was repeated with a 0.07mm effective diameter choke (Figure 2.6) and these results were used to predict time constants for smaller volumes and fed back into equation [2.1] in the manner already described.

2.5 Validation Experiment

The data obtained from the predicted pressure trace was put into the AAD Signal Injection test rig to analyse the damping pressure error. This is a software test program written to specifically test pressure traces taken from actual parachute descents. Ref[7].

The criteria for the choke to fail, was ± 500ft. Although this is the total permitted error for the AAD, the tests provided an effective means to measure the efficiency of each choke arrangement. See Figure 2.9 for the output results from the test rig.

An altitude lag (refer to Section 2.6) is introduced by the damping but is not considered in the signal injection tests. The data points used to calculate firing altitude by the test rig were taken from the damped data and therefore did not take a lag into account. Adequate damping is achieved with a long time constant, but minimal lag error requires a short time constant. A compromised time constant of approximately 1 second was seen to be effective from these tests.

[7] Williams. PM, 2001, *AADSignal Injection Test Rig*, IGQ TR 005, Irving GQ Ltd

RAW DATA TRACE Lift0692

INJECTION FILE NAME: c:\aaaa\ar2data\lift0692.pr2 **(undamped)**

RUN No.	RUN	MAIN ACT. ALT. (ft)	RES. ACT. ALT. (ft)	MAIN ACT. Time(sec)	RES. ACT. Time(sec)	MAIN +250ft ERR	MAIN ± 500ft ERR	MAIN FAIL	RESERVE +250ft ERR	RESERVE ± 500ft ERR	RESERVE FAIL
1	2	5710	3419	38.25	50.45	210					-581
2	2	5701	4329	38.4	45.7	201				329	
3	2	5645	3762	38.5	47.2	145			-238		
4	2	5677	4278	38.45	45.75	177				278	
5	2	5707	3419	38.3	50.45	207					-581
6	2	5714	2634	38.2	54.35	214					-1366
7	2	5645	3466	38.5	50.2	145					-534
8	2	5761	3438	38.05	50.3		261				-562
9	2	5532	2792	38.8	53.05	32					-1208
10	2	5761	3438	38.05	50.3		261				-562

2ml Volume, 25mm Length Choke, 0.02mm diameter

INJECTION FILE NAME: c:\aaaa\ar2data\ch692022502.pr2 **(tc = 0.395 secs)**

RUN No.	RUN	MAIN ACT. ALT. (ft)	RES. ACT. ALT. (ft)	MAIN ACT. Time(sec)	RES. ACT. Time(sec)	MAIN +250ft ERR	MAIN ± 500ft ERR	MAIN FAIL	RESERVE +250ft ERR	RESERVE ± 500ft ERR	RESERVE FAIL
1	2	5744	4284	38.4	45.8	244				284	
2	2	5659	3503	38.7	50.45	159				-497	
3	2	5674	3517	38.65	50.4	174				-483	
4	2	5615	3474	38.85	50.55	115					-526
5	2	5628	3490	38.8	50.5	128					-510
6	2	5705	3517	38.55	50.4	205				-483	
7	2	5731	3439	38.45	50.65	231					-561
8	2	5659	3503	38.7	50.45	159				-497	
9	2	5615	3474	38.85	50.55	115					-526
10	2	5753	3457	38.35	50.6		253				-543

20ml Volume, 25mm Length Choke, 0.15mm diameter

INJECTION FILE NAME: c:\aaaa\ar2data\ch6922025.pr2 **(tc = 1.284 secs)**

RUN No.	RUN	MAIN ACT. ALT. (ft)	RES. ACT. ALT. (ft)	MAIN ACT. Time(sec)	RES. ACT. Time(sec)	MAIN +250ft ERR	MAIN ± 500ft ERR	MAIN FAIL	RESERVE +250ft ERR	RESERVE ± 500ft ERR	RESERVE FAIL
1	2	5734	3629	39.25	50.5	234				-371	
2	2	5716	4215	39.4	46.75	216			215		
3	2	5748	4056	39.1	47.45	248			56		
4	2	5738	4240	39.2	46.45	238			240		
5	2	5734	3618	39.25	50.55	234				-382	
6	2	5707	4215	39.45	46.75	207			215		
7	2	5761	4243	39	46.4		261		243		
8	2	5734	3629	39.25	50.5	234				-371	
9	2	5754	4243	39.05	46.4		254		243		
10	2	5729	3629	39.3	50.5	229				-371	

Figure 2.9: Output results from the Signal Injection Test Rig

With a view to analysing smaller chamber volumes, the assumption was made that the relationship between the area of choke and the time constant is linear over the area of interest as the change is very small there. With this assumption, results could be predicted for smaller diameter chokes and smaller volumes of chamber at 25mm length.

Points were plotted from the results of the 25mm length choke experiments, plotting the multiplication factor (tc/vol) against the area. The resulting trend line equation could then be transposed to give equation 2.2, that could then be used to find the volume required to achieve a time constant of 1 second. Figure 2.10 shows the graph used to obtain equation [2.2].

$$\frac{tc}{volume} = -6 \times 10^6 \times area + 168881 \qquad \text{Equation [2.2]}$$

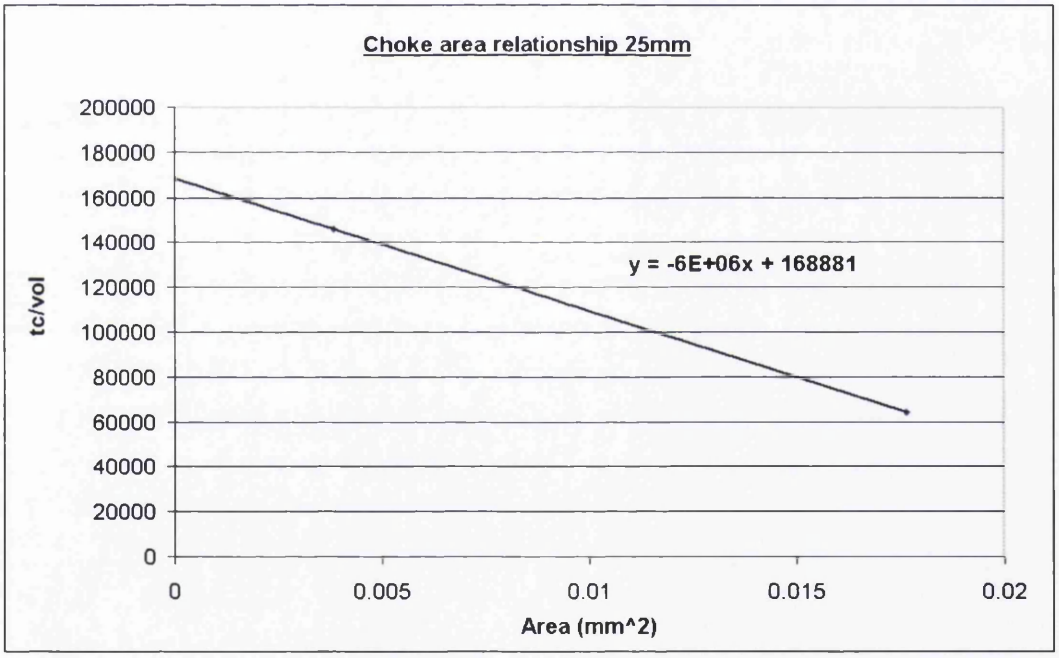

Figure 2.10: Relationship between choke effective area and time constant (25mm length only).

The smallest diameter choke believed possible was 0.02mm ($0.000314mm^2$), resulting in a minimum chamber volume that would display acceptable damping of 6 ml.

$$\frac{tc}{volume} = -6 \times 10^6 \times area + 168881$$

$$\frac{tc}{volume} = -6 \times 10^6 \times 0.000314 + 168881$$

$$\frac{tc}{volume} = 166997$$

Using the assumption that tc = 1 sec:

$$volume = \frac{1}{166997} = \underline{5.988\ ml}$$

2.6 Further Tests

A third series of experiments were carried out with longer chokes (40mm), in order to decrease the required chamber volume further. A new wire was used in this configuration that resulted in an effective diameter of 0.06mm (area = 0.002827mm^2). Figures 2.11 and 2.12 show the results obtained.

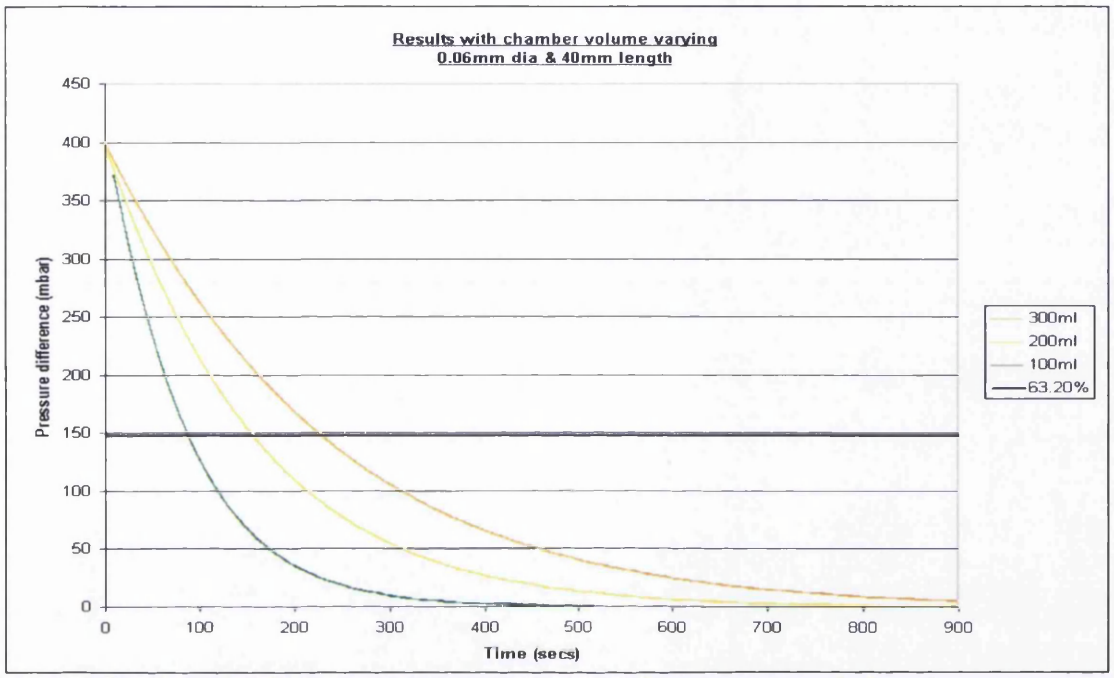

Figure 2.11: Results showing the time taken for the pressurised chamber to equalise through a 0.06mm diameter x 40mm choke with varying chamber volumes.

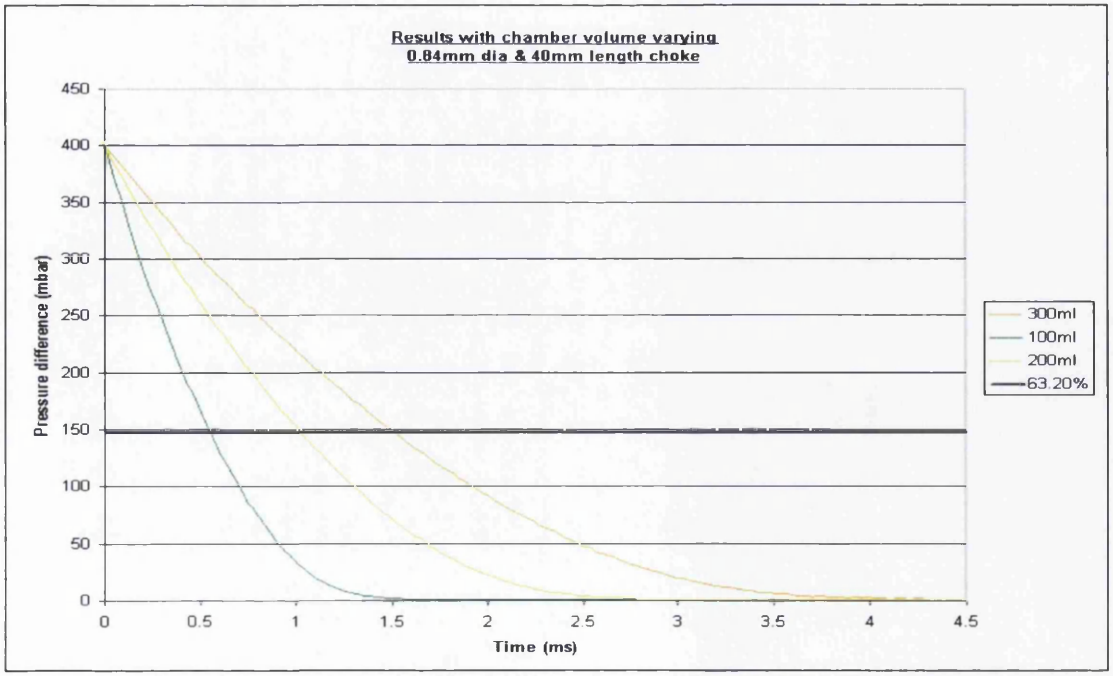

Figure 2.12: Results showing the time taken for the pressurised chamber to equalise through a 0.84mm diameter x 40mm choke with varying chamber volumes.

The results taken from Figures 2.11 and 2.12 were then plotted with the time constant values against the volume, to produce equations for working out the time constants at other volumes. See Figure 2.13 and Table 2.2.

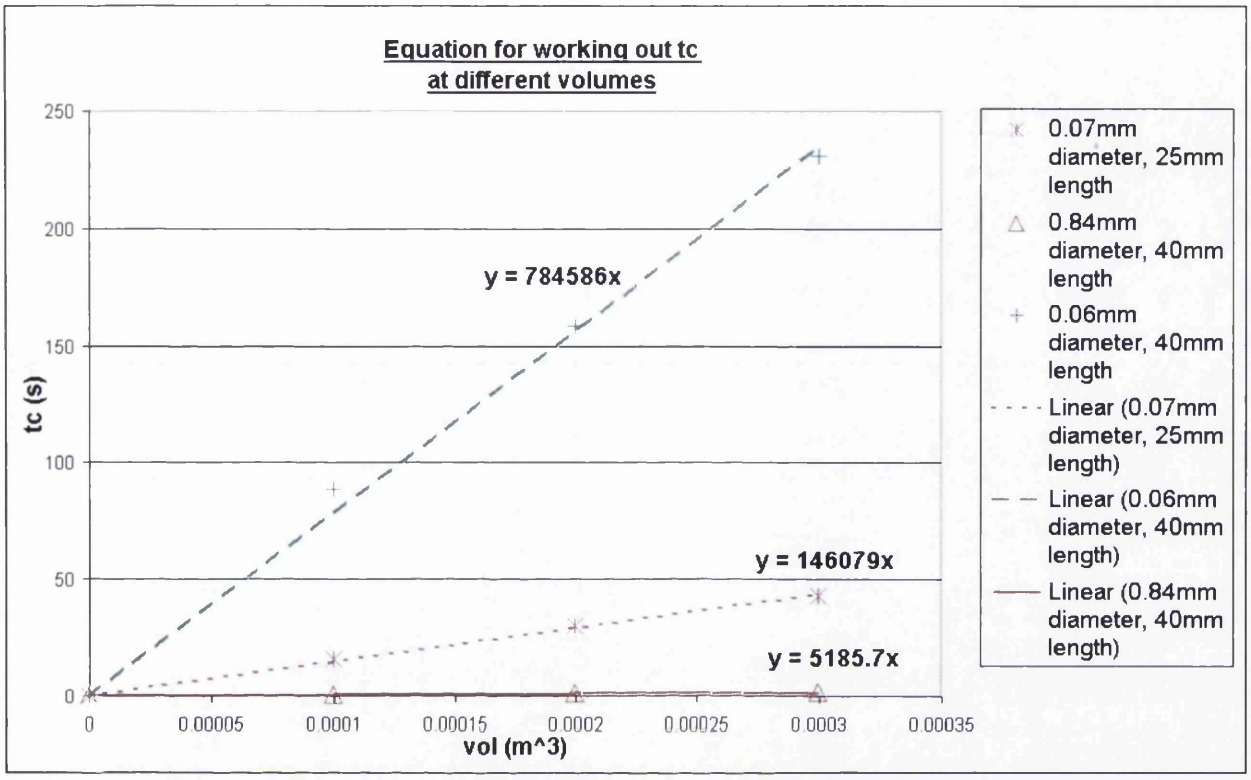

Figure 2.13: Graphs and equations used for working out the time constant at smaller volumes continued from Figure 2.7.

Diameter of choke	Length of choke	Time constant equation
0.07mm	25mm	tc = 146079 V
0.84mm	40mm	tc = 5185.7 V
0.06mm	40mm	tc = 784586 V

Table 2.2: Time constant equations taken from graph

The equations found in Table 2.2 could then be used to predict the optimum chamber volume to be used with choke configuration 0.06mm diameter, 40mm length:

$$tc = 784586 \times volume$$

Using tc = 1 sec, volume = 1.275ml.

The volume found in the tubes leading from the AAD to the static ports is between 1 and 1.7ml. Therefore this choke arrangement should result in adequate damping. It should be noted that this volume is variant on flexure in the tubes and individual fit. The tubes may also generate pressure errors or noise by the walls of the tubes being dynamically crushed or vibrated.

2.7 Error Due to Damping

To establish the signal lag caused by damping, an ideal descent was plotted against a damped descent. The signal lag manifests itself as an altitude error or offset. This error is also dependent on rate of change of pressure signal or rate of descent. Figure 2.14 shows an example of the error found due to damping in two different cases, 250 ft/sec and 100 ft/sec. The time constant was taken as 1 second.

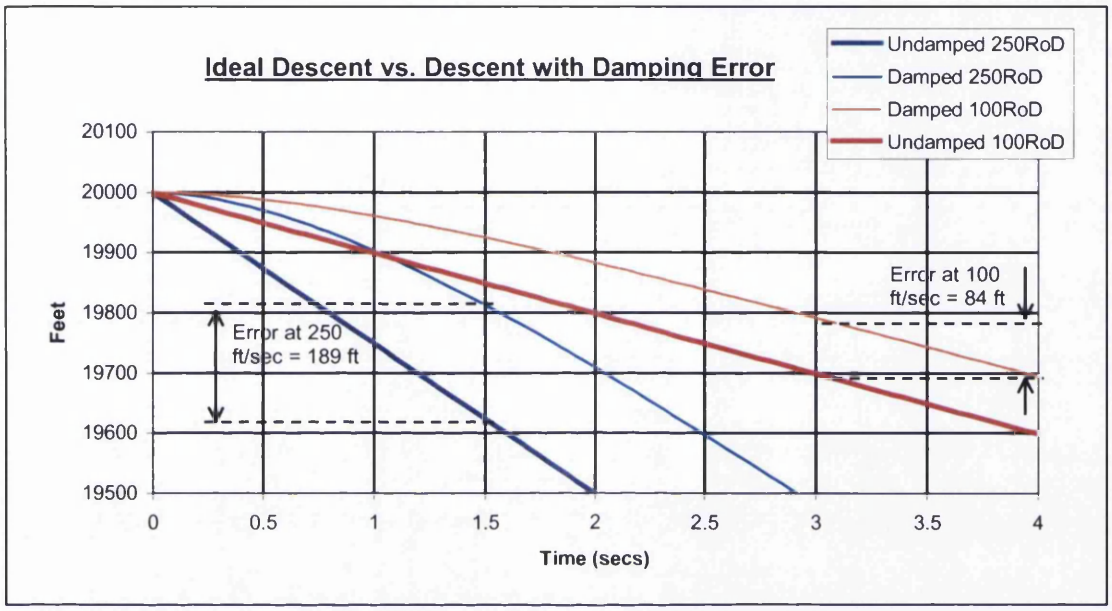

Figure 2.14: Examples of the error generated by damping with a 1 second time constant.

Different rates of descent and time constants were compared through the damping program and the relationships found are shown in Figure 2.15.

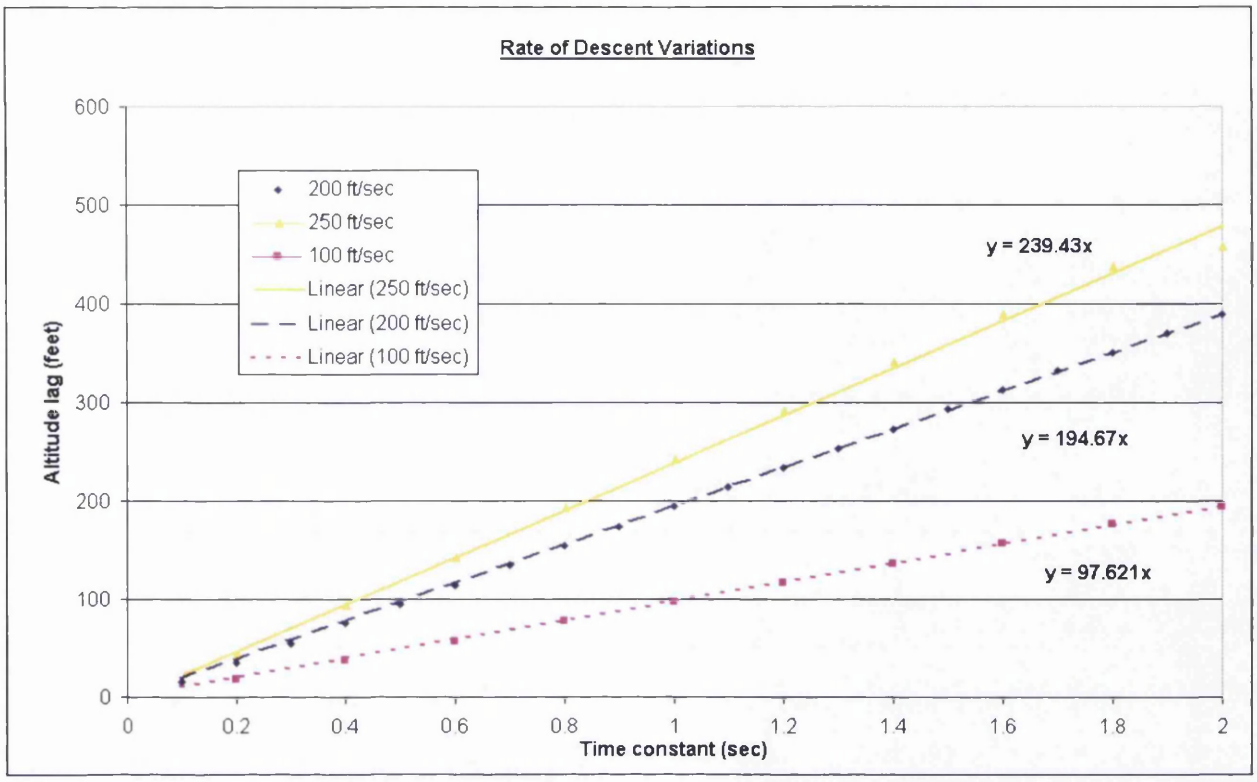

Figure 2.15: Relationships in altitude lag, rate of descent and time constants.

Since the rate of descent will vary in practice from one jump to the next and during a single descent as a result of density/altitude variation and parachutist body position, an average rate of descent was taken as 200 feet per second.

Using the relationships shown in Figure 2.15, the error due to damping can be worked out for each time constant and rate of descent.

2.8 Effects of Absolute Pressure

An investigation was carried out to establish the effect of absolute pressure on the damping. The initial experiments were repeated but for the purposes of this investigation the choke was opened into a pressure equal to that at 20000 ft (460mbar), rather than to sea level pressure (1013mbar). The chamber was evacuated by 200mbar and the time to equalise to 460mbar was measured. Figure 2.16 compares the graphs measured at ground pressure to those at altitude.

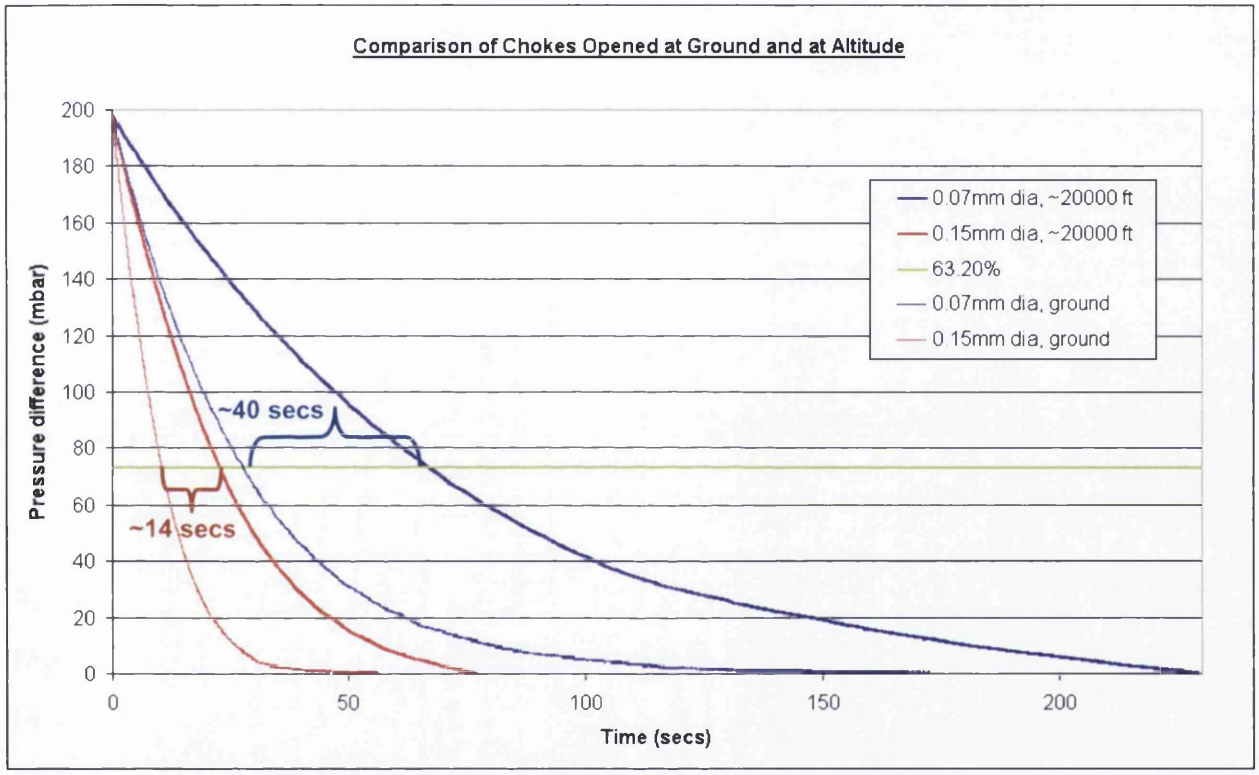

Figure 2.16: Results taken at altitude compared to those taken at ground pressure.

Figure 2.16 shows that the time constant varies with altitude. With reference to the data generated in Figure 2.16 the assumption was made that with each choke arrangement, the magnitude of the time constant multiplies by a factor of 2.86 when equalising to 20000ft equivalent pressure as opposed to equalising to ground pressure. Therefore a time constant could be predicted for each intermediate height.

Using this assumption, an equation was produced for each initial ground time constant to produce a varying time constant with altitude. This was used in the damping program and traced against the raw data to model the damping. An example is shown in Figure 2.17.

Feet	factor	tc(ground)	tc(altitude)
20000	2.86	1.176879	2.353758
19000	2.767		2.2949141
18000	2.674		2.2360701
17000	2.581		2.1772262
16000	2.488		2.1183822
15000	2.395		2.0595383
14000	2.302		2.0006943
13000	2.209		1.9418504
12000	2.116		1.8830064
11000	2.023		1.8241625
10000	1.93		1.7653185
9000	1.837		1.7064746
8000	1.744		1.6476306
7000	1.651		1.5887867
6000	1.558		1.5299427
5000	1.465		1.4710988
4000	1.372		1.4122548
3000	1.279		1.3534109
2000	1.1186		1.2945669
1000	1.093		1.235723
0	1		1.176879

40mm long, 1.5ml chamber volume, 0.06mm diameter choke: tc = 1.176879

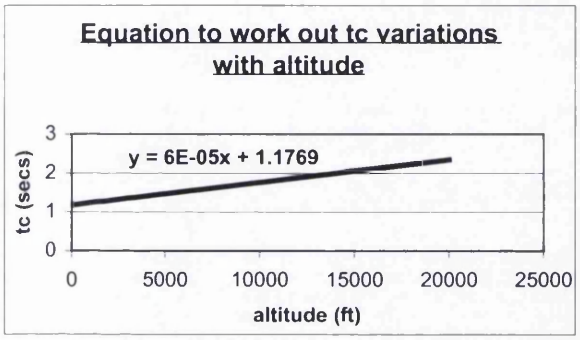

$tc = 6 \times 10^{-5} \times \text{altitude} + 1.1769$

Figure 2.17: Example of time constant variations with altitude.

Further choke configurations were run in the damping program with the altitude error taken into consideration, and plotted against the worst-case descent. Figure 2.18 shows how the smaller the chamber volume, the smaller the error to the pressure readings. However, the smaller the chamber volume the less the pressure variations are damped.

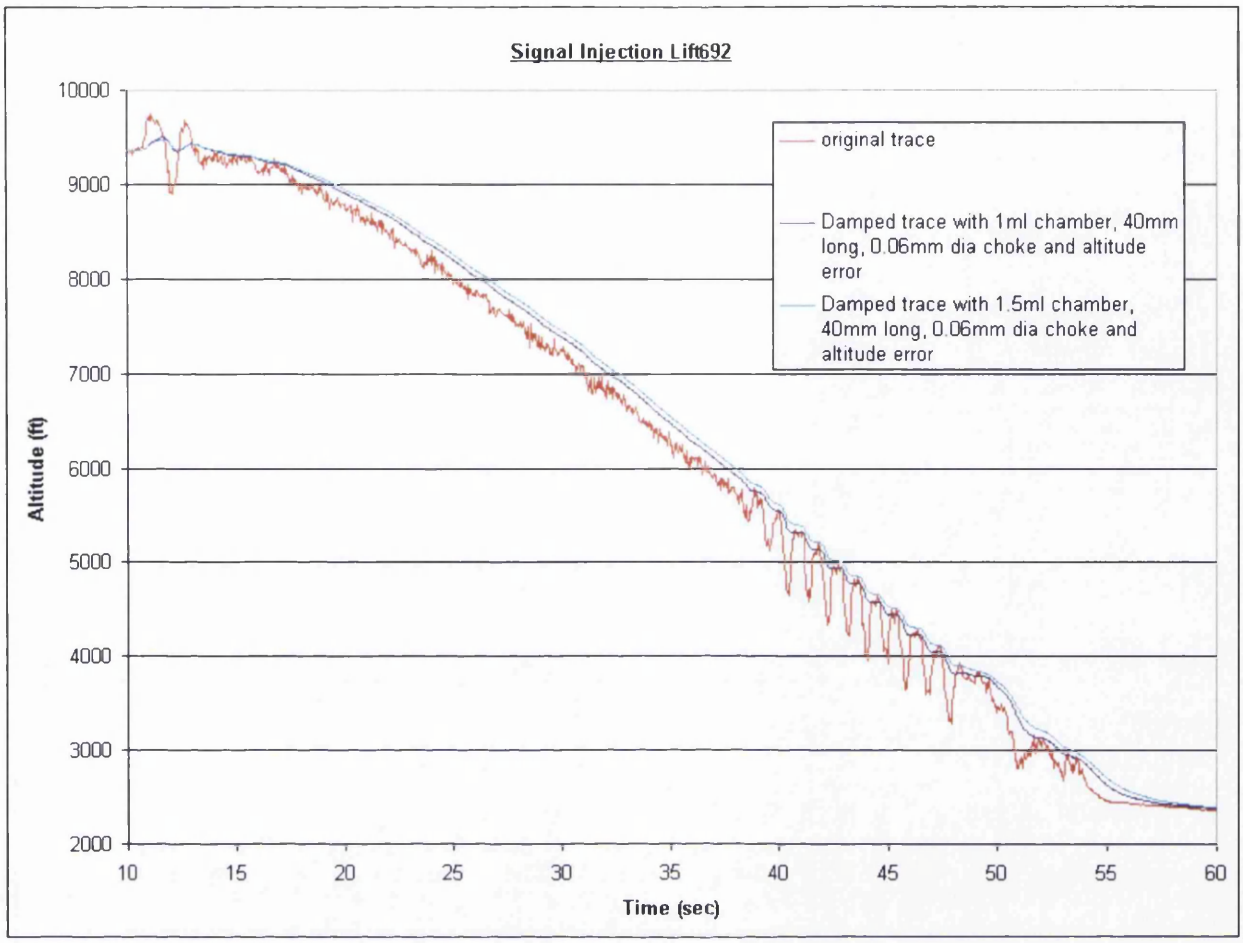

Figure 2.18: Signal Injection Lift 692 (worst case descent) against modelled pressure damping using choked pressure inlet.
Graph showing the different error due to altitude and damping.

2.9 Error Due to Altitude and Damping

The total damping error was found to be the combination of the error due to altitude and the error due to damping. Figure 2.19 shows an error graph with and without the altitude consideration, with parachutist exiting the aircraft at 20000ft and 10000ft.

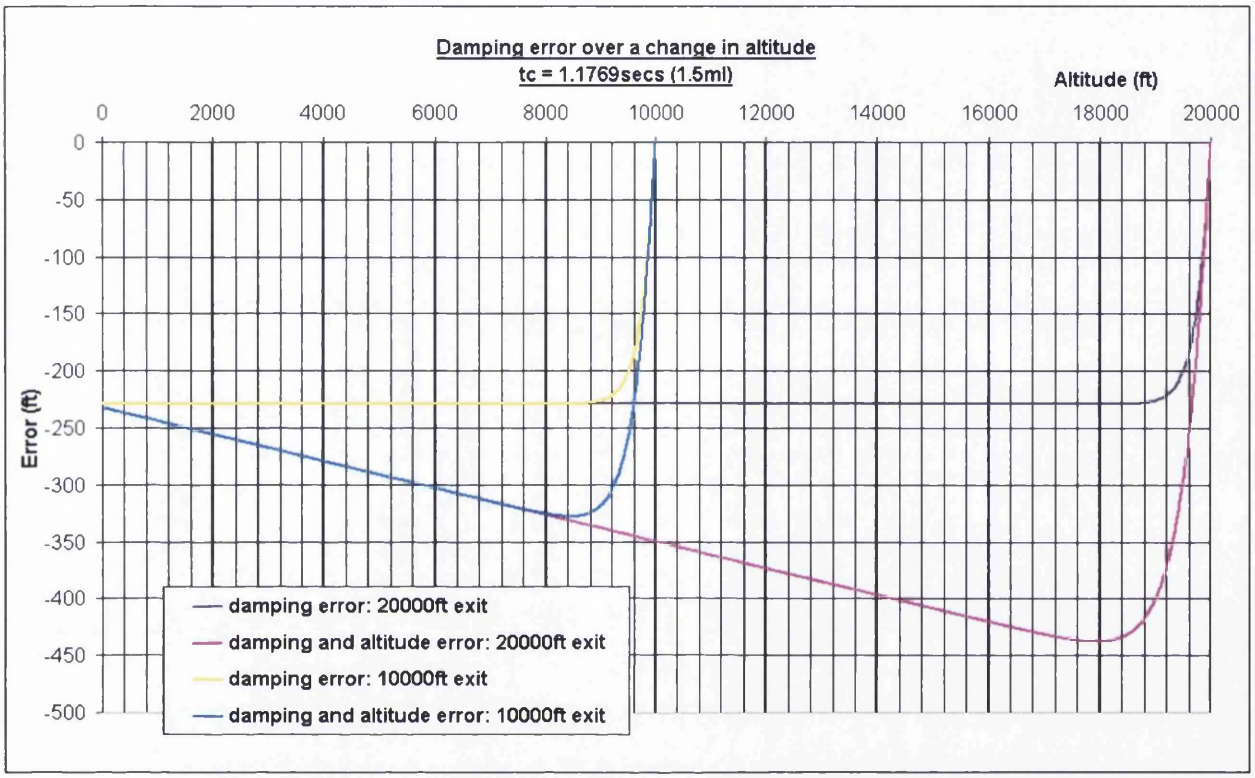

Figure 2.19: Total damping error with altitude

It can be seen from Figures 2.18 and 2.19 that the more damping applied to the pressure variations, the larger the resulting error. The maximum error due to altitude and damping is 438 feet at 18000ft (2.43% error) at 200 ft/sec.

2.10 Conclusions

An investigation has been carried out to see if a choked pressure inlet could be used to damp the erratic inlet pressure that is read by the pressure transducer in the AAD. Work has been carried out to determine the volumes of the choke and chamber to check the viability of the device.

It has been found that the damped pressure inlet alone is not a viable option for the AAD as the required dimensions are not practical. It was found that a 40mm long, 0.06mm diameter choke would be required with a 1-1.5ml chamber, to achieve an acceptable damped pressure reading. A 40mm length is not practical as it may be susceptible to damage during use and would present integration problems.

2.10.1 Assumptions

Several assumptions have been made during this study:

- The damping equation is a perfect exponential decay.
    - The experimental results produced a graph that could be closely modelled to an exponential decay, to give a first order transfer function. However, the experimental curve does not model a theoretical exponential decay perfectly.
    - The time constant used for calculations is taken at 63.2% of the pressure difference and this first section of the graph does model the exponential decal graph closely. Therefore, the assumption made is defendable.

- The relationship between the effective area of the choke and the time constant is linear at small volumes.
    - The relationship between the effective area of the choke and the time constant varies on a curved graph for each choke arrangement, however at such a small scale, the relationship is assumed to be linear as the difference is so small (between 0 and 0.5mm^2).
    - Using this assumption, results could be predicted for smaller diameter chokes and smaller volumes of chamber.

- The ideal time constant is 1 second.
    - Tests on the AAD signal injection test rig displayed a series of results from different tc values (tc = 0.48136, 0.96272, 0.64178, 1.28356, 0.730395, 0.98871 and 0.395484).
    - The minimum error resulted from test tc = 0.98871.
    - This suggested that a time constant of 1 second was ideal, to give a suitably damped pressure reading.

- An average rate of descent was taken as 200 feet per second.
    - The rate of descent will vary in practice from one jump to the next (from 140feet/sec to 280feet/sec) depending on mass and body position. Speed will also vary constantly throughout the descent.
    - An average rate of descent (200 feet per second) was taken in order to proceed with the calculations.

2.11 Recommendations

The software algorithm filters high frequency noise (±500ft) but medium frequency errors (±200ft) are caused by noise of clothing flapping, acoustic noise, vortex shedding, and wake effects. This error will be reduced using the choked pressure inlet investigated in this chapter to damp the pressure signal. However, this is at the expense of introducing a lag offset.

It is concluded from this chapter, that a choked pressure inlet, 40mm long, 0.06mm diameter (achieved by using a hypodermic tube with a wire inserted), will result in effective damping. The total volume in the tubes between the AAD and the static ports inlets is 1.5ml ±10%, and therefore of adequate volume to damp the readings satisfactorily. It must be noted that the larger the volume in these tubes, the larger the error that will be produced, but the more pressure attenuation will be gained.

The MOD AAD uses distributed static port venting to take pressure readings from around the body. The actual low frequency noise filtering effect of distributed static port venting is assessed in the following chapter. With this information the choke configuration, recommended in this report, can be reduced in length, as the choke will only be required to damp a treated pressure signal as opposed to a raw signal.

Chapter 3 - Distributed Static Port Venting

3.1 Introduction

Work has previously been carried out to investigate the effect of static inlet porting (GQ TR 01001) that takes an average of two pressure readings from around the body. It was found that this reduces the effects of changing body position and hence attenuates the low frequency noise. Wind tunnel tests were carried out at Sky Venture, Florida to examine the effects of static porting on recorded pressure readings with differing parachutist's attitude to the airflow. This chapter analyses the results obtained in the tests to obtain a quantitative effect of static inlet porting.

3.2 Test Procedure

A vertical wind tunnel was used to investigate the effect of distributed static port venting. The benefit of using a wind tunnel as opposed to real descents is that experiments can be repeated quickly, you have a longer period of time to gather data, and the whole experiment may be observed and filmed from the side. This particular wind tunnel allowed three people to 'fly' in its cross section. The test parachutist wore a foam parachute pack with the AAD with static ports and measuring instrumentation attached to it, and two men helped to position the parachutist in different body positions in the airflow. Pressure traces were recorded by the instrumentation and used to analyse the noise seen at the AAD. Ref [10] and [11].

3.3 Summary of Wind Tunnel Test Results

Wind tunnel tests were carried out prior to my involvement in this project. They were carried out in accordance with trials specification GQ TR 01017 on 14th April 2001 at Sky Venture, Florida. Tests were conducted with and without the static port venting, with different equipment configurations (see Table 3.1 and Figures 3.1 to 3.9), and in six different body positions to the airflow.

---

[10] Ewing EG, Bixby HW and Knake TW, 1978, *Recovery Systems Design Guide*, Ohio, Air Force Flight Dynamics Laboratory

[11] Hoerner SF, 1965, *Fluid – Dynamic Drag*, Albuquerque, Hoerner Fluid Dynamics

A summary of the results obtained is given in Figure 3.10. The results were obtained from taking the average altitude offset error from the pressure data readings taken, caused by equipment configuration and body position. The equipment consists of typical kit required by paratroopers when despatched from aircraft such as an oxygen tank, Bergen and a weapon.

Run 1	Clean Fatigue, Static Tube not connected
Run 2	: *Run ignored due to static tube coming out during run*
Run 3	Oxygen fitted, static tube not connected *– no data recorded (repeat required)*
Run 4	Bergen, Oxygen, weapon, static tube not connected
Run 5	Bergen, Oxygen, weapon, static tube connected
Run 6	Bergen, Oxygen not fitted, static tube not connected
Run 7	Bergen, Oxygen not fitted, static tube connected
Run 8	Oxygen fitted, static tube not connected
Run 9	Oxygen fitted, static tube connected
Run 10	: *Run abandoned, ran out of time – no data*
Run 11	Clean Fatigue, static tube not connected
Run 12	Clean Fatigue, static tube connected

Table 3.1: Test Configuration

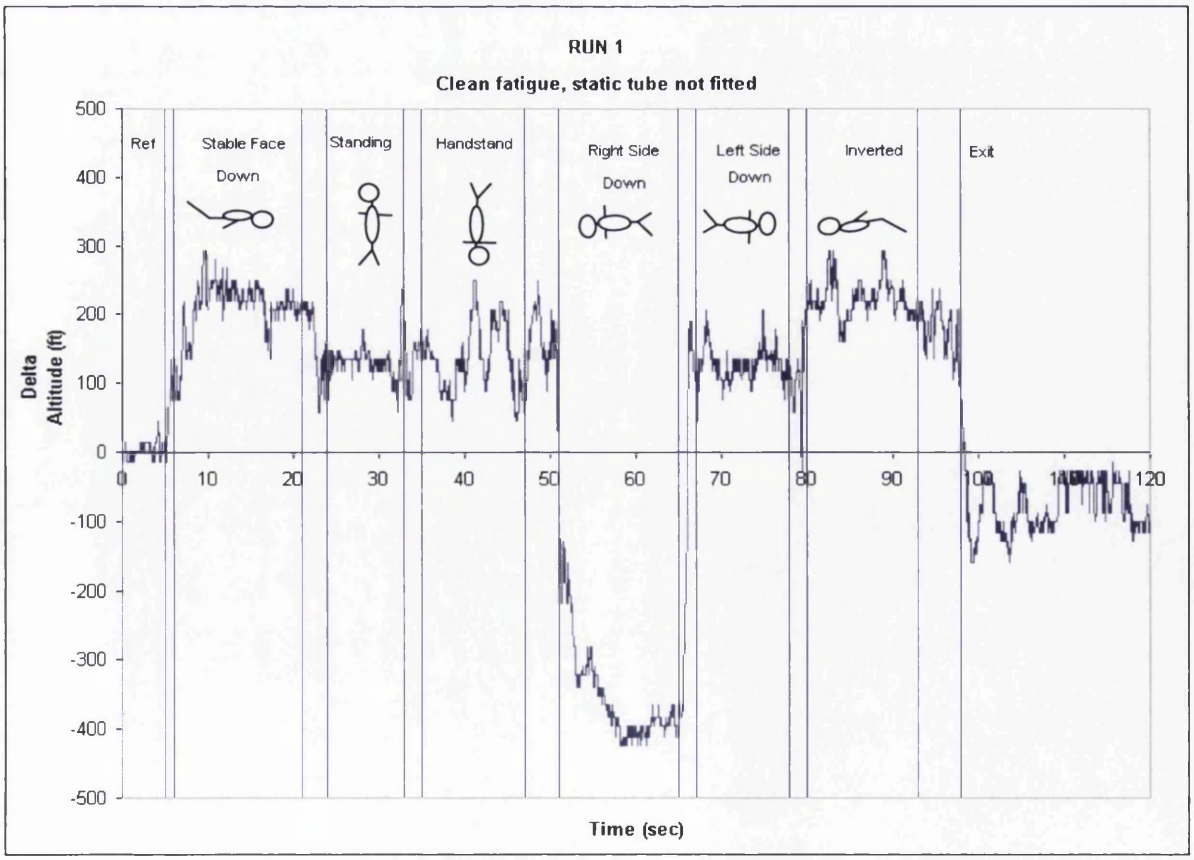

Figure 3.1: Results from Run 1

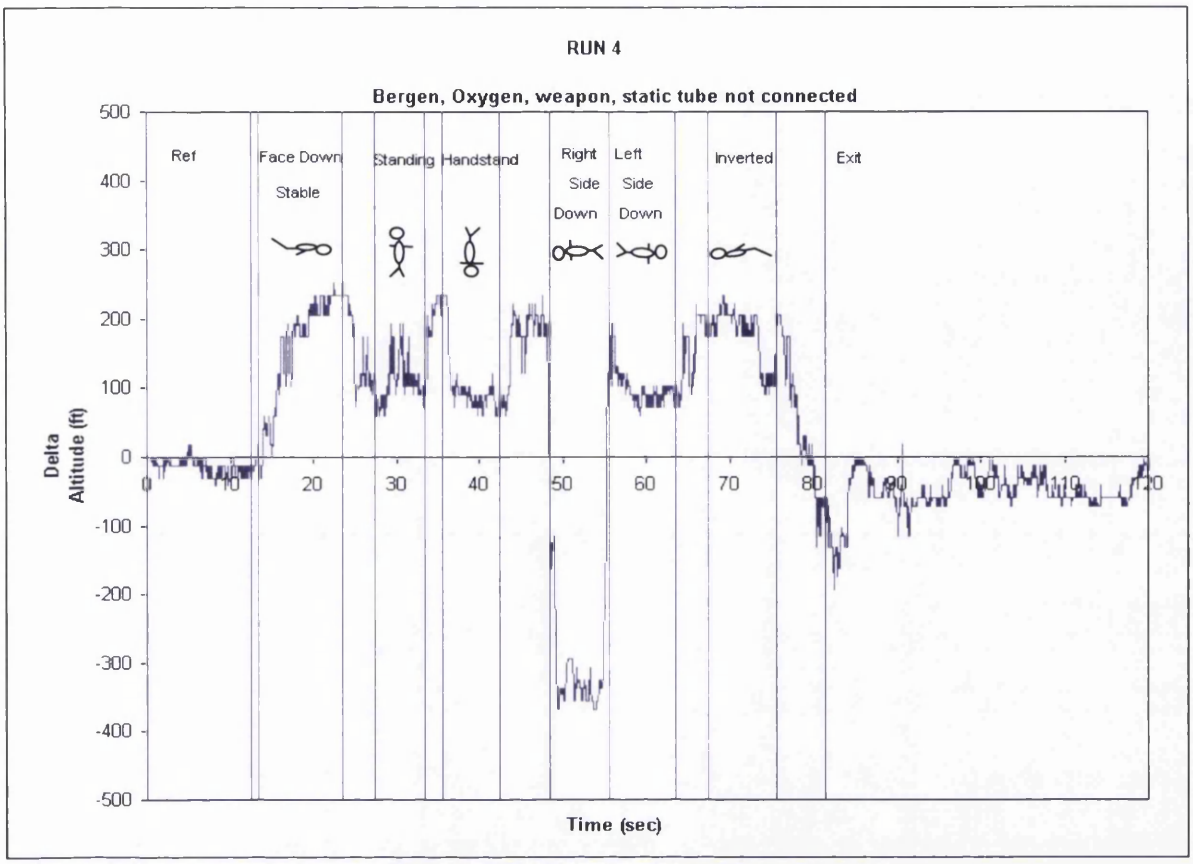

Figure 3.2: Results from Run 4

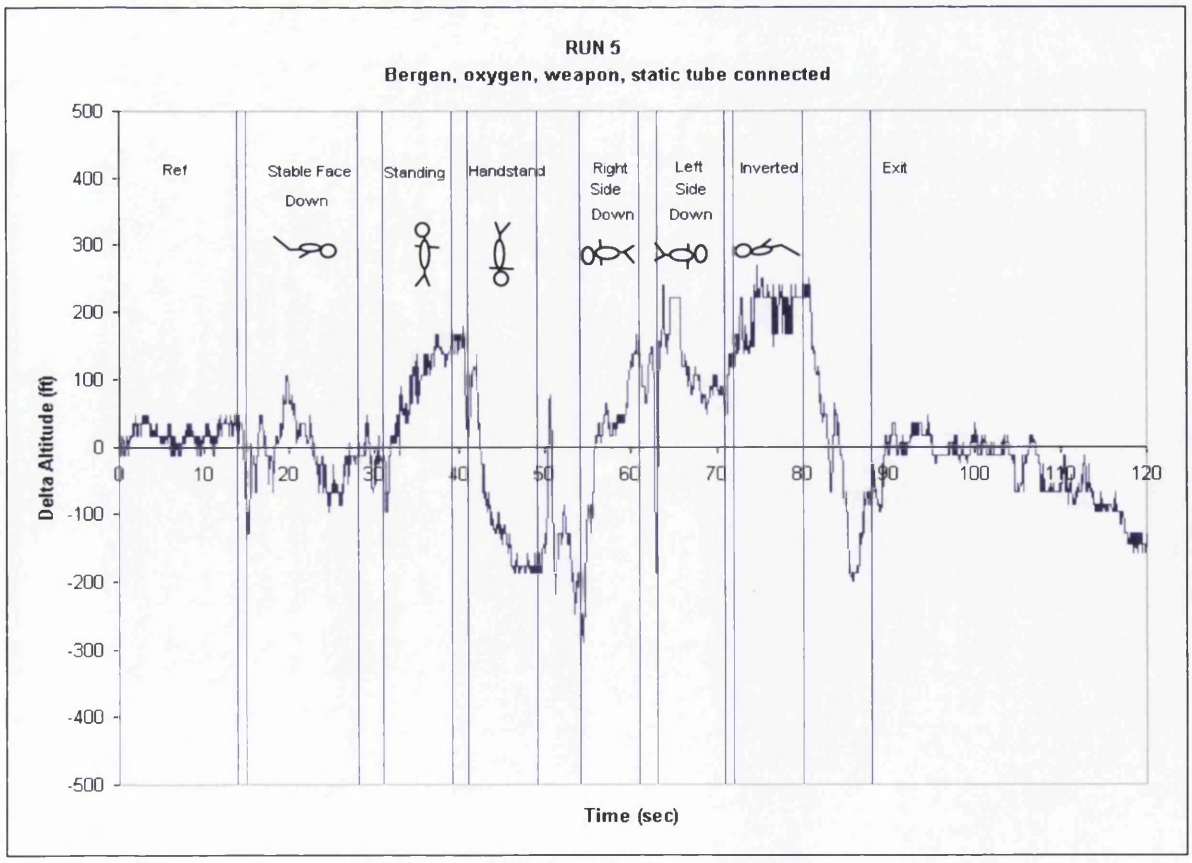

Figure 3.3: Results from Run 5

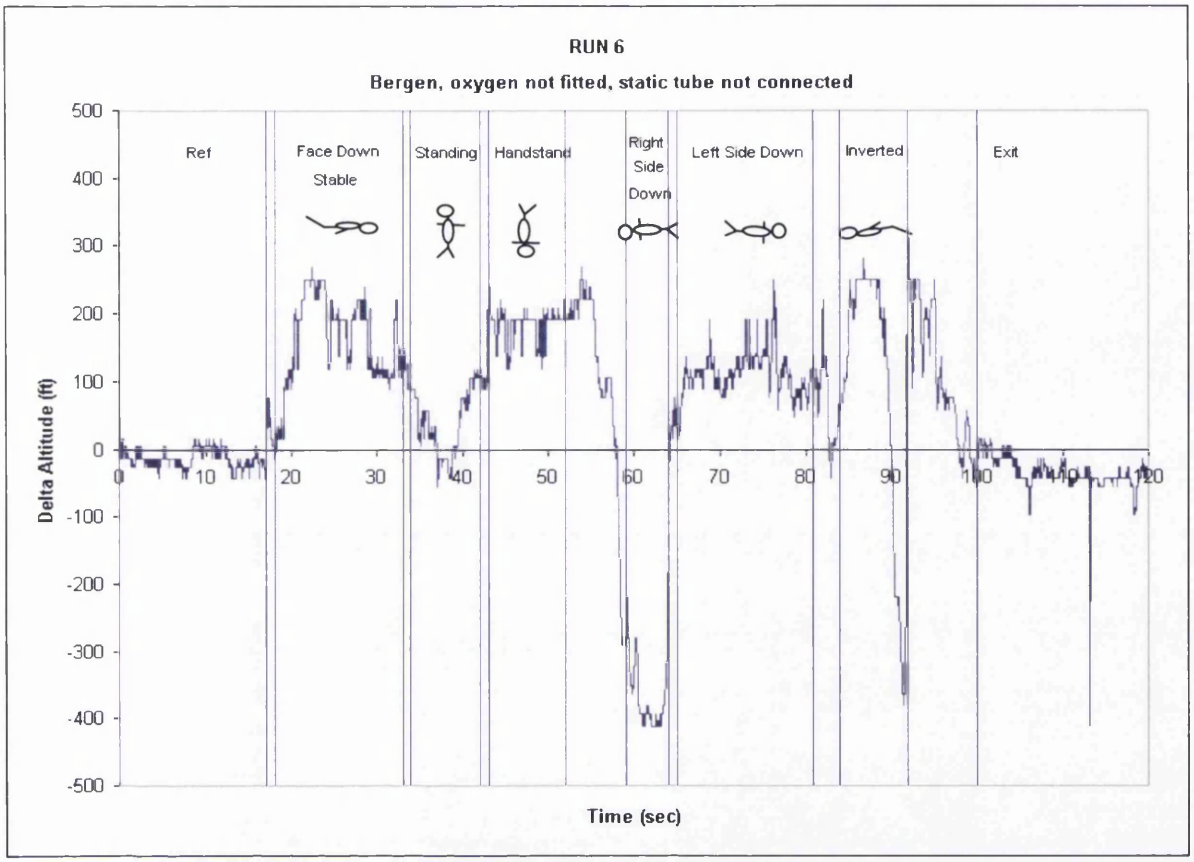

Figure 3.4: Results from Run 6

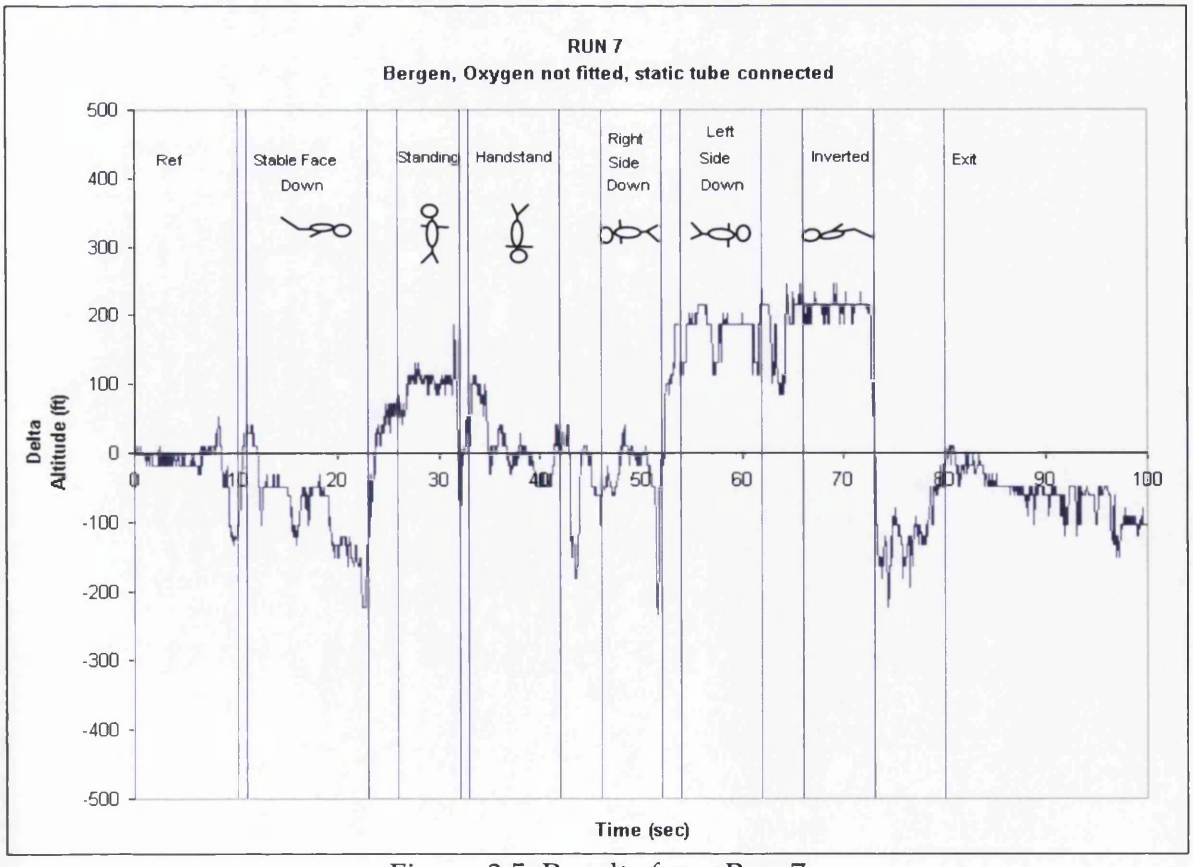

Figure 3.5: Results from Run 7

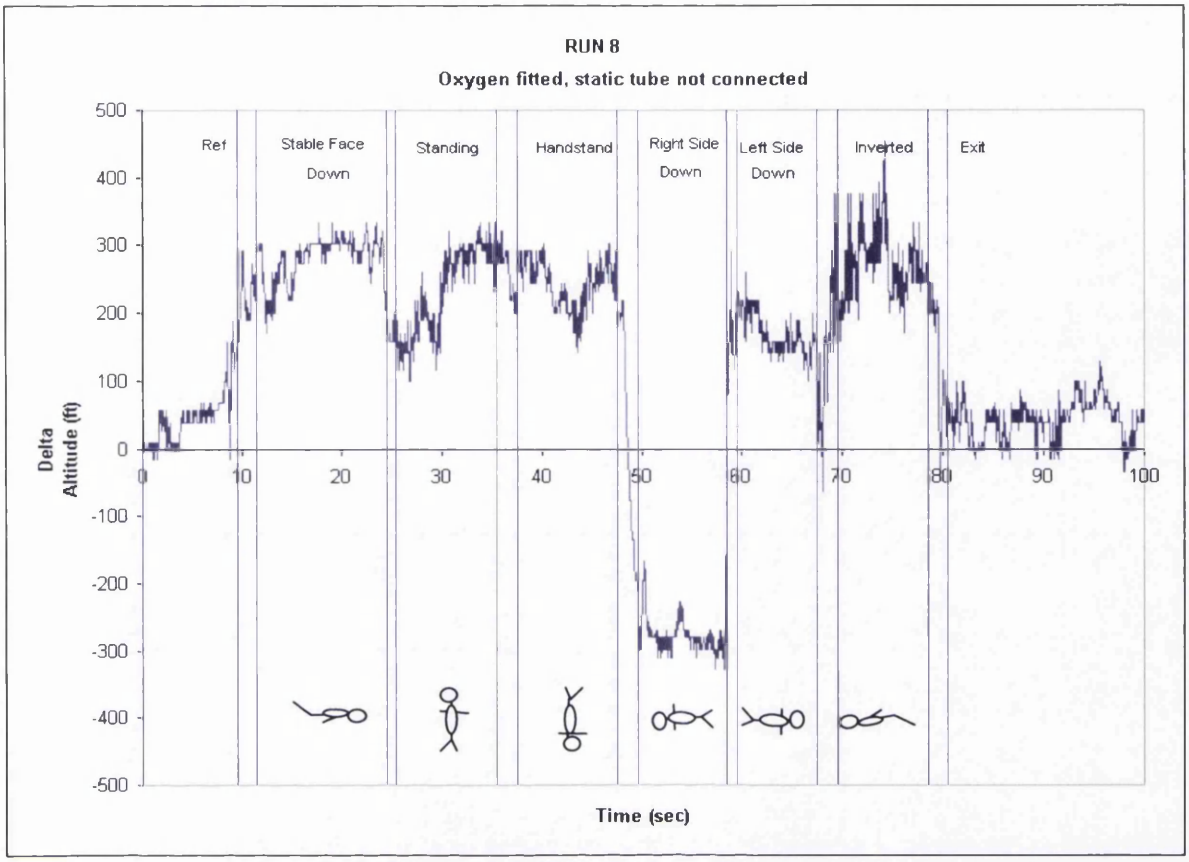

Figure 3.6: Results from Run 8

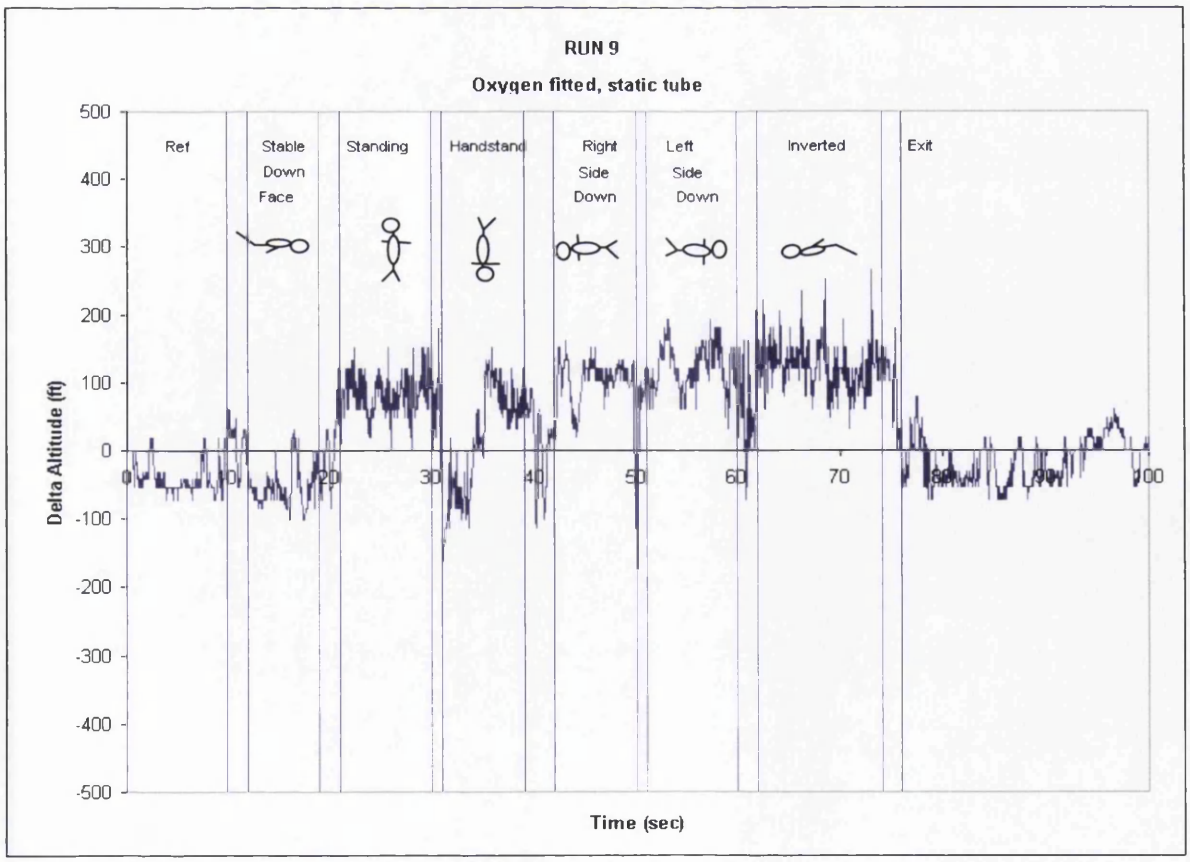

Figure 3.7: Results from Run 9

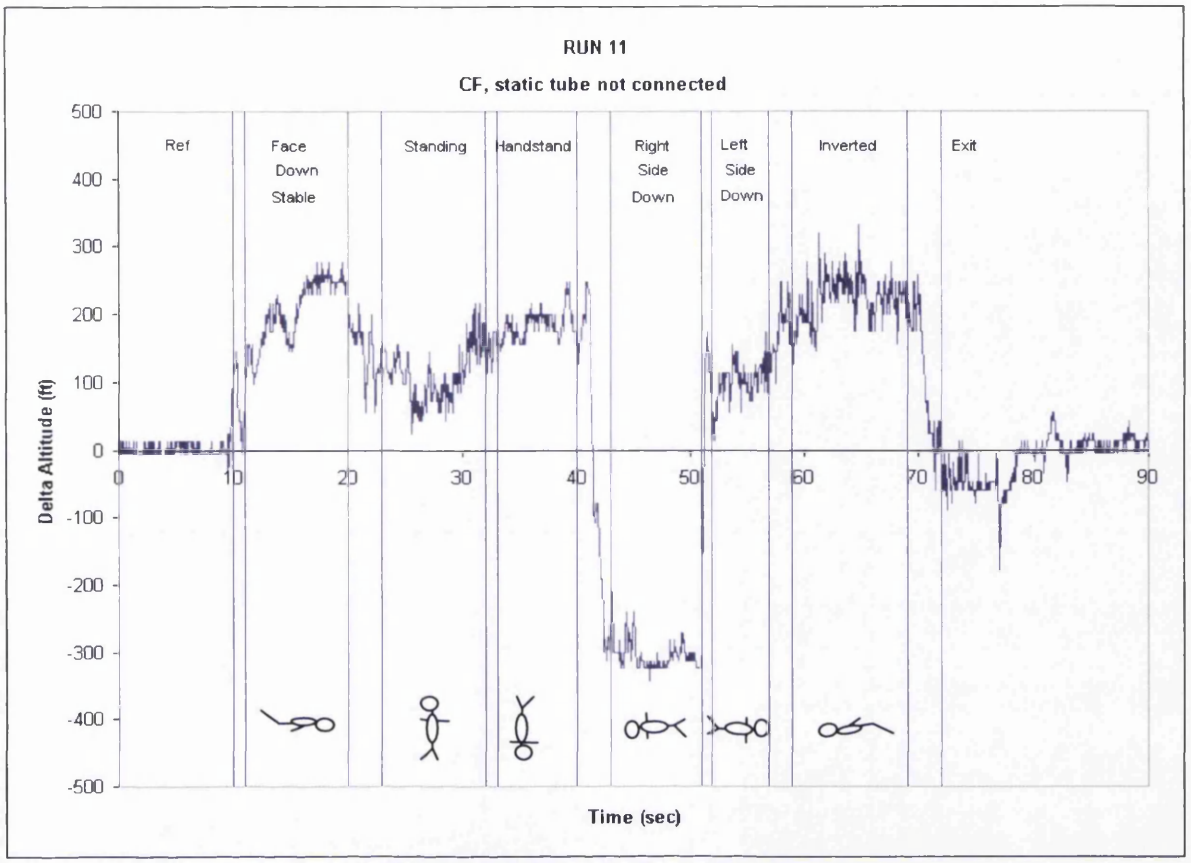

Figure 3.8: Results from Run 11

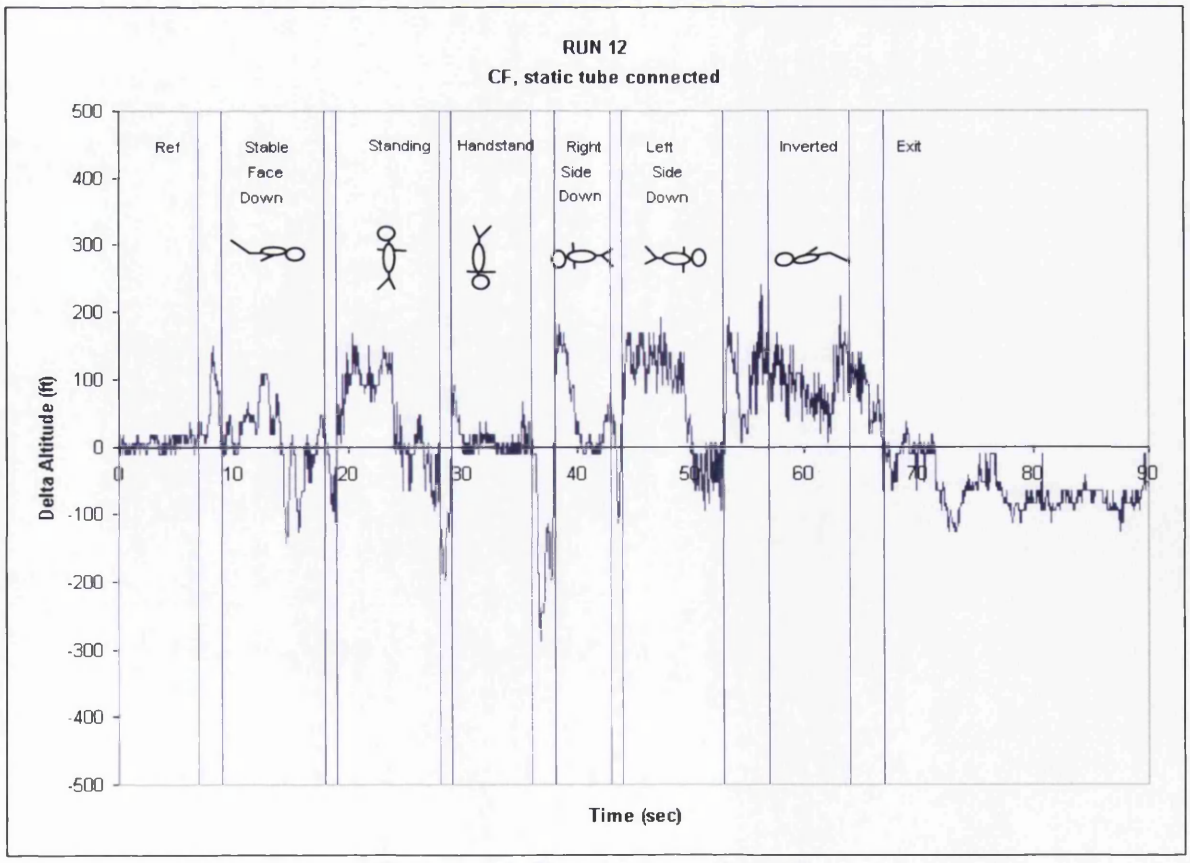

Figure 3.9: Results from Run 12

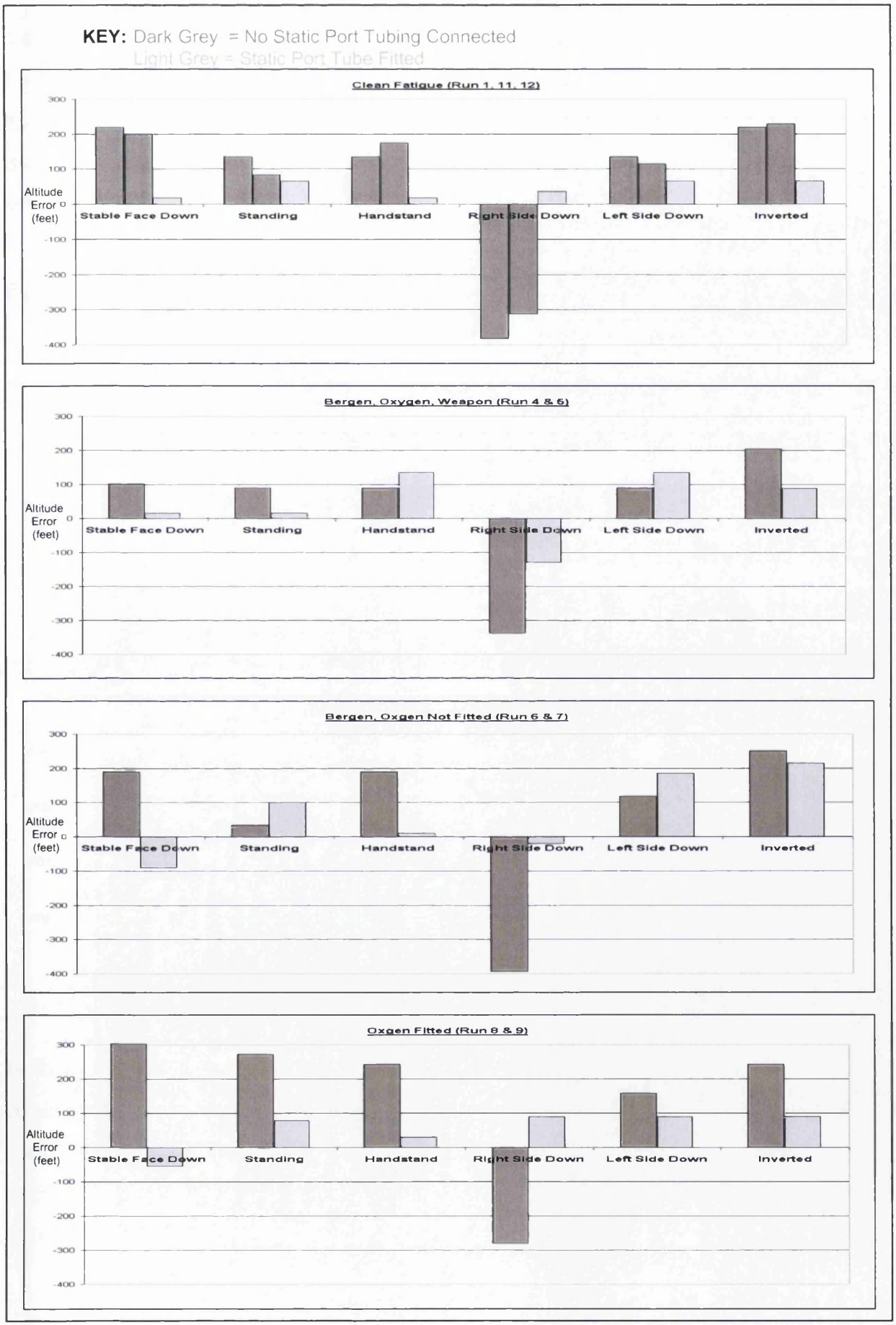

Figure 3.10: Average altitude offset error (feet) caused by equipment configuration and body position.

3.4 Analysis of Results

Further analysis was required to quantify the effectiveness of the static port venting. It had been found that static porting substantially reduced errors. The maximum error displayed by an individual reading, without the static inlet port, was –393 feet, compared to the maximum error with the static inlet port of 221 feet (a reduction of 44%).

Figure 3.11 shows the average error observed from 4 different equipment configurations.

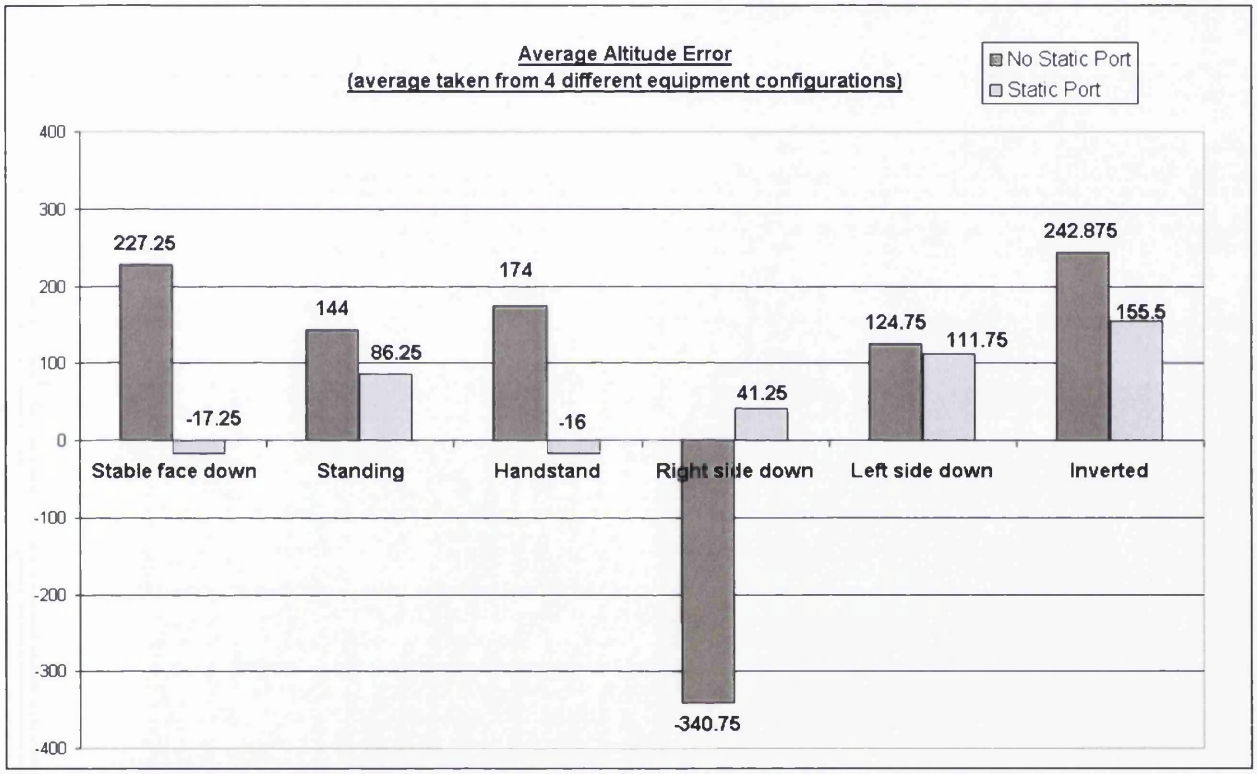

Figure 3.11: Average Altitude Error with and without static inlet porting.

Both maximum errors resulted from the Bergen without oxygen or weapon fitted configuration. A comparison was made of the results from different equipment configurations (see Figure 3.12). Although several individual results show greater error with the static inlet ports present, the graphs demonstrate the general reduction of altitude error with static inlet porting.

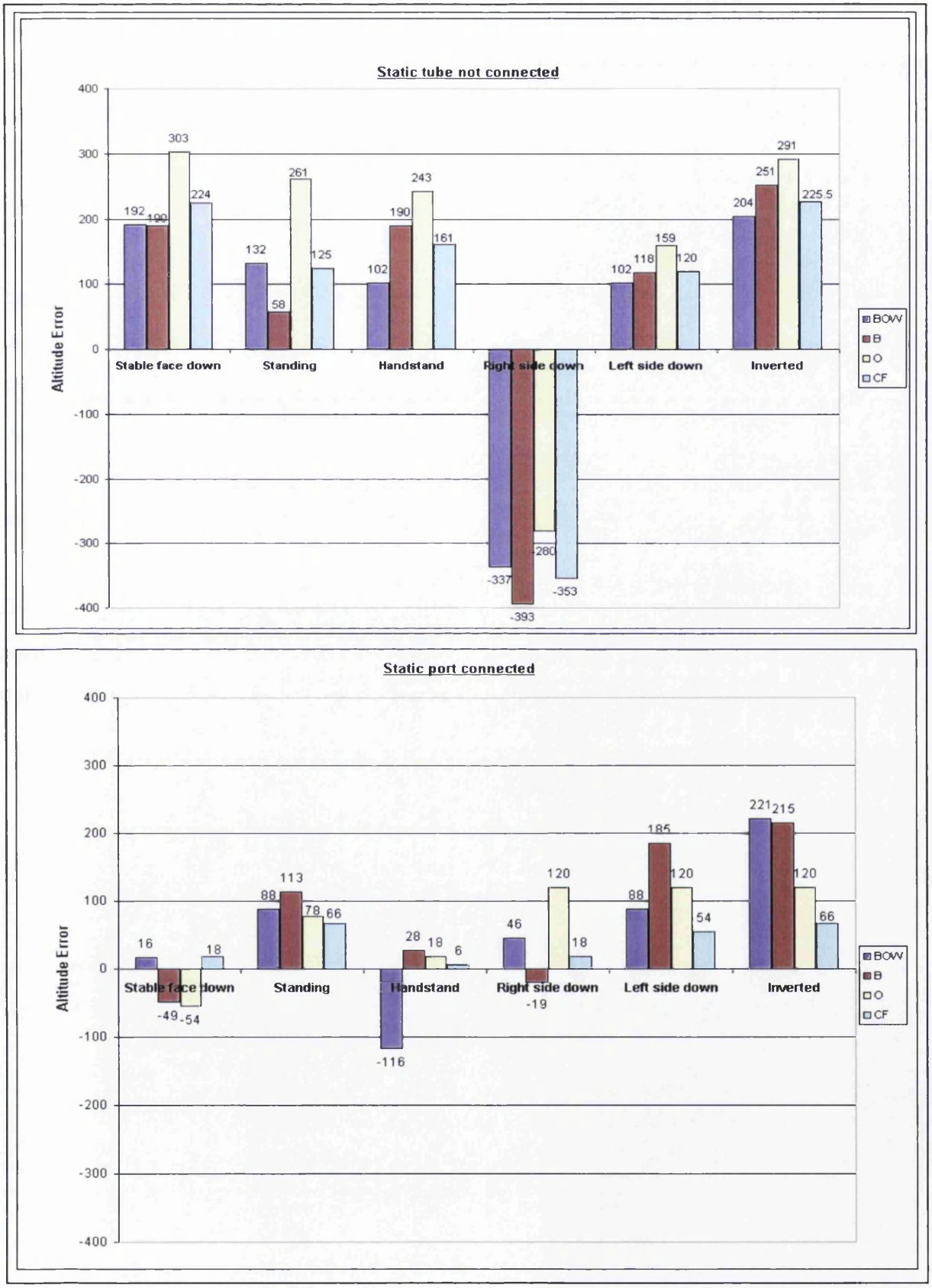

Figure 3.12: Graphs showing comparison of results with and without the static porting tube.

Due to the nature of the wind tunnel and the equipment worn it was necessary for two assistants to hold the parachutist in the assigned positions. This procedure also helped the parachutist stay in the middle of the airflow. However, the presence of the assistants could contribute to errors observed in the results if, for example, they caused a disturbance in the airflow or covered a static port inlet during their activities.

Figure 3.13 tabulates the results of the wind tunnel trial. The shaded boxes highlight unusual pressure variations observed from the output data. The percentage difference between static port and no static port is also shown. The percentages shown in italics highlight the runs where static porting actually increases the error. This may be due to the assistants coving an inlet, particularly the shoulder inlet, accidentally during certain positions.

The easiest and most natural position to adopt during freefall is the stable face down position (stomach towards the ground). It is encouraging to see that in all runs in the stable face down position, there is a high percentage improvement in accuracy.

	Static Tube not connected	Static Tube connected	
	Av. Run 1&11	Run 12	
Position	**CF**	**CF**	**% Improvement in accuracy**
Stable face down	224	18	91.96429
Standing	125	66	47.2
Handstand	161	6	96.27329
Right side down	-353	18	94.90085
Left side down	120	54	55
Inverted	225.5	66	70.73171

Run 12, left side down, showed an anomalous change in pressure on the graph. An average was taken.

	Static Tube not connected	Static Tube connected	
	Run 8	Run 9	
	O	O	**% Improvement in accuracy**
Stable face down	303	-54	82.17822
Standing	261	78	70.11494
Handstand	243	18	92.59259
Right side down	-280	120	57.14286
Left side down	159	120	24.5283
Inverted	291	120	58.76289

Run 9, handstand, showed an anomalous change in pressure on the graph. An average was taken.

	Static Tube not connected	Static Tube connected	
	Run 6	Run 7	
	B	B	**% Improvement in accuracy**
Stable face down	190	-49	74.21053
Standing	58	113	*-94.8276*
Handstand	190	28	85.26316
Right side down	-393	-19	95.16539
Left side down	118	185	*-56.7797*
Inverted	251	215	14.34263

	Static Tube not connected	Static Tube connected	
	Run 4	Run 5	
	BOW	BOW	**% Improvement in accuracy**
Stable face down	192	16	91.66667
Standing	132	88	33.33333
Handstand	102	-116	*-13.7255*
Right side down	-337	46	86.35015
Left side down	102	88	13.72549
Inverted	204	221	*-8.33333*

Average % Improvement in Accuracy: 48.4 %

Figure 3.13: Altitude error results, showing percentage difference between static port and no static port.

Average of all Static Port altitude error results = 80.1 feet

Average of all no static port altitude error results = 208.9 feet

Percentage difference = 61.7 %

Error resulting from a change in body position (attitude) was combined to show the effect of spinning or tumbling on the pressure data. Two examples are shown in Figure 3.14. The table below shows the combination of body positions that make up the movement.

Back loop with full turn:		**Front somersault:**	
Position number	**Position**	**Position number**	**Position**
1	Stable	1	Stable
2	RS down	2	Headstand
3	Inverted	3	Inverted
4	Standing	4	Standing
5	Stable	5	Stable
6	LS down		
7	Inverted		
8	Headstand		
9	Stable		

Table 3.2: Combination of body positions resulting in parachutist manoeuvre

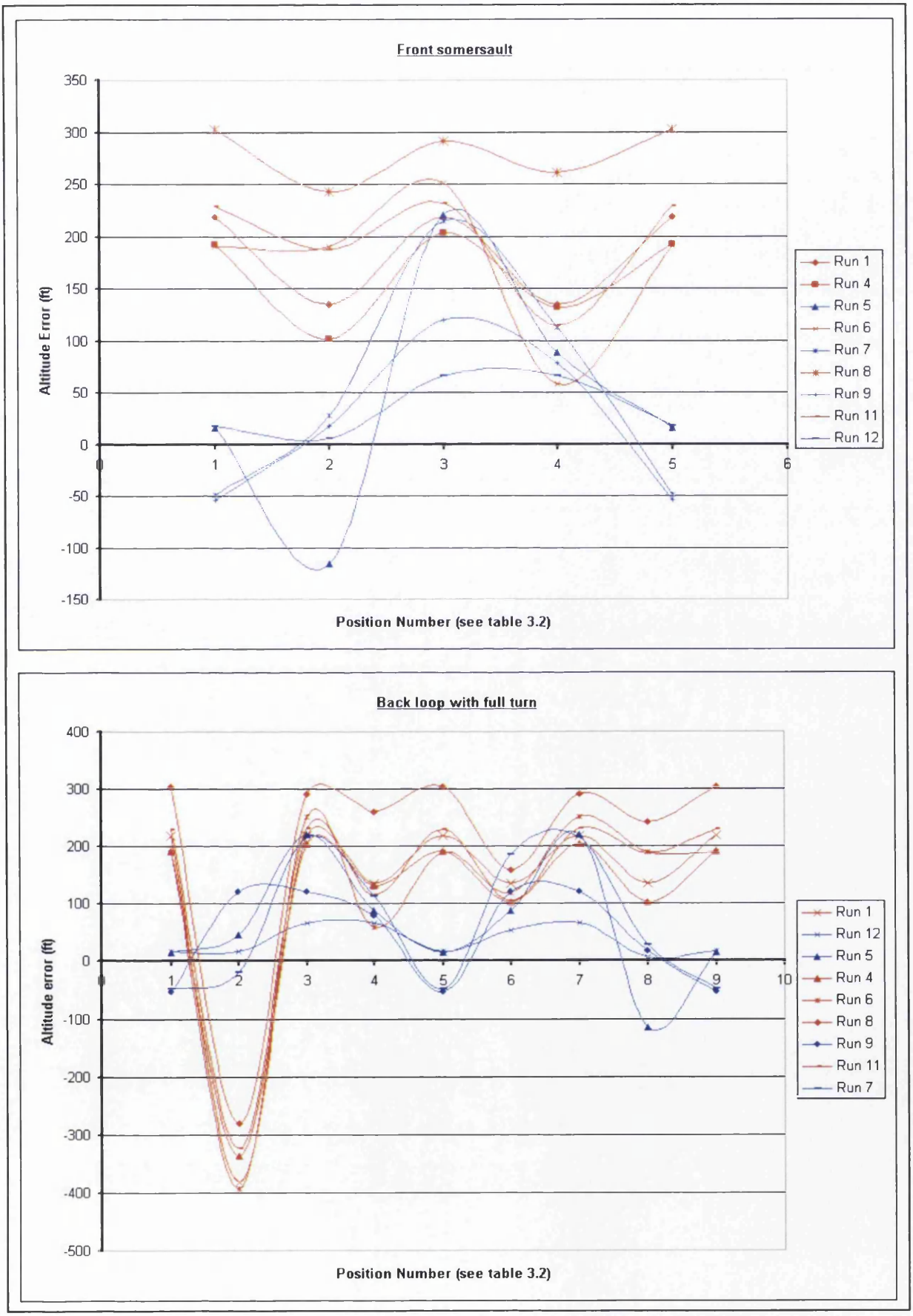

Figure 3.14: Error resulting from changing body position.

The graphs in Figure 3.14 show the altitude error over a change in body position. It is observed that the runs without a static port fitted, have a consistently higher altitude error than those without the static port. The back loop with full turn gives a maximum error of 393 feet, compared to 221 feet resulting from the static port. This gives a 44% improvement. The somersault results in a smaller error due to the free faller not turning onto his side. The right side down position displays the largest altitude error. The maximum error without the static port is 303 feet compared to 221 feet with the static port, resulting with a 27% improvement.

4.1 Conclusions

An analysis study has been carried out in this section, to quantify effect of static inlet porting. It is concluded that static inlet porting produces an average of 45% attenuation of the pressure signal. This average was taken from the improvement in results recorded both statically and dynamically and reported in this study.

Chapter 4 - Choked Static Port Venting

4.1 Introduction

Work has been carried out in the previous chapter, investigating the use of static inlet porting that takes an average of two pressure readings from around the body. This reduces the effects of changing body position and hence attenuates the low frequency noise. The actual effect of static porting was investigated, and an average attenuation of 45% was found by using static inlet porting.

Work has also been conducted investigating the concept of a choked pressure inlet recorded in Chapter 2 that could be used to damp the pressure input seen by the transducer. It was found that the choked pressure inlet alone could not damp the pressure adequately without excessive lag to the static pressure measured.

This chapter is a numerical study that investigates the effect of combining the choked pressure inlet with the static porting arrangement.

4.2 Descent Data

In November 1997, a number of parachute jump trials were recorded for pressure readings in the El Centro AR2 Descents. The jumps were recorded on video QC6934A.

This pressure data was used in Chapter 2 of this study, 'Choked Damping', by applying a damping equation (Equation 2.1) to the measured pressure data to produce a damped pressure trace. The damped pressure trace was then used in the signal injection rig (IGQ TR 0005) to analyse the damping pressure error.

The video was reviewed to see if some of the worst-case traces could be eliminated. It was found that the low frequency effects seen in the graphs could not be eliminated as these results actually occurred during the live drops, and would therefore be seen to be realistic. The low frequency noise could not be eliminated, but a smaller choke arrangement is still necessary.

The volume in the pipes leading from the AAD to the static ports is 5.4119ml. A practical choke configuration was seen to be 10mm long with a 0.07mm diameter (achieved by inserting a wire into the bore of a hypodermic tube). Referring to Equation [1] in Chapter 2, this configuration resulted in a time constant of 0.2666 seconds.

4.3 Applied Damping

The damping program used in Chapter 2, was modified to include a 45% reduction for each change in pressure, to simulate the effects of static inlet porting. This had noticeable effect on the high frequency noise but not on low frequency. Equation 2.1 was then applied to the new trace, using a time constant of 0.2666 seconds. This damping substantially attenuated the low frequency noise. The resultant pressure trace is shown in Figure 4.1.

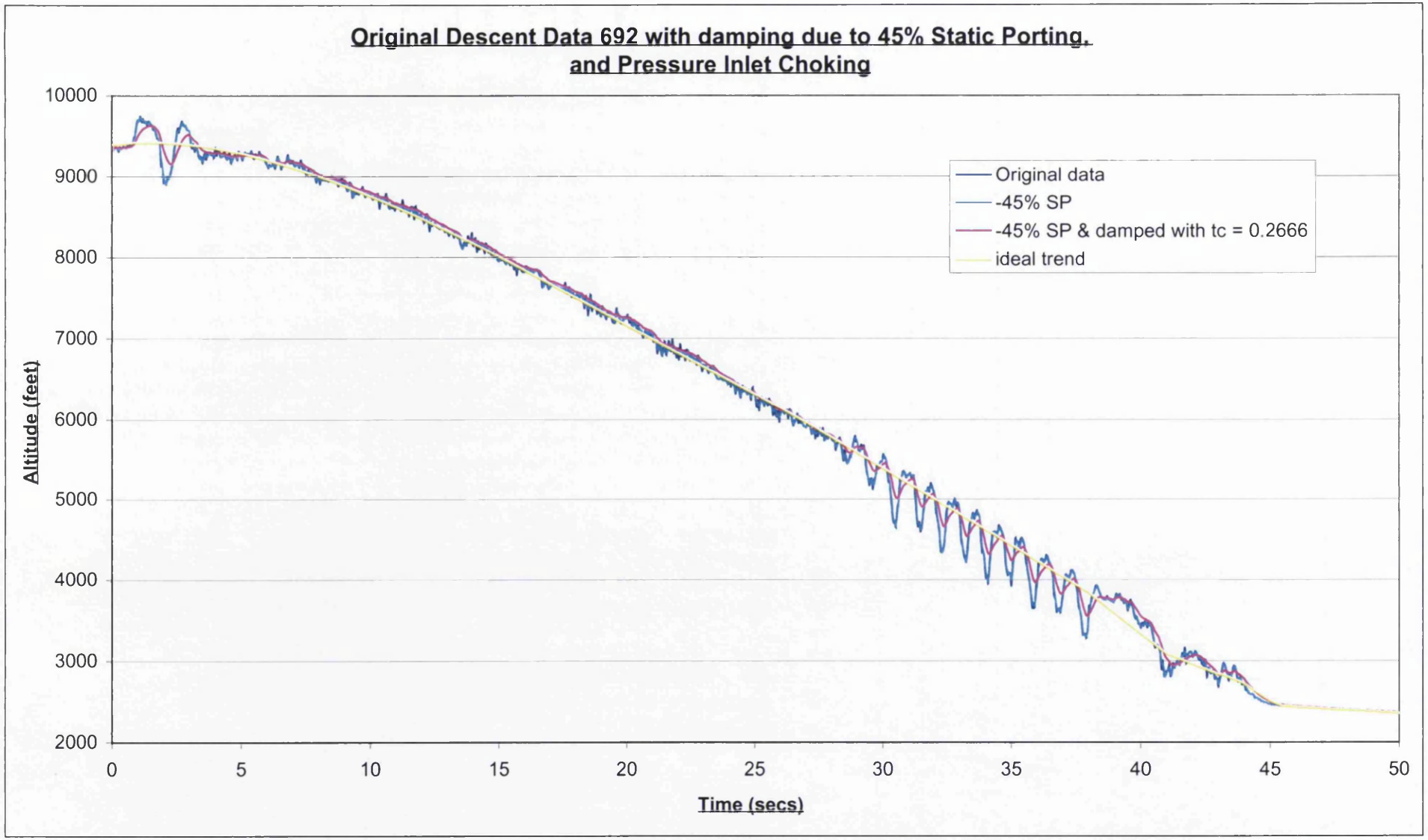

Figure 4.1: Graph showing original worst-case descent data, with damping due to static porting and pressure inlet choking.

4.4 Results

The resultant pressure trace was then tested using the signal injection rig (IGQ TR 0005) described in Chapter 2 that analysed the damping pressure error. Results are shown in Figure 4.2. It was found that the descent now incurred no error greater than 233 feet.

5.4119ml Volume, 10mm Length Choke, 0.07mm diameter

RUN No.	INJECTION FILE NAME	RUN	MAIN ACT. ALT. (ft)	RES. ACT. ALT. (ft)	MAIN ACT. Time(sec)	RES. ACT. Time(sec)	MAIN +250ft ERR	MAIN + 500ft ERR	MAIN FAIL	RESERVE +250ft ERR	RESERVE + 500ft ERR	RESERVE FAIL
1	c:\aaaa\ar2data\40ml1.pr2	r	5643	4190	39.9	47.65	143			190		
2	c:\aaaa\ar2data\40ml1.pr2	r	5696	4148	39.55	47.9	196			148		
3	c:\aaaa\ar2data\40ml1.pr2	r	5673	4149	39.7	48.95	173			149		
4	c:\aaaa\ar2data\40ml1.pr2	r	5684	4179	39.8	47.55	184			179		
5	c:\aaaa\ar2data\40ml1.pr2	r	5684	4215	39.7	47.55	184			215		
6	c:\aaaa\ar2data\40ml1.pr2	r	5684	4230	39.75	47.6	184			230		
7	c:\aaaa\ar2data\40ml1.pr2	r	5696	4148	39.7	48.9	196			148		
8	c:\aaaa\ar2data\40ml1.pr2	r	5651	4149	39.85	47.7	151			149		
9	c:\aaaa\ar2data\40ml1.pr2	r	5651	4201	39.9	47.7	151			201		
10	c:\aaaa\ar2data\40ml1.pr2	r	5692	4233	39.45	47.75	192			233		

Figure 4.2: Signal Injection Test Results, tc = 0.2666 seconds.

Figure 4.1 shows an ideal trend of descent 692. It was generated to show what the ideal data recording of that descent would be. The original data, and the damped data traces were then compared to the ideal trend to find a resultant altitude error. The results in Figure 4.3 show the reduction in error due to static inlet porting and the choke arrangement.

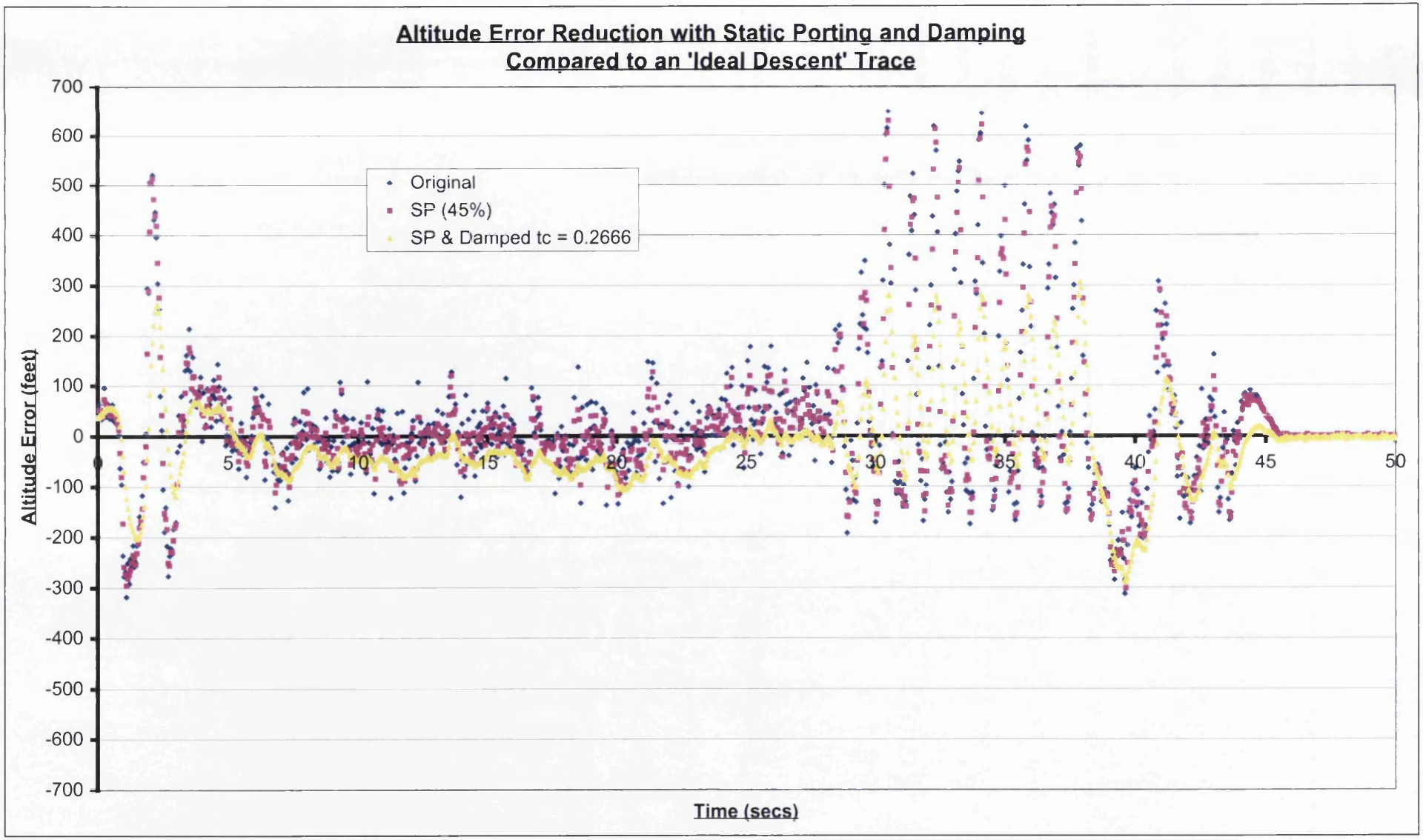

Figure 4.3: Altitude error reduction with static porting and damping using a time constant of 0.2666 seconds.

4.5 Conclusions

An investigation has been carried out to see if a choked pressure inlet with the use of static inlet porting, could be used to damp the erratic inlet pressure that is read by the pressure transducer in the AAD. Work has been carried out to determine the effect of static porting, and the volumes of the choke and chamber that will attenuate the readings sufficiently.

It was found that the static inlet porting results in a 45% error reduction that may be used with a 10mm long, 0.07mm diameter choke with a 5.4119 ml chamber (volume found in the static tubes), to achieve an acceptable damped pressure reading. This configuration gives a maximum error of 300 feet, where the original descent data gives an altitude error of up to 650 feet. This is an improvement of 54%.

Chapter 5 - Wind Tunnel Verification

5.1 Introduction

Work has been carried to out investigate the use of static inlet porting (GQ TR 01001), that takes an average of two pressure readings from around the body. This reduces the effects of changing body position and hence attenuates the low frequency noise. The actual effect of static porting was investigated in Chapter 3, and an average attenuation of 45% was found by using static inlet porting.

Work has also been conducted investigating the concept of a choked pressure inlet (Chapter 2) that could be used to damp the pressure input seen by the transducer. It was found that the choked pressure inlet alone could not damp the pressure adequately without excessive lag to the static pressure measured.

Furthers studies have been conducted to see if a choked pressure inlet together with the use of static inlet porting, could be used to damp the erratic inlet pressure that is read by the pressure transducer in the AAD (Chapter 4). Work was carried out to determine the effect of static porting, and the volumes of the choke and chamber that will attenuate the readings sufficiently.

Wind tunnel trials have been conducted on the choked static port configuration determined in Chapter 4, to verify its function and attenuation of the pressure signal. It was discovered while analysing the results however, that the prepared sample was miscalculated and the sample actually tested was a 13mm long, 0.98mm effective diameter choke with a 12.078ml chamber.

This chapter details the results produced by the wind tunnel tests, but further studies shall be required with a more accurate sample configuration.

5.2 Method

The purpose of the wind tunnel trial was to gather pressure data read by a choked static port assembly and then to compare the trace with an un-choked static port assembly. Noise variations were measured to compare the damping characteristics of each device using data capture equipment (as detailed in Irvin GQ document ITW 3746), including a PICO data recorder and laptop computer.

The static port assemblies were mounted together on a block with the two nozzles of each assembly facing different directions on the airflow, and the inlet nozzles of both assemblies positioned together on two perpendicular faces (see Figure 5.1). A diagram of the choke configuration used in the wind tunnel tests is shown in Figure 5.2.

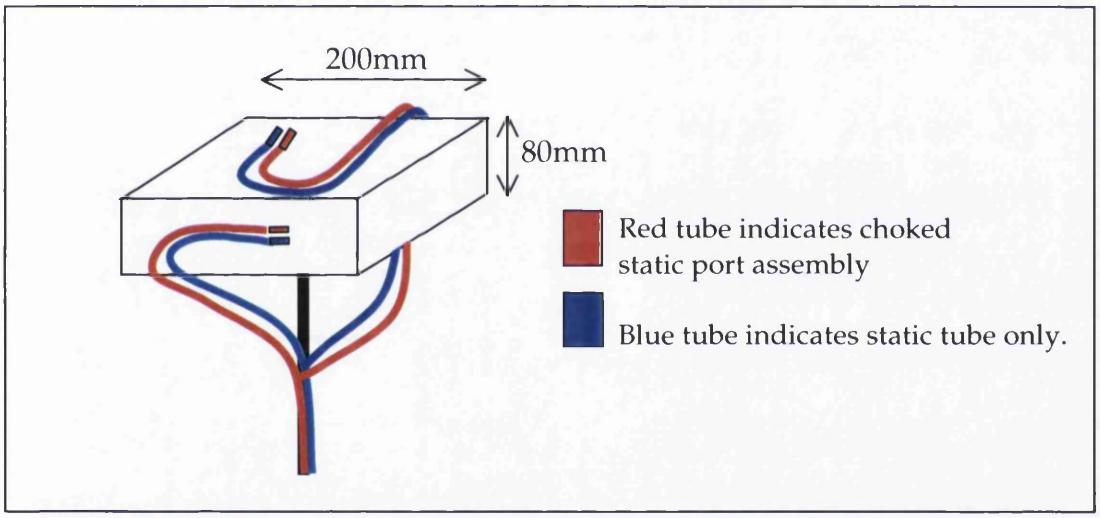

Figure 5.1: Static port assemblies as mounted on block.

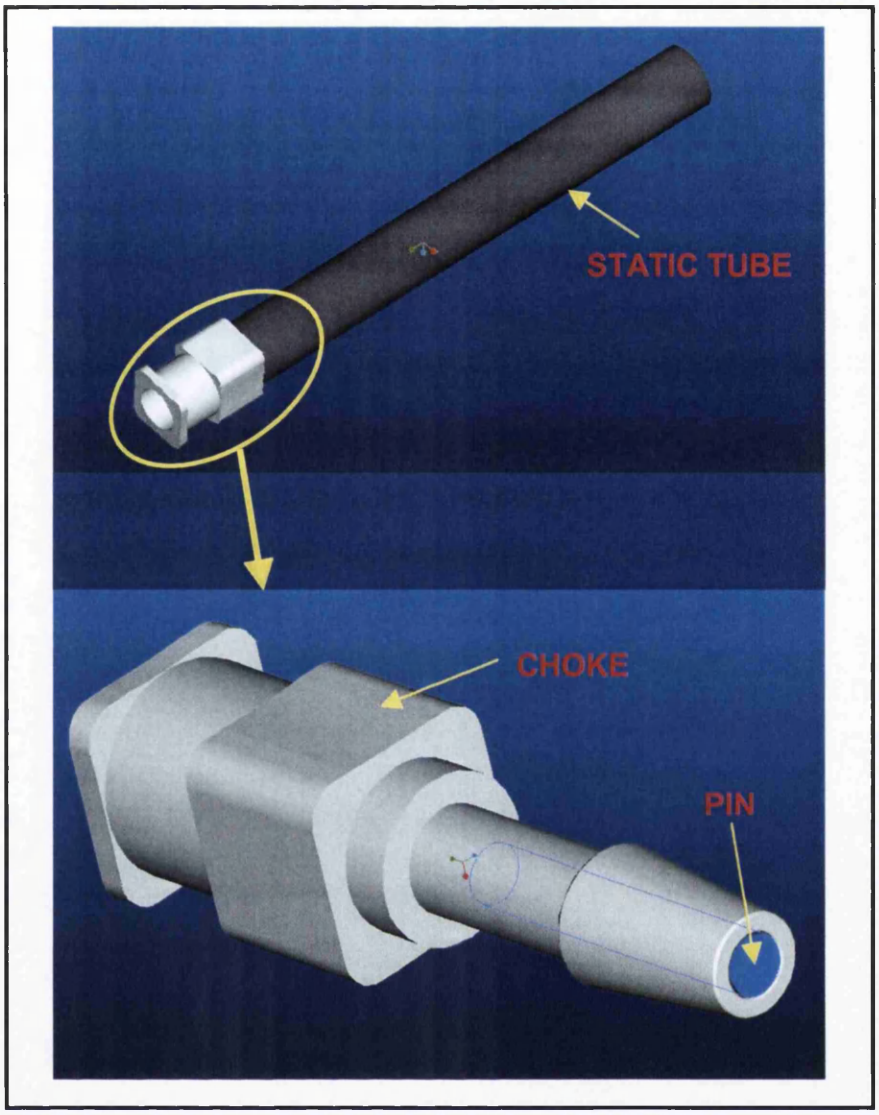

Figure 5.2: Diagram showing components of choke assembly used in wind tunnel tests.

A control tube was placed upstream of the block to measure the flow occurring at the static port tubes. An initial test was recorded before the wind tunnel was turned on to check the operation of the pressure sensors. Placing a baffle upstream of the block generated a disturbed airflow that helped to demonstrate a noisy input. Tests were conducted with the block in four different orientations, for static tests in clean and disturbed airflow. Figures 5.3 – 5.6 show the block in the wind tunnel, set in the four orientations. Direction of airflow is left to right.

The PICO data recorder was set to measure the pressure every 5 milliseconds (200Hz), to run for 60 seconds. The recording was started with the tunnel turned off and then

recorded as the tunnel started up to approximately 35 m/s, running for about twenty seconds and then shutting off.

Dynamic tests were then conducted by rotating the block slowly about the attachment pillar, while the tunnel was turned on and run for two minutes. The rotations were recorded on video IGQ DV034, to assist in the post-test analysis of the results.

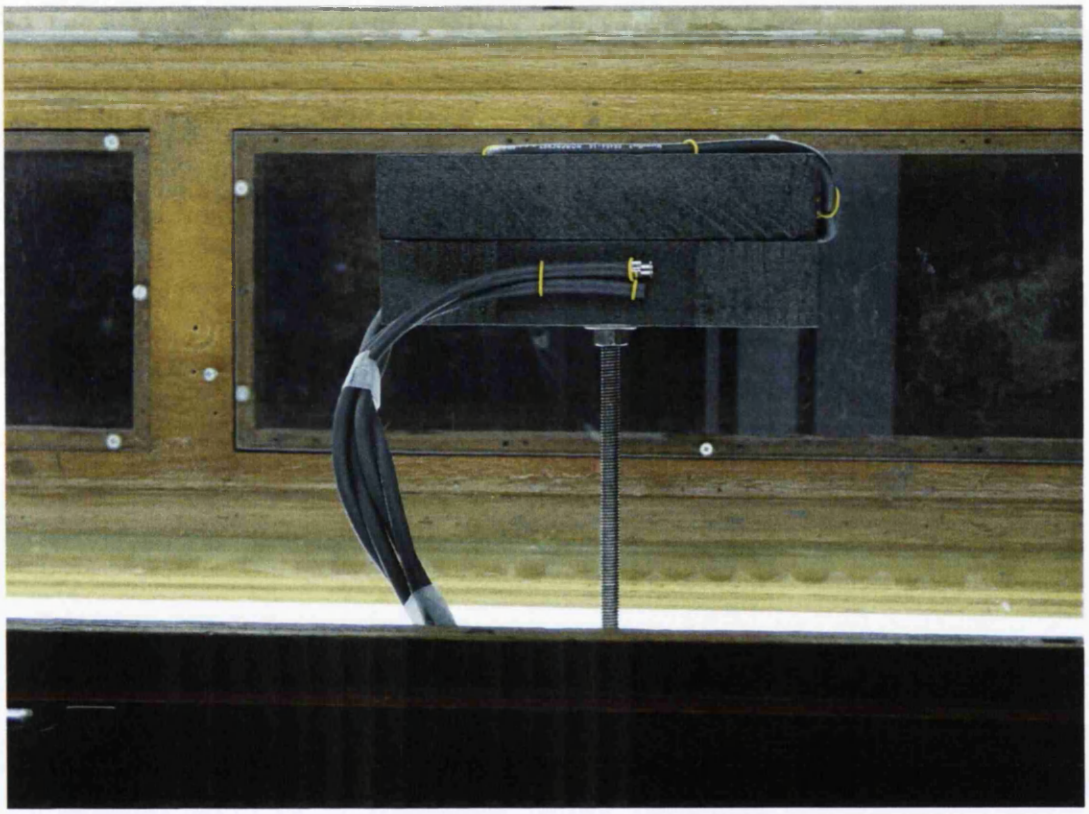

Figure 5.3: Block in Position 1

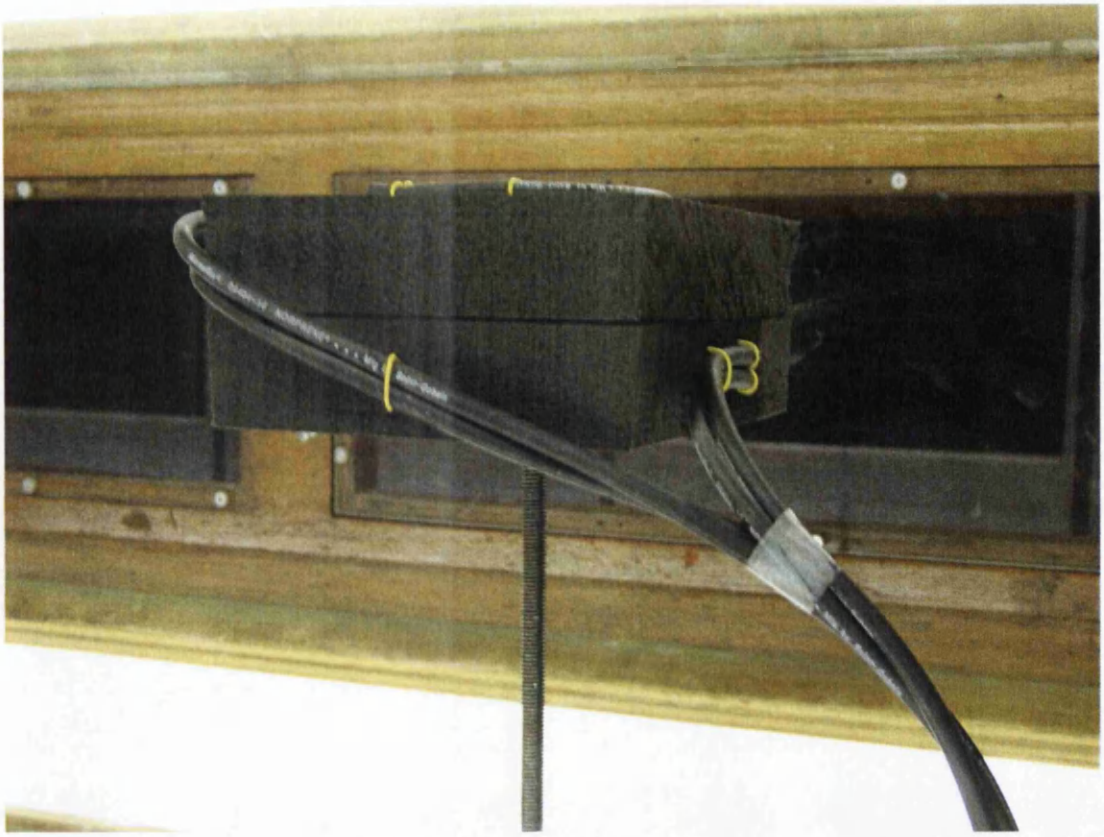

Figure 5.4: Block in Position 2

Figure 5.5: Block in Position 3

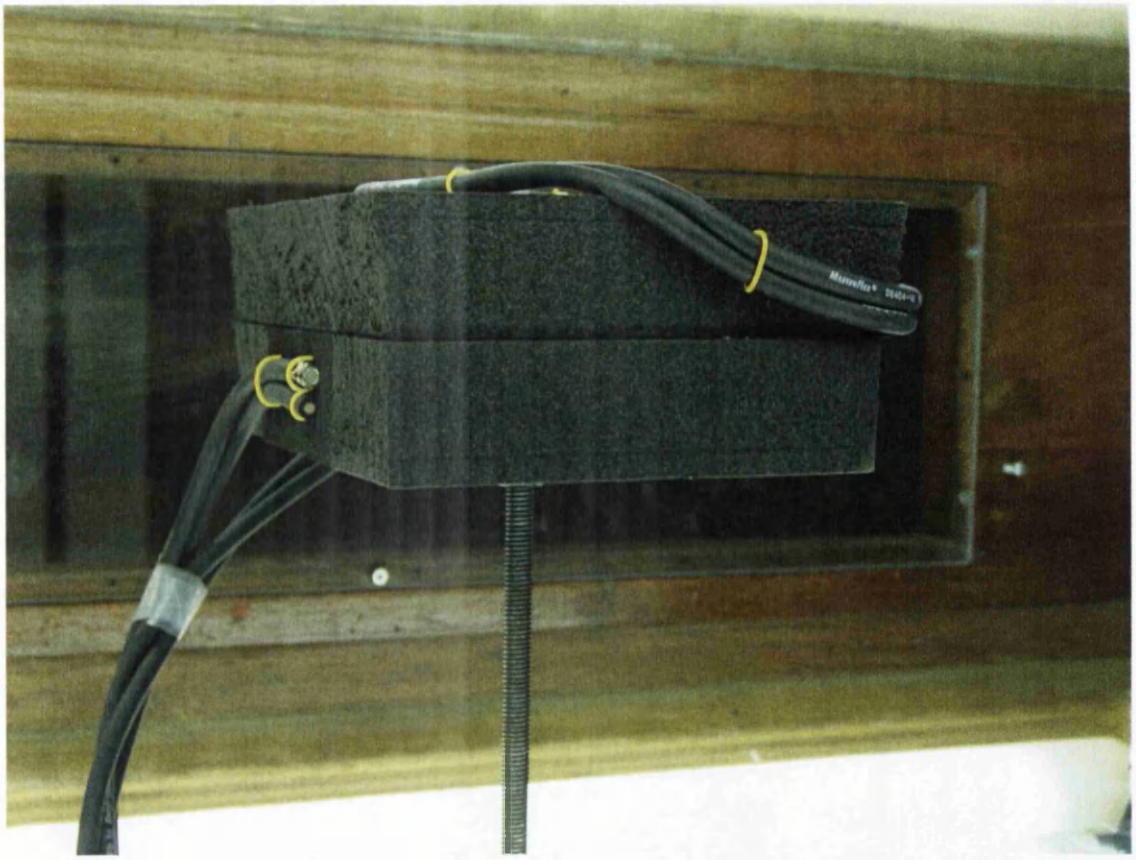

Figure 5.6: Block in Position 4

5.3 Static Results

Results from the static tests are showed in Figures 5.7 – 5.14 for clean and disturbed airflow. Each graph shows the wind tunnel starting up, running at constant/maximum speed and then running down.

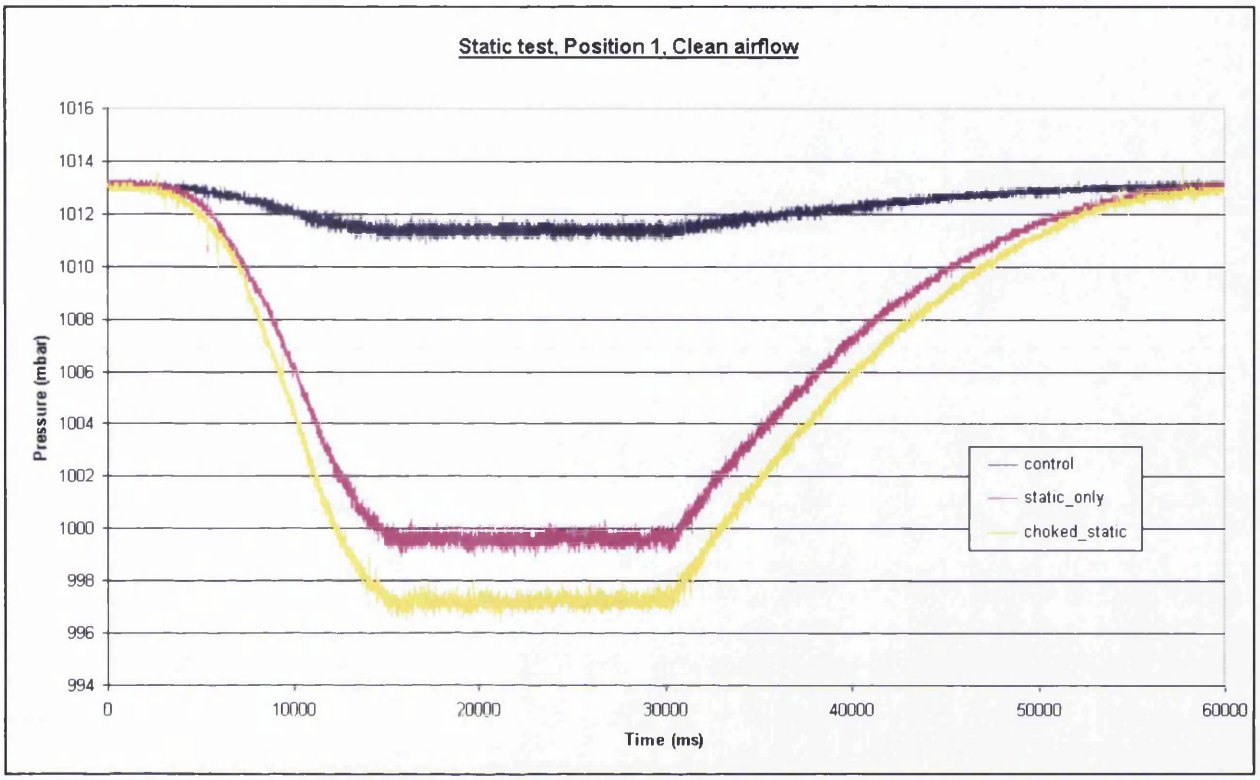

Figure 5.7: Static test position 1, clean airflow

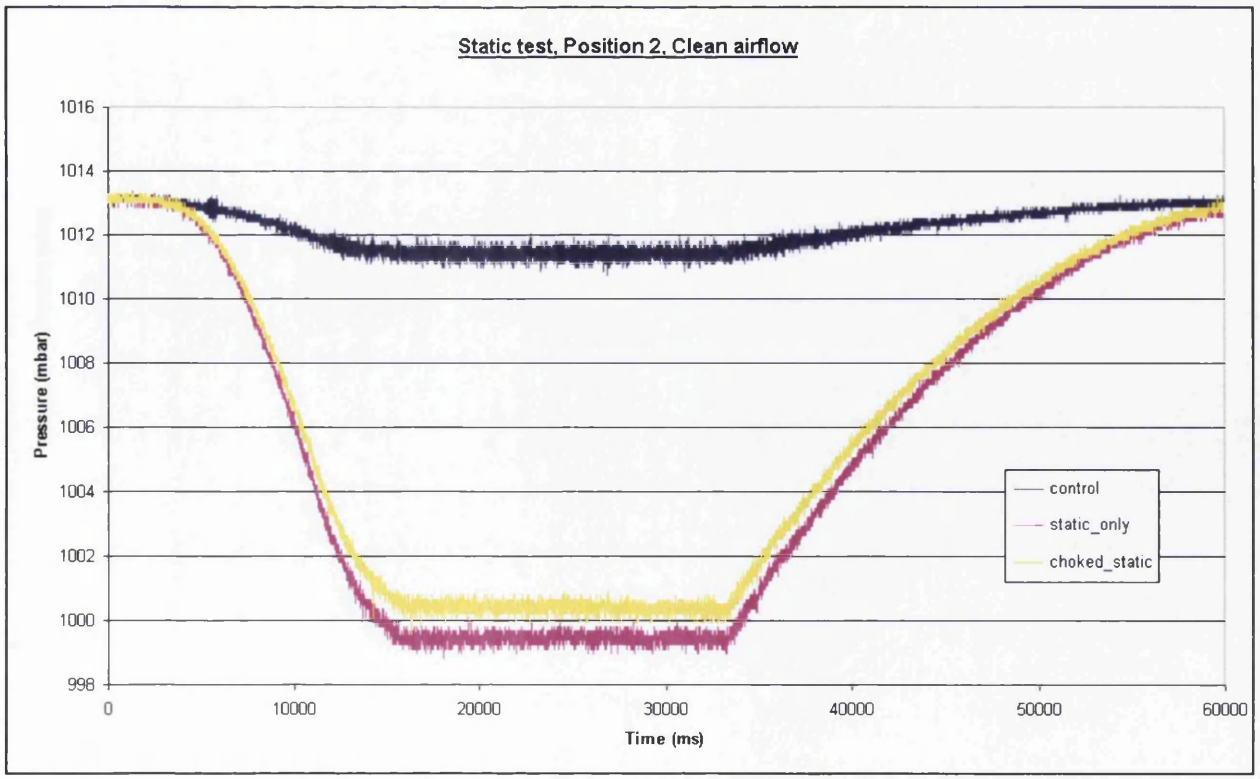

Figure 5.8: Static test position 2, clean airflow

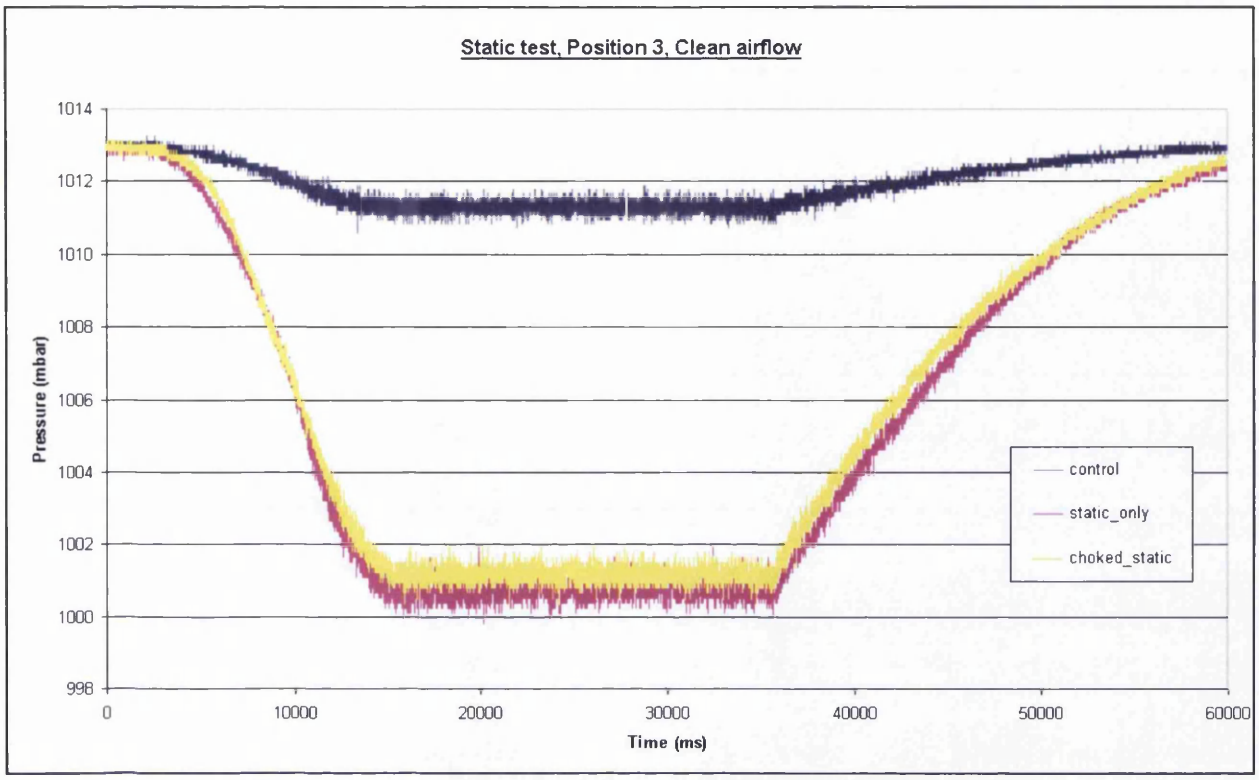

Figure 5.9: Static test position 3, clean airflow

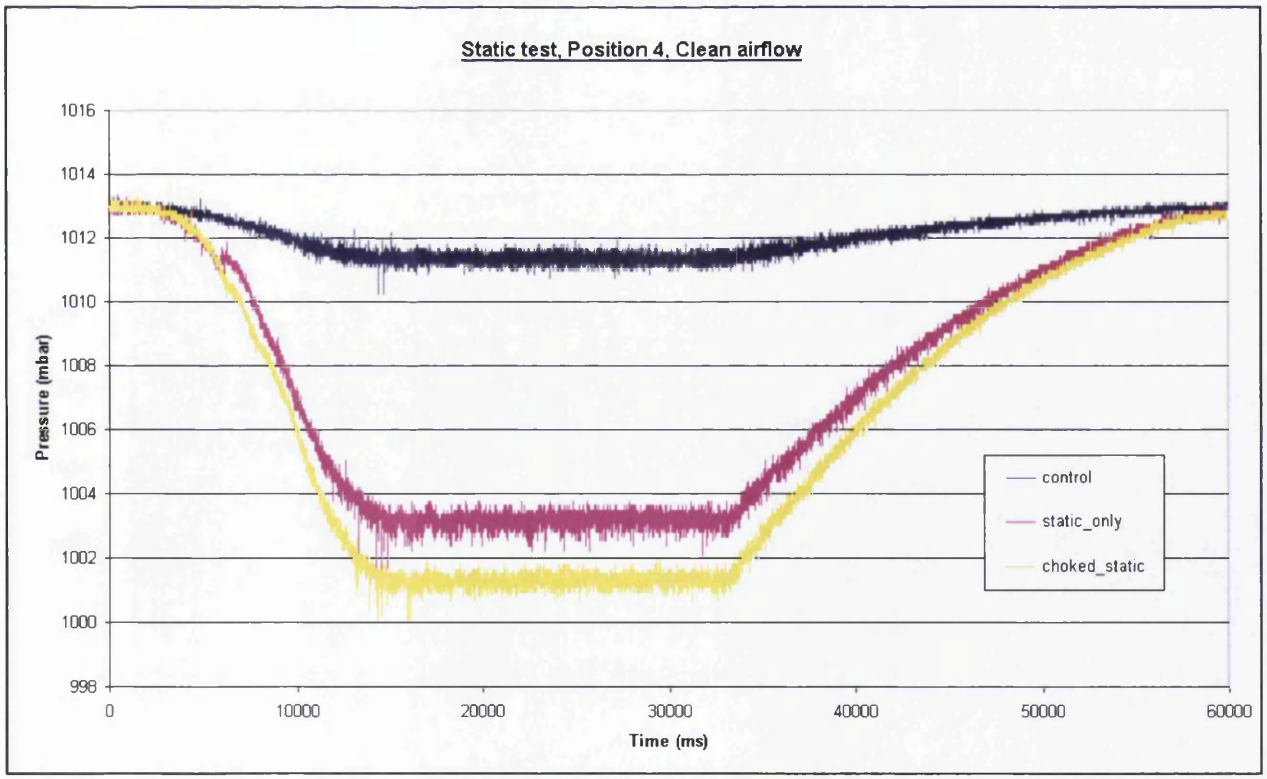

Figure 5.10: Static test position 4, clean airflow

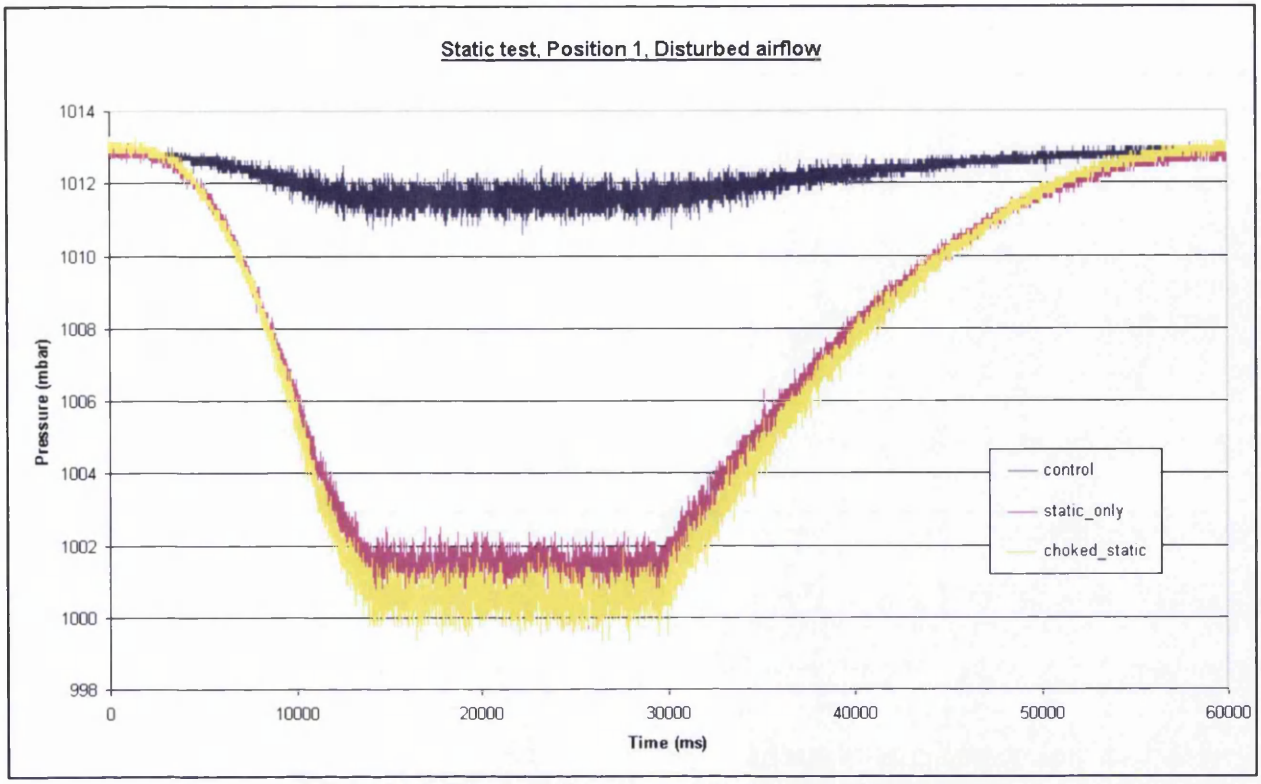

Figure 5.11: Static test position 1, disturbed airflow

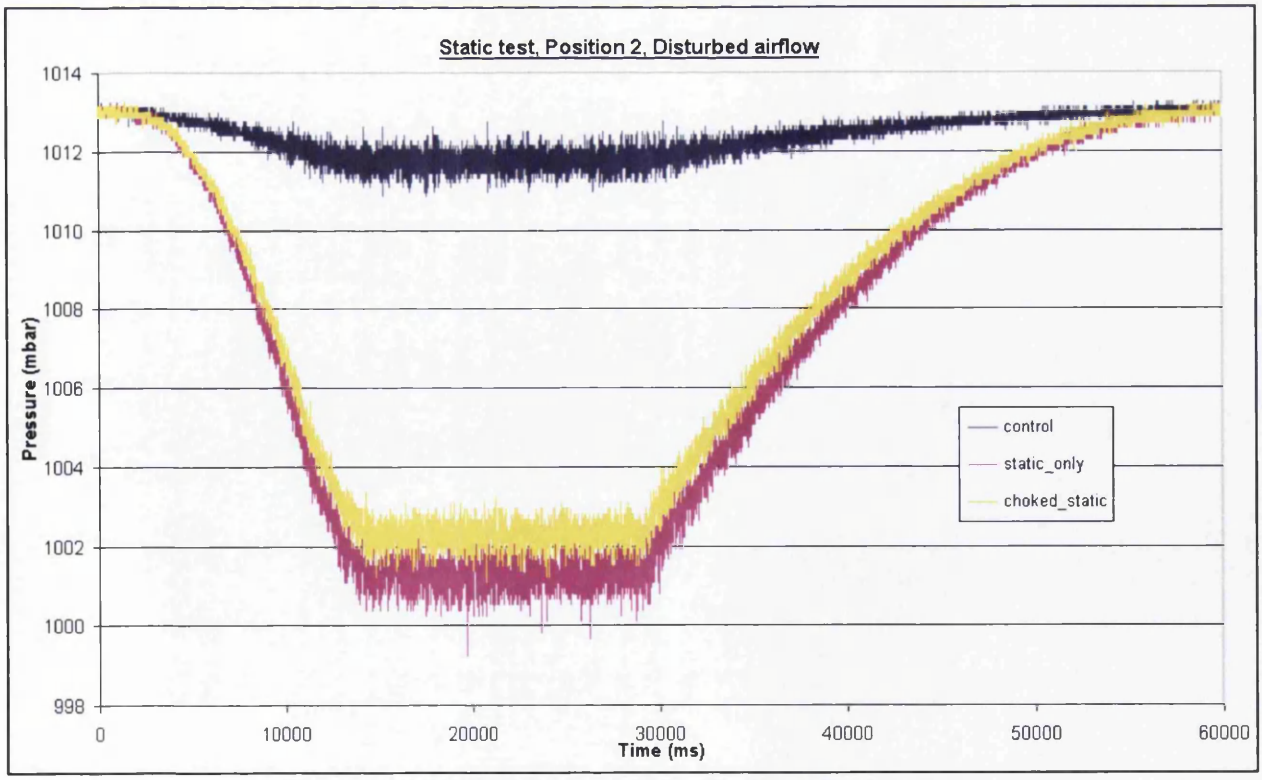

Figure 5.12: Static test position 2, disturbed airflow

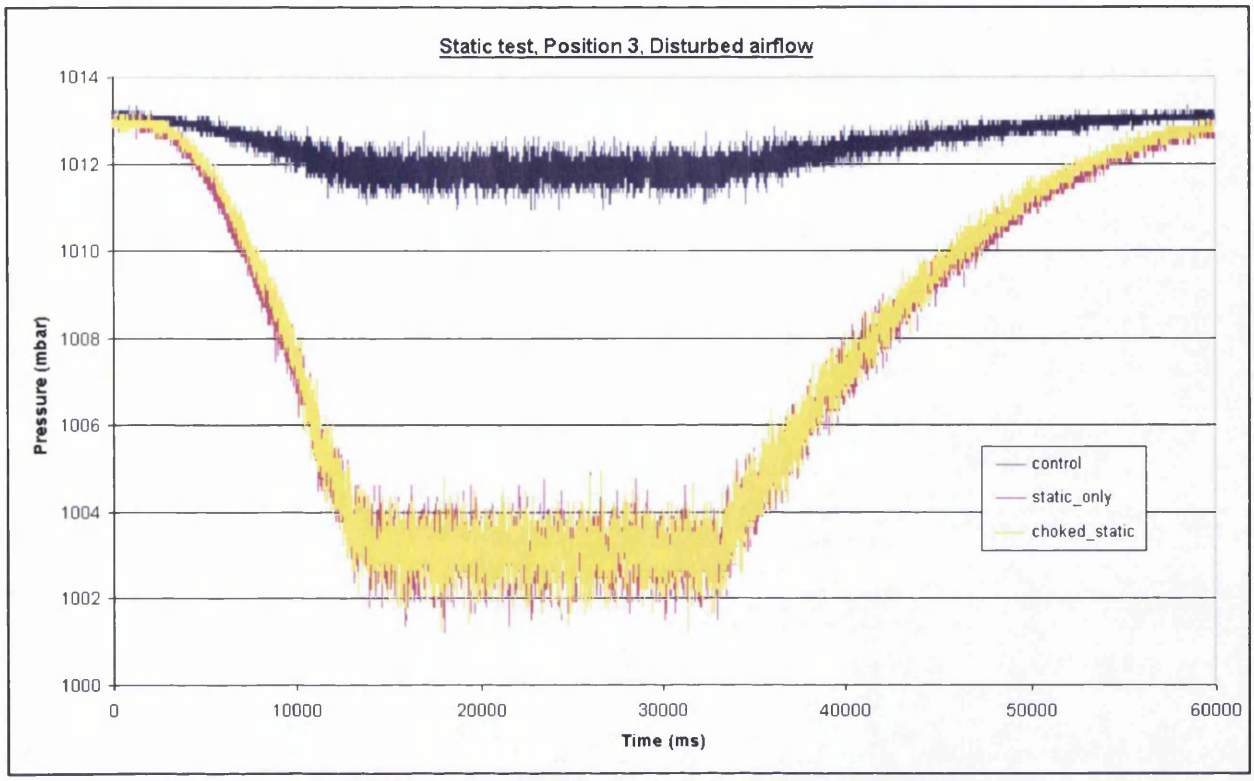

Figure 5.13: Static test position 3, disturbed airflow

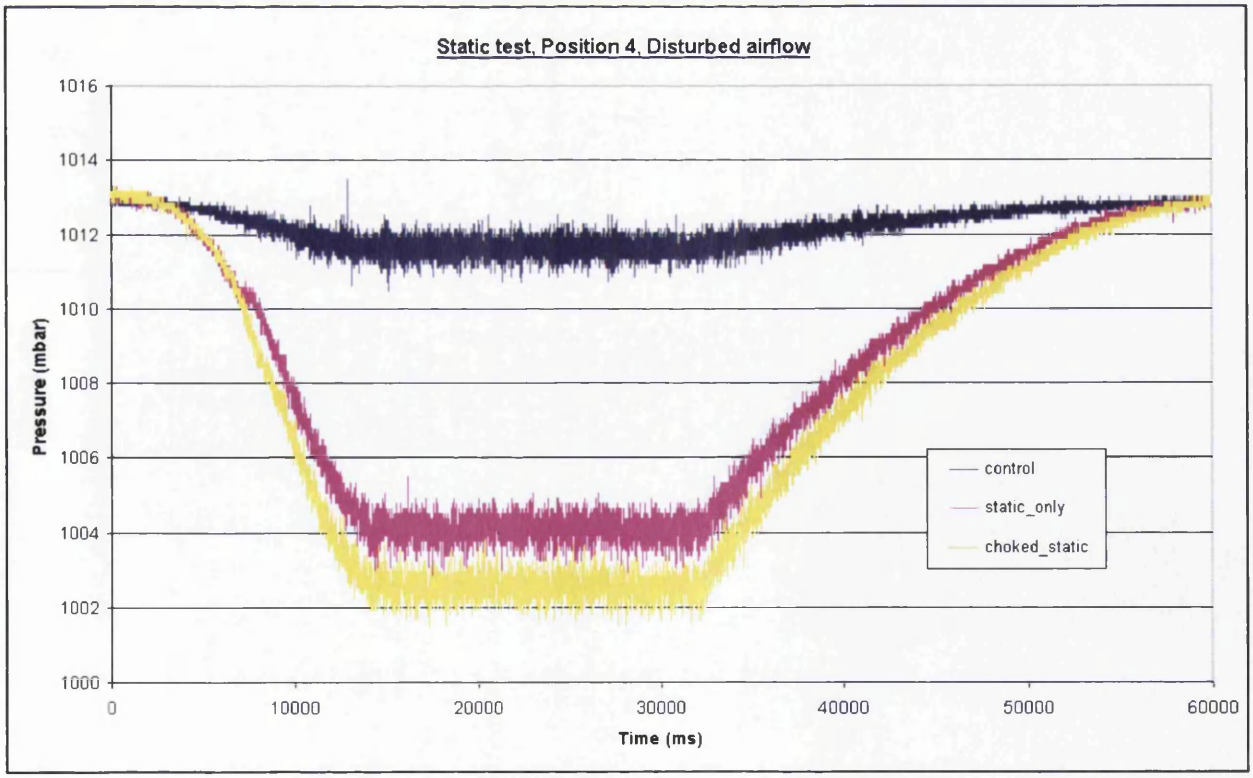

Figure 5.14: Static test position 4, disturbed airflow

5.4 Dynamic Results

Results from the dynamic tests are shown in Figures 5.15 – 5.20 for clean and disturbed airflow. The graphs show a ten point moving average along the dynamic part of the trace to simplify the data, and show a clearer display of the noise. The numbers shown in red, correlate to positions observed on the video.

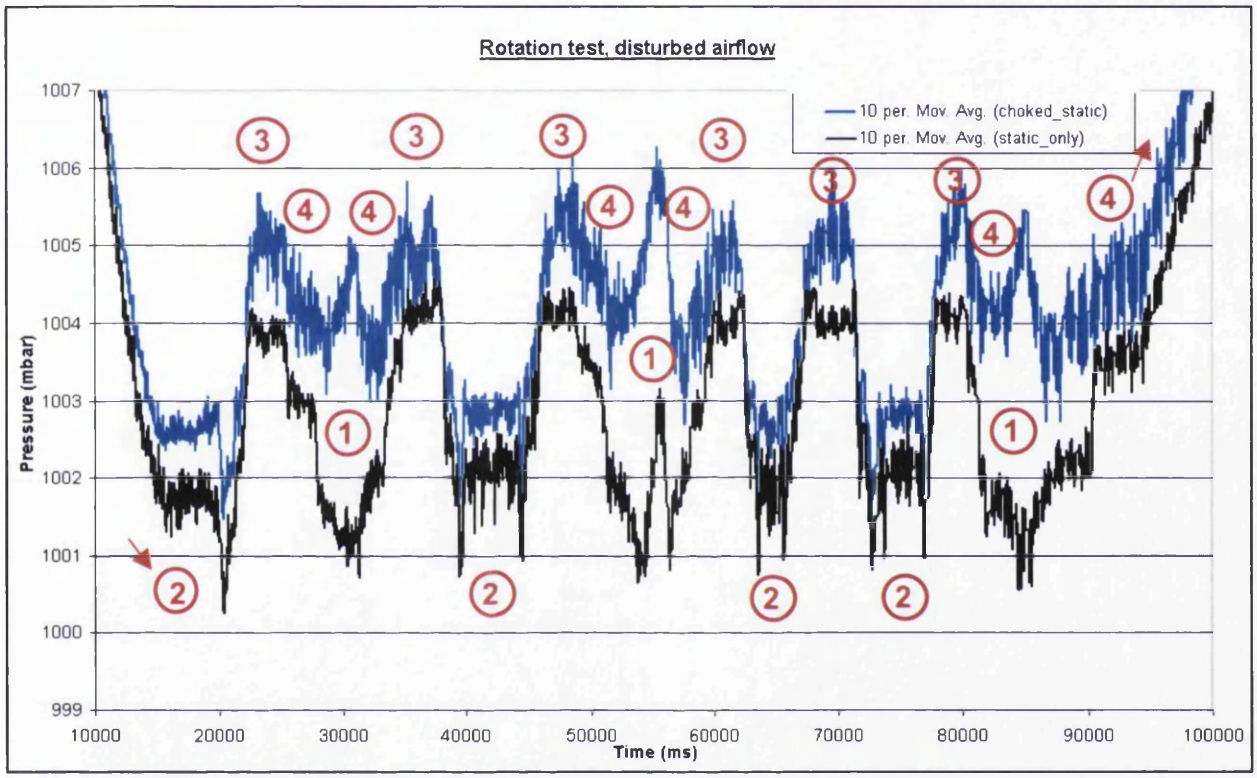

Figure 5.15: Rotation test with disturbed airflow

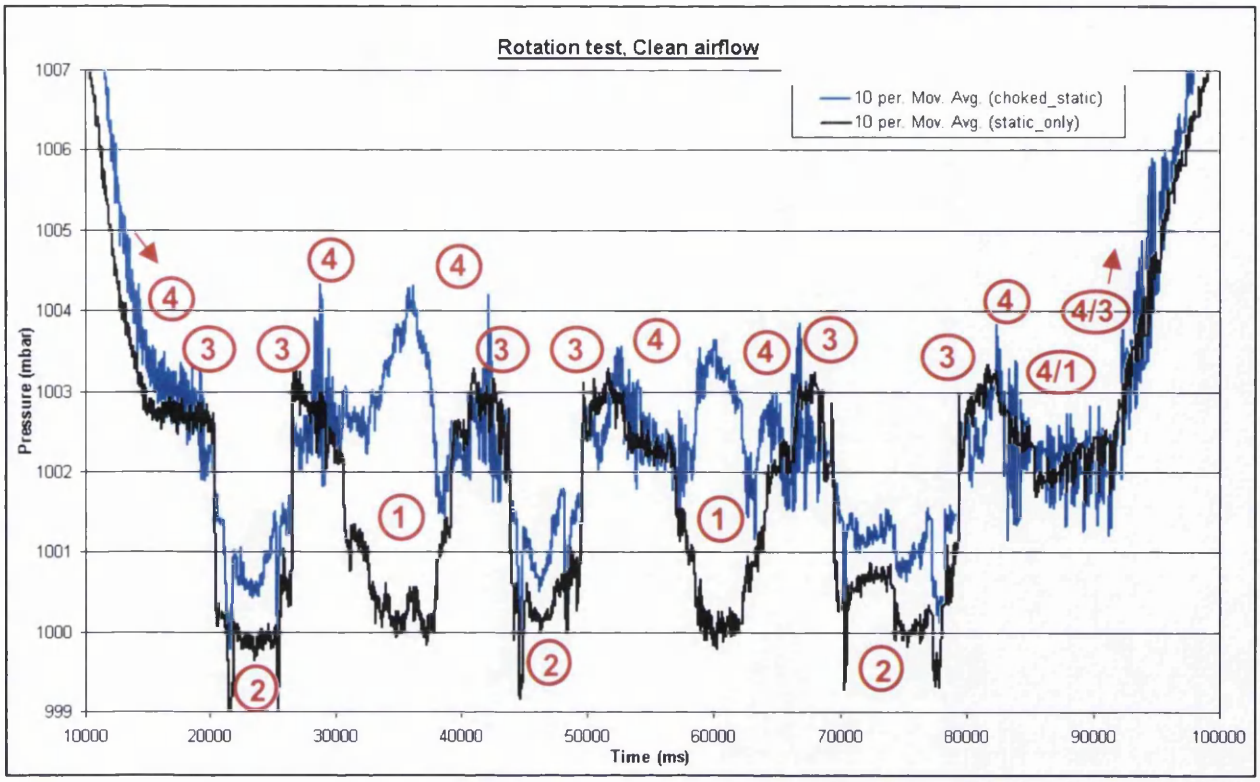

Figure 5.16: Rotation test with clean airflow

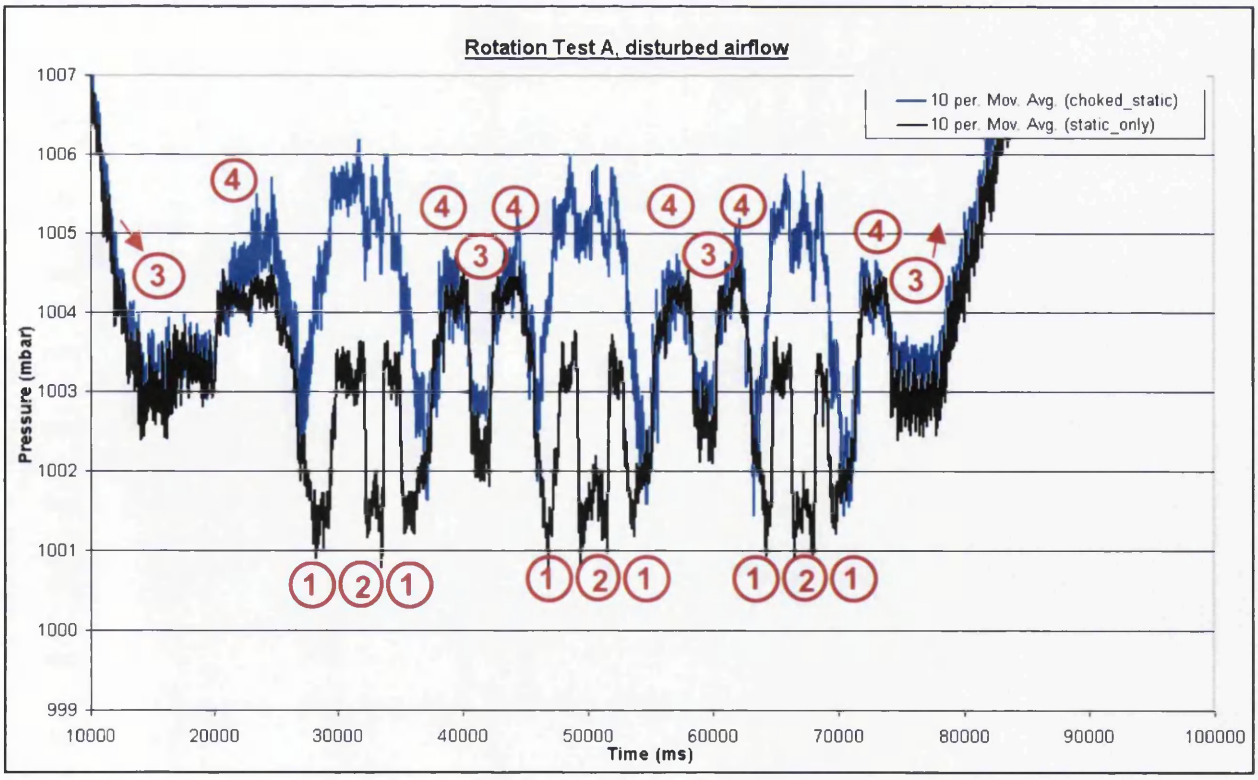

Figure 5.17: Rotation test A with disturbed airflow

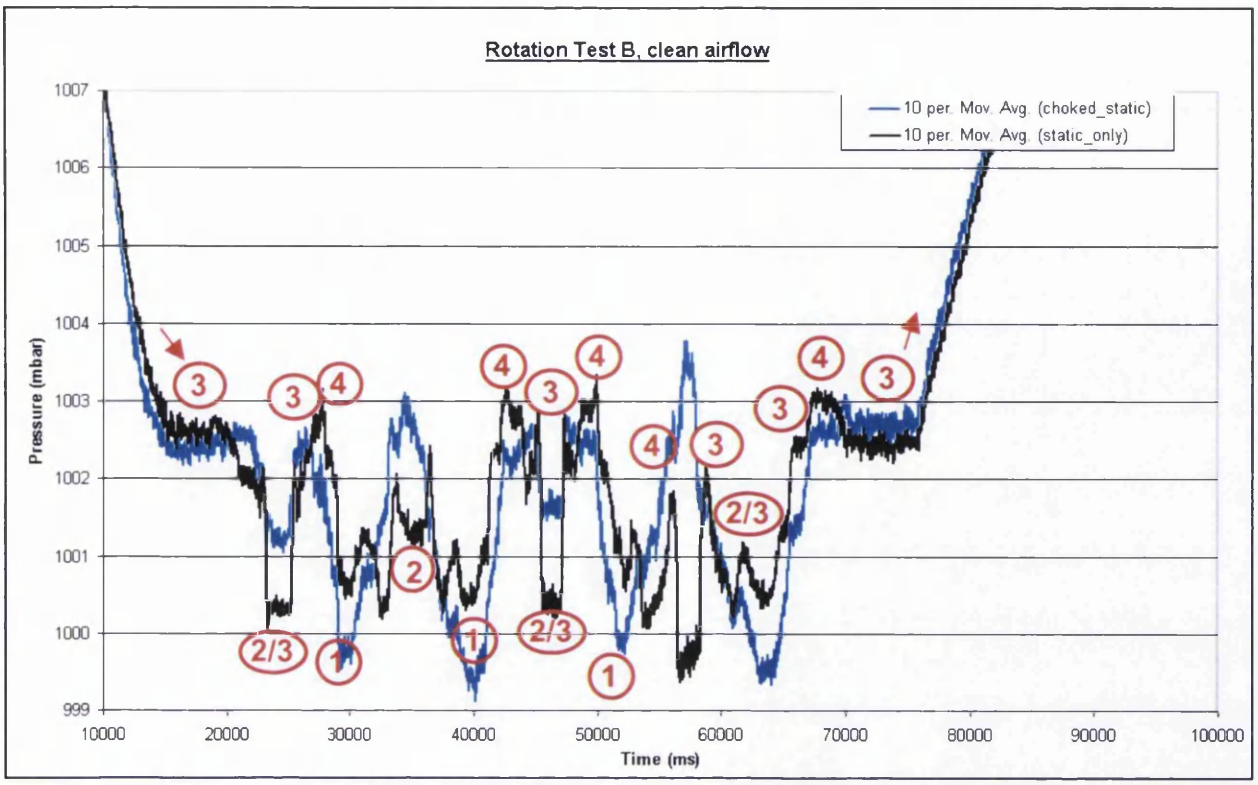

Figure 5.18: Rotation test B with clean airflow

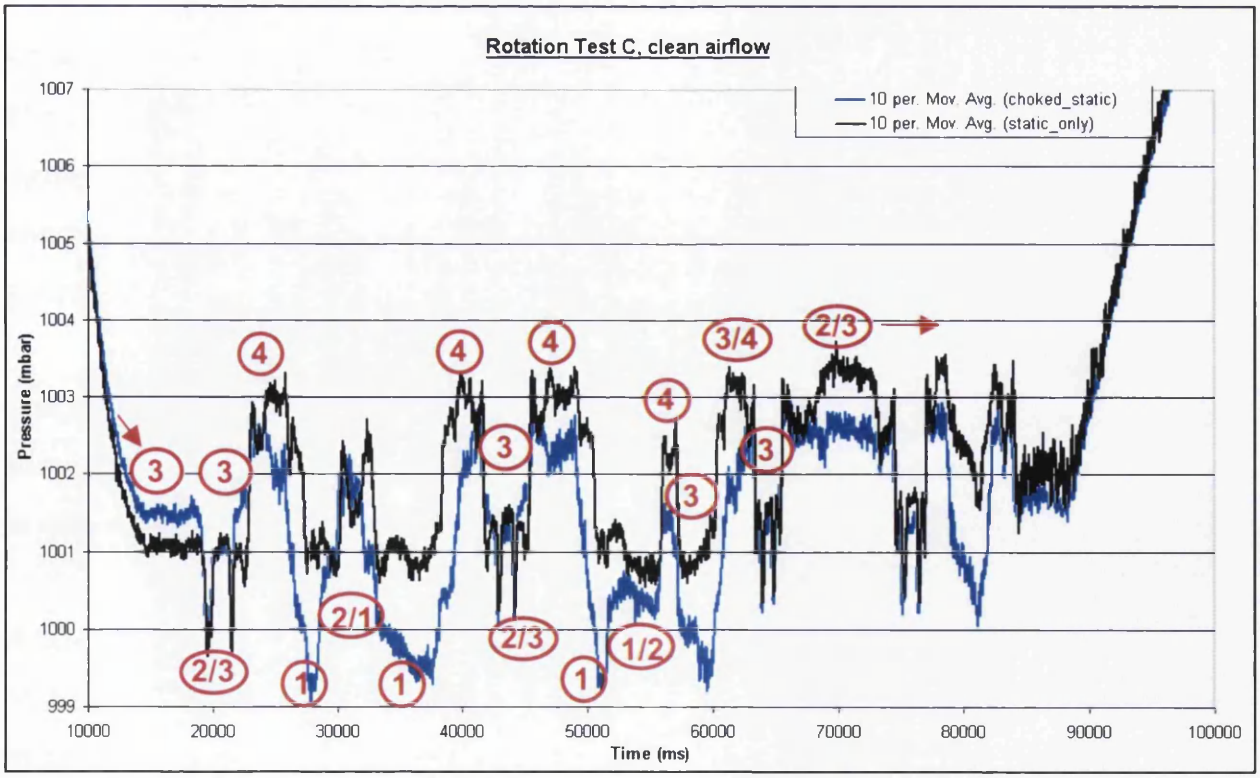

Figure 5.19: Rotation test C with clean airflow

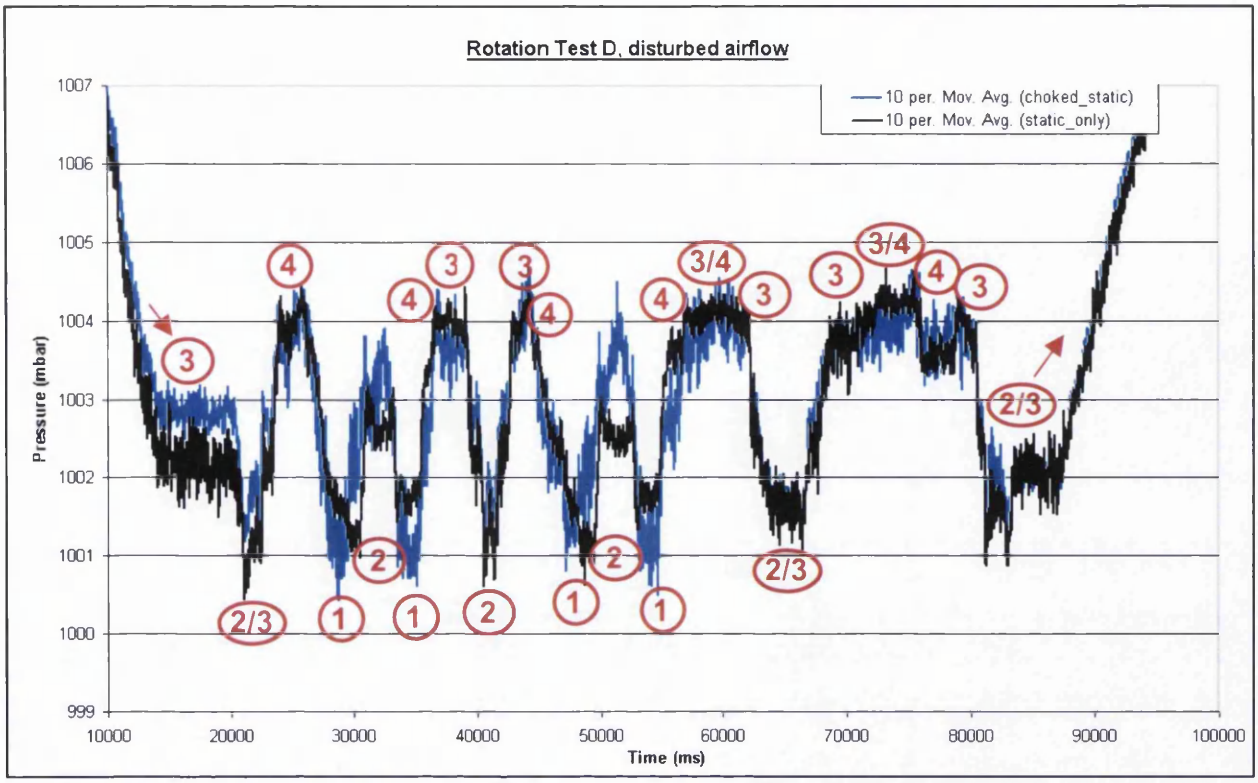

Figure 5.20: Rotation test D with disturbed airflow

5.5 Analysis of Results

The choked pressure traces recorded from the wind tunnel trials did not attenuate the signal as much as expected. Calculations and computer simulations predicted 9% attenuation from the choked static port, compared to the un-choked static port device, giving a total damping effect of 54%.

The results taken from the wind tunnel tests seem to be erratic and unpredictable. They show that in certain positions the Choked Static Port attenuates the signal quite well, but in other positions it seems to add more noise.

A 20-point moving average was taken on the static test results (figures 5.7 – 5.14) to obtain an average maximum and minimum value for each static port. These were than compared to find the damping between the two static ports, and also to compare the values to the control tube average value. (See Table 5.1)

		Static Port (SP) (mbar)			Static Port & Choke (SP&C) (mbar)		
Position	Airflow	min	Max	Average	min	max	Average
1	Clean	999.352439	999.8158537	999.58414	996.9865854	997.45	997.2182927
2	Clean	999.235294	999.6117647	999.42352	1000.229412	1000.552941	1000.391177
3	Clean	1000.48	1001.04	1000.76	1001	1001.38	1001.19
4	Clean	1002.89583	1003.40625	1003.1510	1001.041667	1001.5	1001.270834
1	Disturbed	1001.225	1001.85	1001.5375	1000.116667	1001	1000.558334
2	Disturbed	1001.09375	1001.78125	1001.4375	1002.015625	1002.640625	1002.328125
3	Disturbed	1002.56666	1003.593333	1003.08	1002.642222	1003.562222	1003.102222
4	Disturbed	1003.85416	1004.385417	1004.1197	1002.197917	1002.927083	1002.5625

Position	Airflow	Choke Attenuation (feet)	% Attenuation	Control change from ambient (mbar)	SP error compared to control (mbar)	SP&C error compared to control (mbar)	% Choke Improvement
1	Clean	0	**0**	1.597523	11.81833065	14.1841843	**-20.02**
2	Clean	1.69	**14.06**	1.592415	11.9840556	11.0164085	**8.07**
3	Clean	5.76	**32.14**	1.682223	10.557777	10.127777	**4.07**
4	Clean	1.67	**10.20**	1.647243	8.2017155	10.0819235	**-22.92**
1	Disturbed	-8.27	**-41.33**	1.409426	10.053074	11.0322405	**-9.74**
2	Disturbed	2	**9.09**	1.259016	10.303484	9.412859	**8.64**
3	Disturbed	3.41	**10.39**	1.1592	8.7608	8.738578	**0.25**
4	Disturbed	-6.33	**-37.25**	1.37218	7.508028165	9.06532	**-20.74**

Table 5.1: Extract from spreadsheet comparing average static pressures to control pressure

The % Attenuation is:

$$100 - \left(\frac{\text{Max. Static Port \& Choke value} - \text{Min. Static Port \& Choke Value}}{\text{Max. Static Port value} - \text{Min. Static Port Value}} \right) \times 100$$

The % Choke Improvement is:

$$100 - \left(\frac{\text{SP\&C error}}{\text{SP error}} \right) \times 100$$

The percentage attenuation and percentage choke improvement values indicate that positions 2 and 3 seem to attenuate the signal better than positions 1 and 4. This may be due to the nozzles in positions 2 and 3 that are facing directly into the airflow, and hence are receiving a stronger signal.

The average values obtained in Table 5.1 for each position, in both clean and disturbed airflow, were translated onto the rotation traces shown in Figures 5.15 – 5.20. The values were expected to correlate with the positions observed from the video but this was only

the case for the Static Port only trace. The Choked Static Port traces behaved in a very unpredictable manor, particularly in clean airflow. An example is shown in Figure 5.21a and 5.21b.

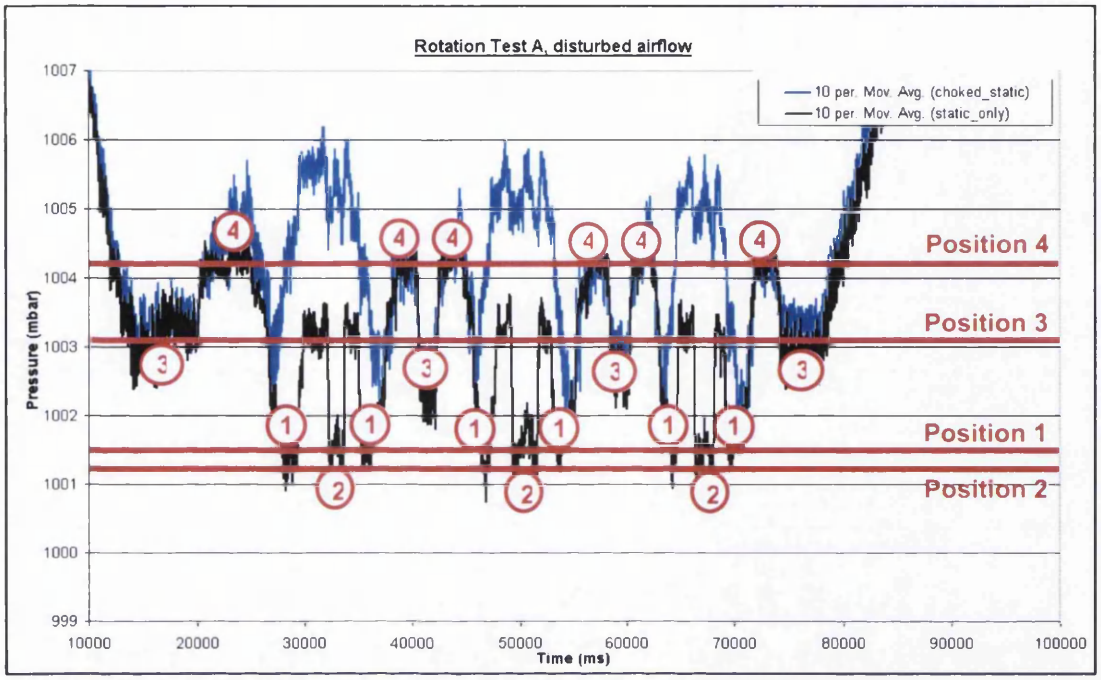

Figure 5.21a: Rotation test A with translated static position pressure values

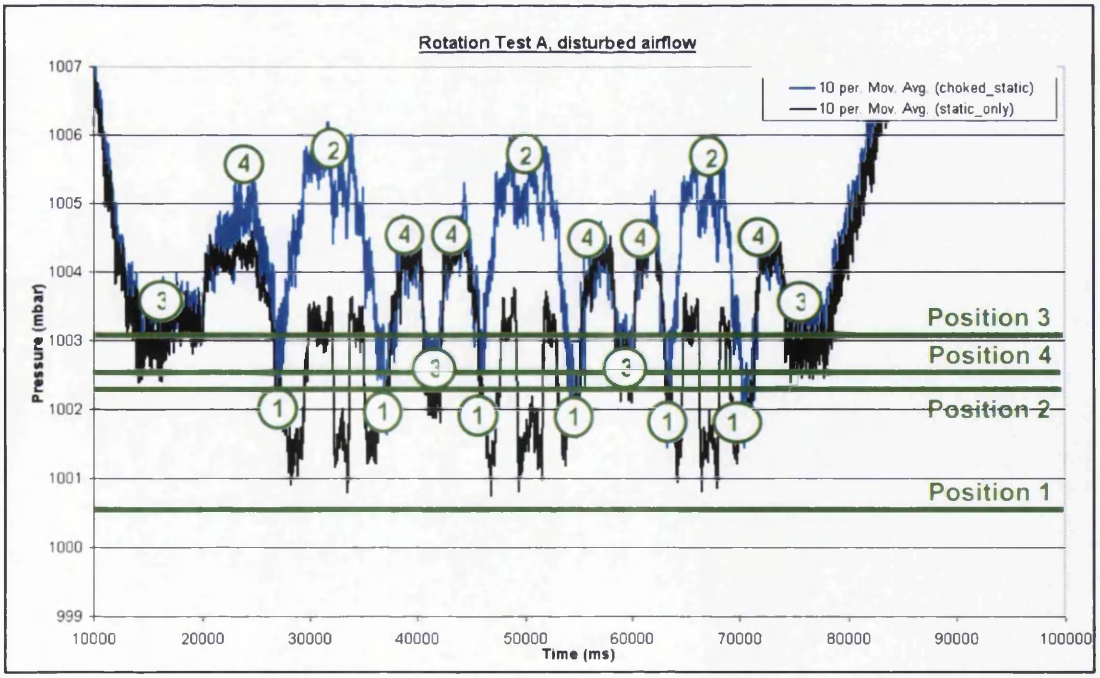

Figure 5.21b: Rotation test A with translated static port with choke position pressure values

Figures 5.21a and 5.21b show the same rotation test (test A) but Figure 5.21a describes the static port only results and 5.21b describes the results of the static port and choke configuration. The position lines 1-4 show the average pressure derived in Table 5.1 for each position in each configuration. This can then be used to compare the rotation result trace with the average static port position values.

It can be seen from Figures 5.21a and 5.21b, that the measured Static Port positions correlate quite well with the static port rotation trace, however the Choked Static Port rotation trace does not follow the choked position values, other than in position 3. This could be due to the lag offset resulting from the choke. The accuracy of position 3 values show that the choke is reading a more accurate or stronger signal in this position.

Figure 5.21b also demonstrates the attenuation at position 2. At this point the trace is nearly 3 mbars (96 feet) away from the predicted pressure value obtained in the static tests, but is closer to the control pressure value. This actually results in a noisier signal than the Static Port only trace, which is not desired, although it would indicate a stronger damping effect, as it is closer to the control value.

5.6 Conclusions

The purpose of this chapter was to verify with an experiment the calculated and simulated function of the Choked Static Port assembly as investigated in the previous chapter.

It was discovered while analysing the results, that the prepared sample had been miscalculated. Instead of the 10mm long, 0.07mm diameter choke, with a 5.4119 ml chamber volume with the predicted attenuation described in the previous chapter, the sample actually tested was a 13mm long, 0.98mm effective diameter choke with a 12.078ml chamber. Therefore the sample did not attenuate the signal as much as expected, and the resulting pressure traces were found to be unpredictable and erratic.

The orientation of the static port inlets gave a noticeable effect on the damping of the signal. Position 2 and 3, where the inlets are positioned facing direct airflow, continually gave more accurate or attenuated pressure readings. Positions 1 and 4 however, often gave a noisier output than the Static only device.

It is difficult to draw any valuable conclusions from the data collected in this trial and further studies shall be required with a more accurate sample configuration. The recommendations of this chapter are to re-visit the design of the choke configuration, and possibly trial different configurations in the wind tunnel to achieve a more valuable choked static port assembly.

Chapter 6 – Orthogonal Array Testing

6.1 Introduction

Wind tunnel trials have been conducted in the previous chapter, on the choked static port configuration, to verify its function and attenuation of the pressure signal. The sample tested did not attenuate the signal as much as expected, and the resulting pressure traces were found to be unpredictable and erratic. The orientation of the static port inlets gave a noticeable effect on the damping of the signal. Orientations where the inlets were positioned facing direct airflow, gave more accurate or attenuated pressure readings. The other positions however, often gave a noisier output with the Choked Static port compared to the Static port only device.

It was difficult to draw any valuable conclusions from the data collected in that trial. Therefore the purpose of this chapter is to re-visit the design of the choke configuration, and test different configurations in the wind tunnel using an orthogonal array technique to design an experiment that will achieve more valuable results.

6.2 Orthogonal Array Analysis

The orthogonal array technique was used to identify the optimum Pressure Inlet configuration in this thesis. The technique helped to design an experiment that would help to analyse every factor involved in the choke assembly.

The purpose of any experiment is to assess the functionality of the given product or process. The function may be affected and therefore possibly improved by any of the many characteristics it has. The traditional way of improving a design is to make changes based on previous experience and enhance the characteristics already known in the product or process that will contribute to an improvement.

In a lot of cases it is known how a product will react to a given test or experiment, based on theory or experience. The main characteristics that contribute to these predicted reactions can then be refined, modified or improved to increase the reliability or functionality of the product. Characteristics that are not commonly tested however, may

contribute more towards the functionality of the product or process than is usually recognised. In order to assess all the characteristics of the product or process, a full factorial approach would be necessary, that would involve a considerable number of experiments. Orthogonal arrays are a subset of the full factorial approach, which allows the total number of experiments required to be considerably reduced. It produces an analysis method where the effect of each of the process parameters, or product characteristics, can be investigated.

There are several methods of optimising a products design. They are based on statistical process control (SPC). SPC is a type of quality control used for mass production components etc. after the design has reached production. It relies on the principle that the pattern of variation in dimension, surface finish and other manufacturing characteristics of the component can be studied and controlled by using statistics. Inspecting a sample of components makes it possible to predict the compliance or non-compliance compared to the specification for the whole batch.

Experimental design is based on the theory that the process or product can be improved at the design stage, before it has reached production, and hence, reduce the cost of defective items that would otherwise occur later. To optimise the design of a process the factors that have the greatest influence, and which produces the most consistent performance must be identified. This has to be done with the minimum number of experiments whether they are on actual components or prototypes, or on mathematical models, such as finite element programmes.

Orthogonal arrays are used in process optimisation methods such as the Taguchi Method (Ref [5]). They help to reduce the experiment to a manageable size whilst allowing independent assessment of each of the factors. The first step in performing a Taguchi experiment is to decide how many process parameters (or factors) there are to test. This may be a variable characteristic such as speed, pressure or temperature. This will determine how many levels you are testing, depending on how many variations of speed, pressure and temperature you want to test.

---

[5] Gethin DT and Claypole TC, 2002, *Process Optimisation Module Notes*, University of Wales Swansea

The next step is to choose an orthogonal array to suit the experiment. This will depend on the number of levels and factors you have chosen and will allocate a certain number of tests that will be required. For example, a typical three two-level factors experiment will have an L4 array that has four experiments. Seven two-level factors will have an L8 array that has eight experiments, and a one two-level and seven three-level factors will have an L18 array.

The use of these orthogonal arrays make it possible to measure an average characteristic for each combination of factors, with a limited number of experiments. No combination of factors is repeated in the design of the array and no experiment is the direct inverse of the other. Also the array is symmetrical so that each level appears the same number of times in each column.

A response table is then constructed alongside the array that calculates the results. The mean result from each experiment is calculated and recorded in column Y (see Figure 1.3, L4 example). The effect of each level is calculated by averaging the mean result from each respective level for each column. The response is calculated by taking the difference between each effect of the levels for each column, and then each factor is ranked depending on the response level.

	Columns			Mean
Experiment	**1**	**2**	**3**	**Y**
Y1	1	1	1	9.0
Y2	1	2	2	7.5
Y3	2	1	2	6.0
Y4	2	2	1	6.5
Effect of level 1	8.3	7.5	7.8	
Effect of level 2	6.3	7.0	6.8	
Response	2.0	0.5	1.0	
Rank	1	3	2	

Figure 6.1: Example of an L4 array.

It may be concluded from Figure 6.1 that the optimum setting would be to have all the factors set to level 2. This is one of the merits of this technique, because this combination

of factors has not been actually used in the experiments but it is possible to examine all the possible combinations using the table. The rank indicates which of the factors is dominant. Factor 1 has the most effect but the effect of factor 2 is minimal and the non optimum setting may be preferred if there is an economic or similar argument in favour of operating with factor 2 set to level 1.

If this experiment were to be carried out using the full factorial approach where each variable is changed while keeping the rest constant, with three variables and two possible settings, it would take eight experiments ($2^3 = 8$). In this example however it has only been necessary to make 4 experiments but it is still possible to analyse all the factors. This is only a small example but this type optimisation method can be used with orthogonal arrays up to L81 that is for forty three-level factors. Using this L81 array, only 81 experiments would be required as opposed to a possible $3^{40} = 1.215 \times 10^{19}$ experiments using the full factorial method. This is an extreme example but it demonstrates the flexibility of using orthogonal arrays to perform the Taguchi method of experimentation.

6.3 Experiment Design

To optimise the design of a process the factors that have the greatest influence, and which produces the most consistent performance must be identified. Orthogonal arrays are used in process optimisation methods such as the Taguchi Method. They help to reduce the experiment to a manageable size whilst allowing independent assessment of each of the factors. The first step in performing a Taguchi experiment is to decide how many process parameters (or factors) there are to test.

There are three variables in the actual choke configuration; choke diameter, choke length, and chamber volume. The chamber volume may be increased for experimental purposes by adding a separate chamber directly after the choke rather than using the volume in the static tubes only. This may not be practical for actual use on the parachute assembly but it will determine the effect of the chamber volume, as this may be a critical factor in the damping.

The required choke diameter is obtained by inserting a pin through the bore of the choke. The choke diameter may be altered, by inserting different diameter pins to obtain a different effective diameter. The length of the choke may be varied, by using the original fitting shown in Figure 5.2 (Chapter 5) for the first length of 13mm, and then using a secondary attachment fitting that increases the length to 45mm. See Figure 6.2.

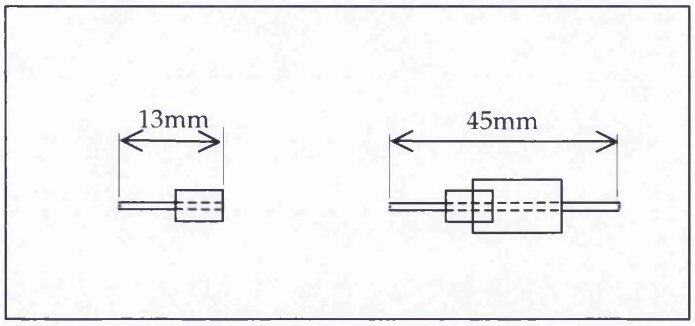

Figure 6.2: Choke lengths 13 and 45mm.

Another factor found to effect the performance of the choke is the direction into the airflow the pressure inlet is facing. When mounted onto the parachute assembly the back inlet is placed inside the parachute container away from direct airflow, but the second inlet is mounted onto the shoulder harness faces direct airflow in certain body positions. The orientation of the choke inlets is therefore be considered as a variable for this experiment.

Work has been conducted investigation the effect of static inlet porting but not with the use of an additional choke. Therefore, another factor to be included in the array will be the number of inlets used. Two inlets will model the static porting and the one inlet will demonstrate the difference.

The final parameters in the orthogonal array determine the type of test to be conducted. Tests shall be conducted in clean and disturbed airflow, by placing a baffle upstream of the testing block to generate the disturbed airflow. Static tests and dynamic tests shall be compared, by rotating the test block about 180^0 and back again for the dynamic tests. Rotating about 180^0 should ensure that the inlets remain in direct or indirect airflow as

required from the array. This will not be controllable in a real life situation but thought to be of value in this experiment to observe any effects they may have.

The next step is to choose an orthogonal array to suit the experiment. This is dependent on the number of levels and factors to be tested, and it allocates a certain number of tests that will be required. In this experiment there are 7 variables. The first configuration level is the choke analysed in chapter 4 and the second level is designed to attempt to increase the damping by decreasing the choke effective diameter, and increasing the length and chamber volume. Therefore and L_8 (2^7) array was chosen, that would require 8 experiments. Table 6.1 shows the choke damping parameters chosen, and Table 6.2 shows the orthogonal array used.

		Level	
		1	**2**
1.	Choke effective diameter (mm)	0.98	0.268
2.	Choke length (mm)	13	45
3.	Chamber Volume (ml or cm^3)	12.078 (tube)	20.55 (tube + chamber)
4.	Number of inlets	2	1
5.	Orientation of inlets	Direct Airflow (nozzle horizontal and facing airflow)	Indirect Airflow (nozzle behind block and facing the wall of the tunnel)
6.	Type of airflow	Clean	Disturbed
7.	Type of test	Static	Rotating

Table 6.1: Choke damping parameters

Experiment number	**Column**						
	1	**2**	**3**	**4**	**5**	**6**	**7**
1	1	1	1	1	1	1	1
2	1	1	1	2	2	2	2
3	1	2	2	1	1	2	2
4	1	2	2	2	2	1	1
5	2	1	2	1	2	1	2
6	2	1	2	2	1	2	1
7	2	2	1	1	2	2	1
8	2	2	1	2	1	1	2

Table 6.2: Orthogonal Array

A response table was then constructed alongside the array that calculates the results. The measure in this experiment is the pressure error offset as described in Chapter 5. The mean pressure spread is compared to the control pressure result from each experiment and a percentage difference is calculated and recorded in the array table. The effect of each level is calculated by averaging the mean result from each respective level for each column. The response is calculated by taking the difference between each effect of the levels for each column, and then each factor is ranked depending on the response level.

6.4 Method

For each experiment the test assembly and control tube were mounted together on a block with the two nozzles of each assembly facing different directions on the airflow. In the case of the static ported assemblies, the inlet nozzles of both assemblies were positioned together on two perpendicular faces of the block (see Figure 6.3). The control tube was of the same length and with the same number of inlets, but with no choking device, and no sintered filter. This measures the un-damped airflow the device is subjected to.

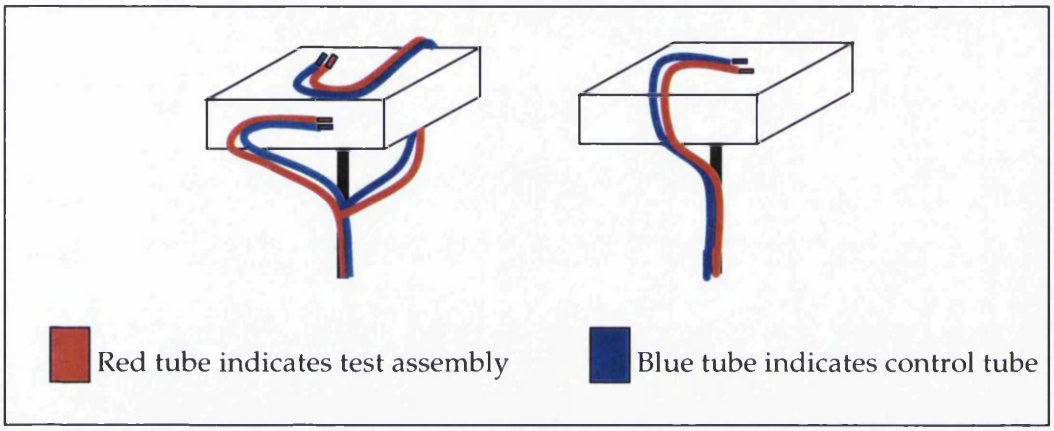

Figure 6.3: Static port assemblies as mounted on block.

Pressure data was recorded using a PICO data logger, at a 5ms (200Hz) sampling rate over a 60 second period. Noise variations were measured to compare the damping characteristics of each device.

Initial tests included taking a data recording before the wind tunnel was turned on to check the operation of the pressure sensors. The rotation tests were recorded on video (IGQ DV038), to assist in the post-test analysis of the results, and to account for any abnormalities in the pressure traces that may occur.

Post-test analysis includes statistical calculations on the pressure traces. The actual results that were included in the orthogonal array were taken as the mean pressure spread over the entire trace. The objective of both the choke and static port device is to minimise the

noise output and dampen the pressure reading, and therefore the measurable characteristic in this array is noise.

The results for each experiment is entered into the array to determine the effect of each level, and the response and rank of each variable. A response graph was constructed to help visualise the effect of each factor, and to indicate the importance of each variable. The interactions between each of the parameters shall be analysed to determine the optimum choke characteristics.

Previous calculations have determined that a long choke, with a small diameter and large chamber volume, with the use of static inlet porting would result in the most effective damping. Limitations in practical size in the parachute assembly and also problems in lag that will occur as a result shall be factors that will help determine the optimised choke configuration.

6.5 Results

The results from the wind tunnel tests were record by a PICO logger and transferred to an Excel spreadsheet for evaluation. The pressure traces were recorded in Volts and zeroed so that the control and test samples could be compared. The graphs for each of the 8 experiments are shown in Figure 6.4.

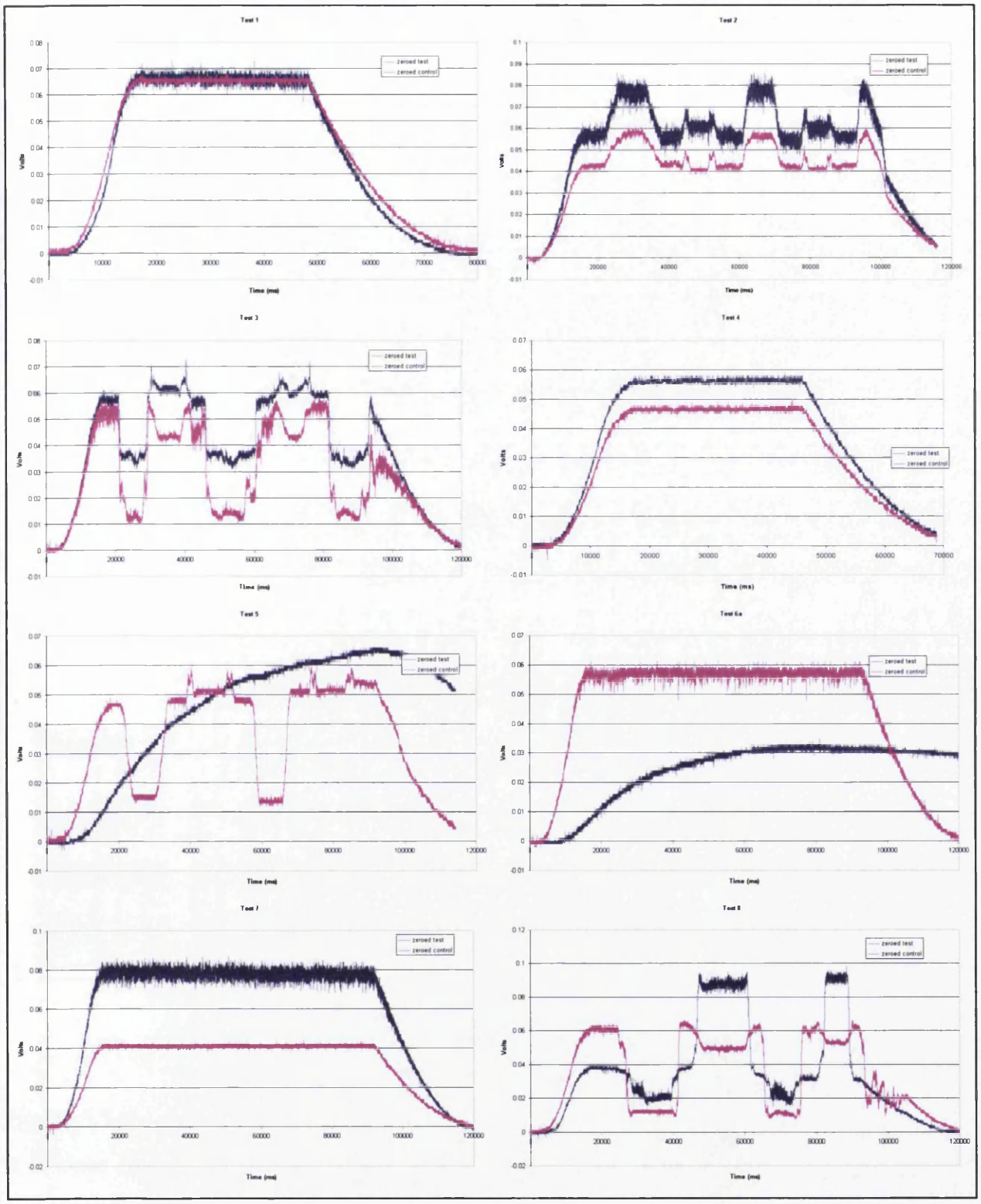

Figure 6.4: Result graphs as recorded by the PICO data logger.

The pressure spread was calculated by taking the maximum and minimum voltage values, avoiding any peak anomalies, from the test and control samples. The mean pressure spread was then calculated from the difference between the maximum and minimum readings. The difference was taken as a percentage between the two samples spread values.

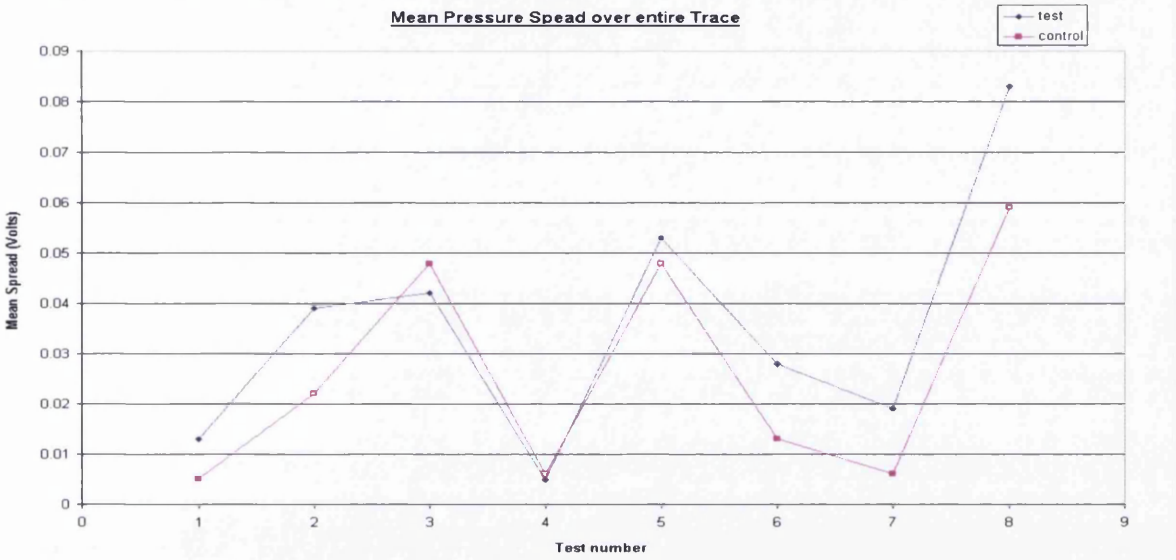

test number	test min	test max	test spread	control min	control max	control spread	% diff
1	0.06	0.073	0.013	0.063	0.068	0.005	61.53846
2	0.047	0.086	0.039	0.039	0.061	0.022	43.58974
3	**0.031**	**0.073**	**0.042**	**0.01**	**0.058**	**0.048**	**12.5**
4	0.054	0.059	0.005	0.044	0.05	0.006	16.66667
5	**0.013**	**0.066**	**0.053**	**0.012**	**0.06**	**0.048**	**9.433962**
6	0.007	0.035	0.028	0.048	0.061	0.013	53.57143
7	0.068	0.087	0.019	0.038	0.044	0.006	68.42105
8	0.015	0.098	0.083	0.007	0.066	0.059	28.91566

Figure 6.5: Mean pressure spread calculation

Figure 6.5 shows the results from each experiment in the form of a mean pressure spread. It is clear from the graph in Figure 6.5, that the results from test 3 only, show the test sample actually reducing the spread from the control. It is also observed that tests 4 and 5 have a smaller difference between the spread in the control and test samples. The percentage difference gives a good indication of this. The results from test number 5 look to be the most effective, followed by test number 3.

This is also evident by examining the graphs in Figure 6.4. Test 3 obviously damps the trace, while test 5 over-damps the trace. The greatest percentage difference is calculated to be in test 7 and test 1, and this too is evident in Figure 6.4.

Using the mean spread percentage difference as the results from the experiments, and bearing in mind that the smaller the spread the better, the orthogonal array results table may be drawn as shown in Figure 6.6.

Test number	Column							Mean
	1	2	3	4	5	6	7	Y
1	1	1	1	1	1	1	1	61.538
2	1	1	1	2	2	2	2	43.589
3	1	2	2	1	1	2	2	12.5
4	1	2	2	2	2	1	1	16.666
5	2	1	2	1	2	1	2	9.4339
6	2	1	2	2	1	2	1	53.571
7	2	2	1	1	2	2	1	68.421
8	2	2	1	2	1	1	2	28.915
Effect of level 1	33.5737	42.0334	50.6162	37.973	39.1313	29.138	50.0494	
Effect of level 2	40.0855	31.625	23.0430	35.685	34.5278	44.520	23.6098	
Response	6.5118	10.407	27.5732	2.2874	4.60353	15.381	26.4395	
Rank	**5**	**4**	**1**	**7**	**6**	**3**	**2**	
Parameter	Diameter	Length	Volume	Inlets	Orientation	Airflow	Type	

Figure 6.6: Response table showing the effect of choke parameters on damping.

The response table in Figure 6.6 shows the effect of each level, the response and the rank of each of the parameters used in designing the pressure damping choke. It shows the most effective parameter is the chamber volume, and least effective is the number of inlets used. This was a surprising result as the static inlet porting has already been proven to dampen the low frequency noise.

A response graph is shown in Figure 6.7 that helps to visualise the effect of each factor. The slope of the graph is indicative of the importance of each factor, and it is also apparent which level should be selected to optimise the process.

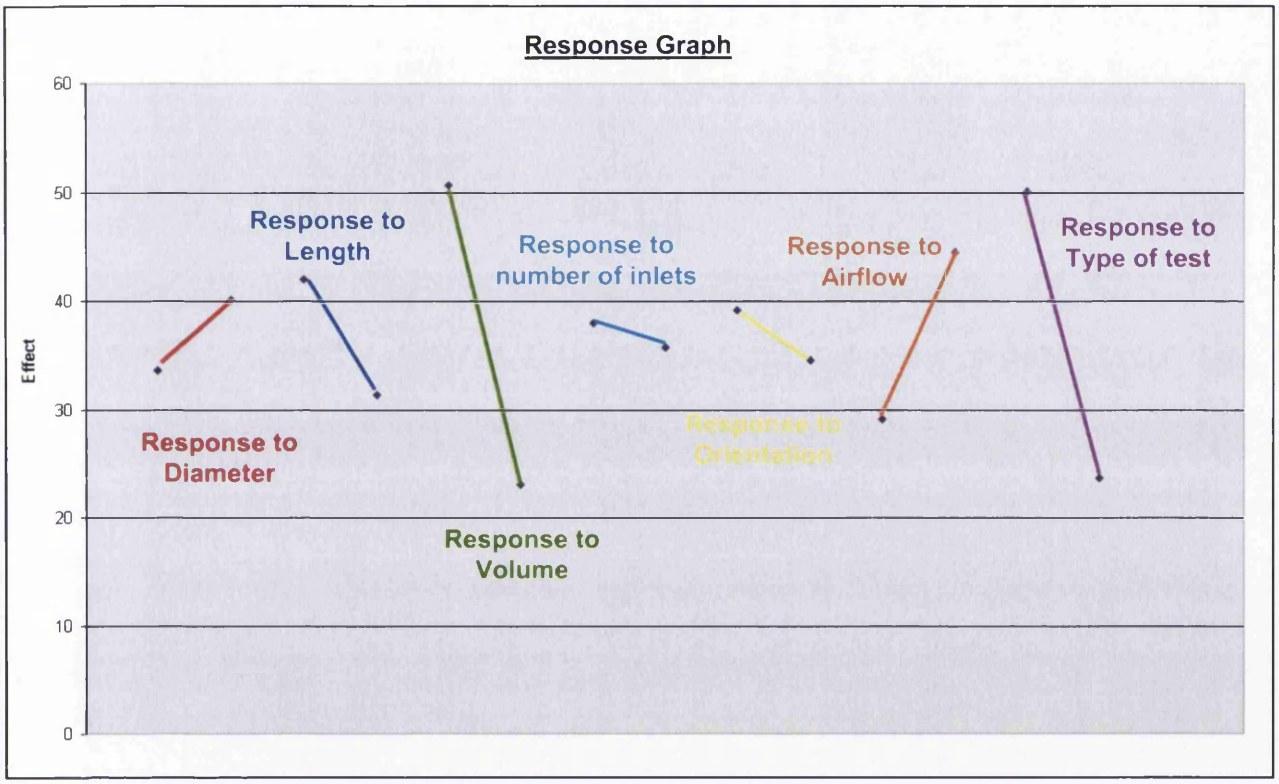

Figure 6.7: Response graph used to visualise the effect of each factor.

The response graph in Figure 6.7 clearly shows the factors with the most effect are the response to volume and the response to the type of test used. However, the response to the type of test, the airflow and orientation, are factors that in the design are uncontrollable. Therefore to optimise the choke design, the volume, length, diameter and number of inlets should be analysed for their interactions.

To analyse the interactions a further matrix is constructed (see Figure 6.8) in which the effect of each of the combinations can be compared. The Y value is the mean pressure error for each experiment where the subscript number depicts the experiment number. Factors 'a' and 'b' are any two parameters tested in the array.

	Factor 'a' at Level 1	Factor 'a' at level 2
Factor 'b' at level 1	$\frac{Y_1 + Y_2}{2}$	$\frac{Y_5 + Y_6}{2}$
Factor 'b' at level 2	$\frac{Y_3 + Y_4}{2}$	$\frac{Y_7 + Y_8}{2}$

Figure 6.8: Interactions matrix.

The values obtained from the interactions matrix can then be plotted graphically to obtain an optimum value for that parameter. Figures 6.9 to 6.14 show the interaction in the pressure damping choke configuration.

	Diameter at level 1	Diameter at level 2
Length at level 1	$Y_1 + Y_2/2$ = 52.56	$Y_5 + Y_6/2$ = 31.50
Length at level 2	$Y_3 + Y_4/2$ = 14.58	$Y_7 + Y_8/2$ = 48.67

	Level 1	Level 2
Choke effective diameter (mm)	0.98	0.268
Choke length (mm)	13	45

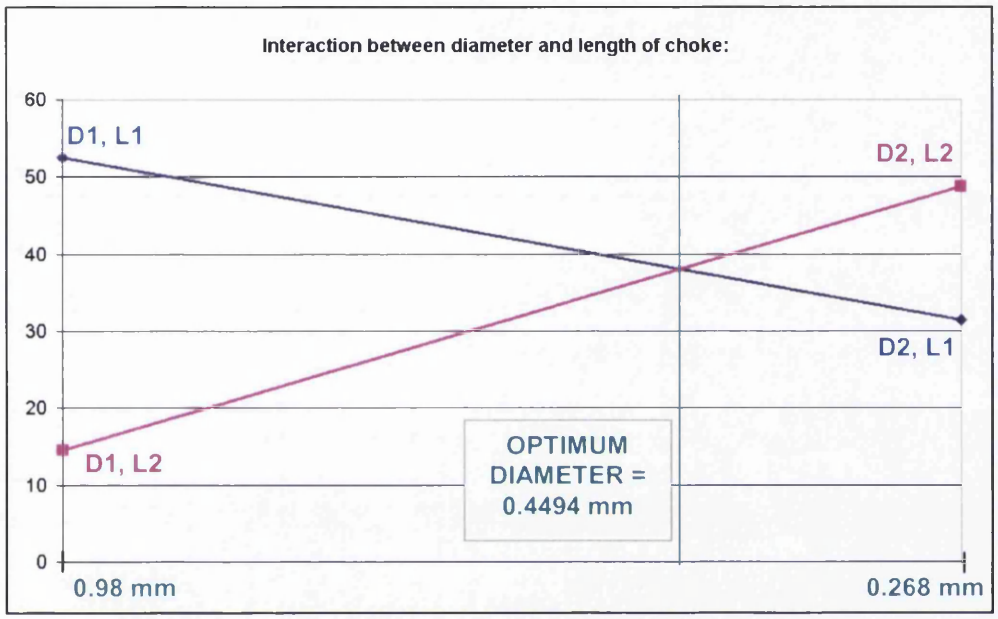

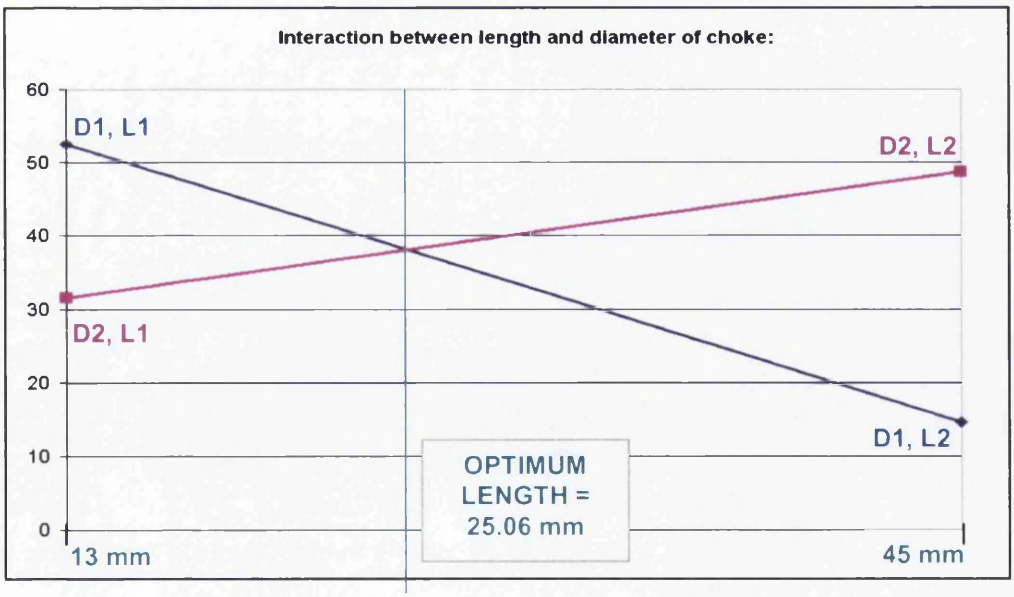

Figure 6.9: Interactions between diameter and length.

	Length at level 1	Length at level 2
Volume at level 1	$Y_1 + Y_2/2 =$ 52.56	$Y_5 + Y_6/2 =$ 48.67
Volume at level 2	$Y_3 + Y_4/2 =$ 31.50	$Y_7 + Y_8/2 =$ 14.58

	Level 1	Level 2
Choke length (mm)	13	45
Chamber Volume (ml or cm^3)	12.078 (tube)	20.55 (tube + chamber)

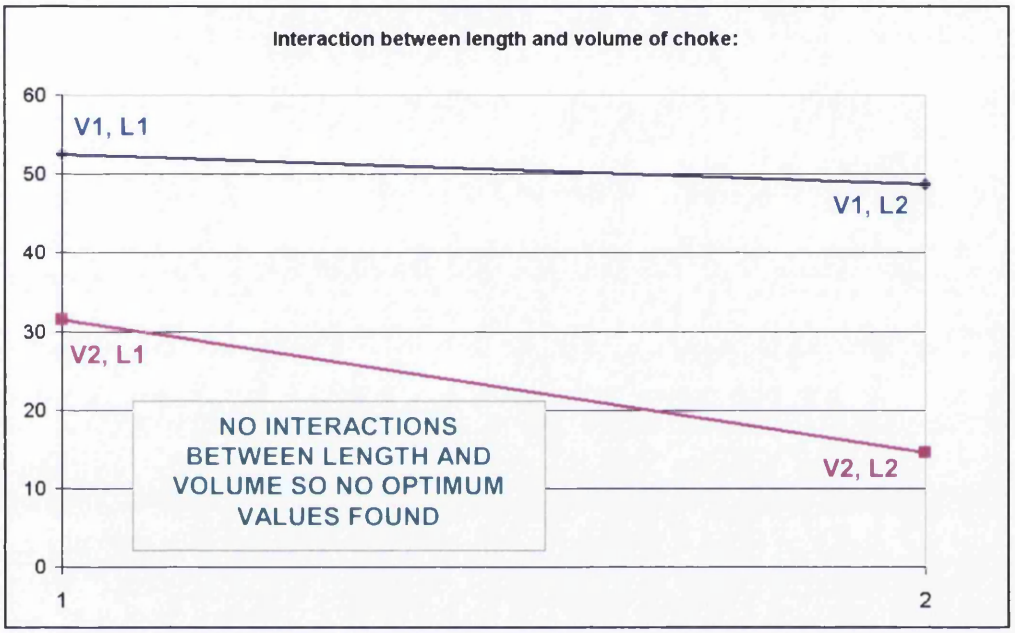

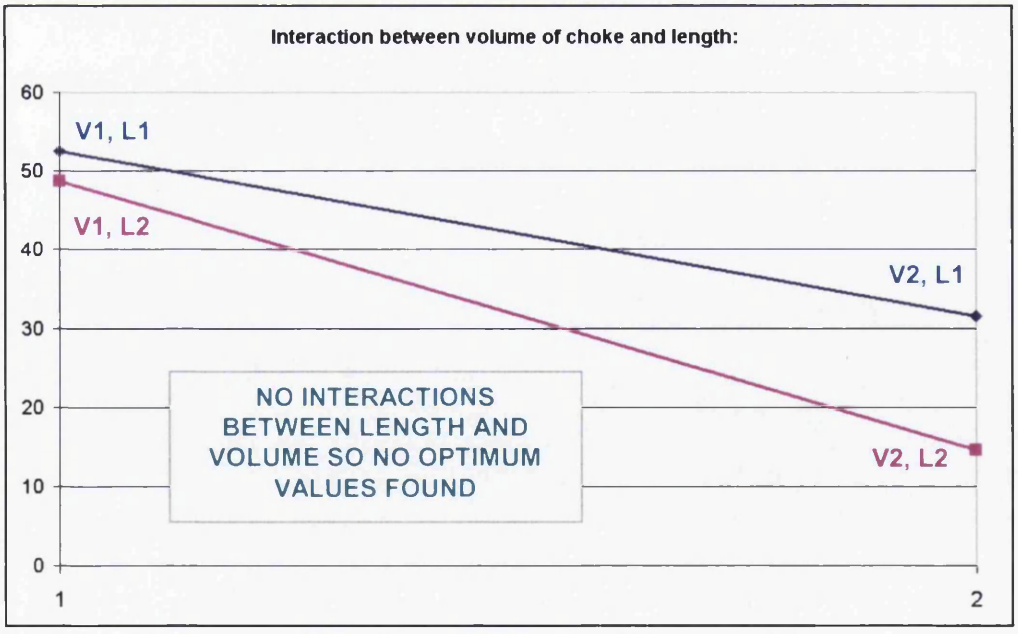

Figure 6.10: No Interactions between length and volume.

	Length at level 1	Length at level 2
Inlets at level 1	$Y_1 + Y_2/2 =$ 35.49	$Y_5 + Y_6/2 =$ 40.46
Inlets at level 2	$Y_3 + Y_4/2 =$ 48.58	$Y_7 + Y_8/2 =$ 22.79

	Level 1	Level 2
Choke length (mm)	13	45
Number of inlets	2	1

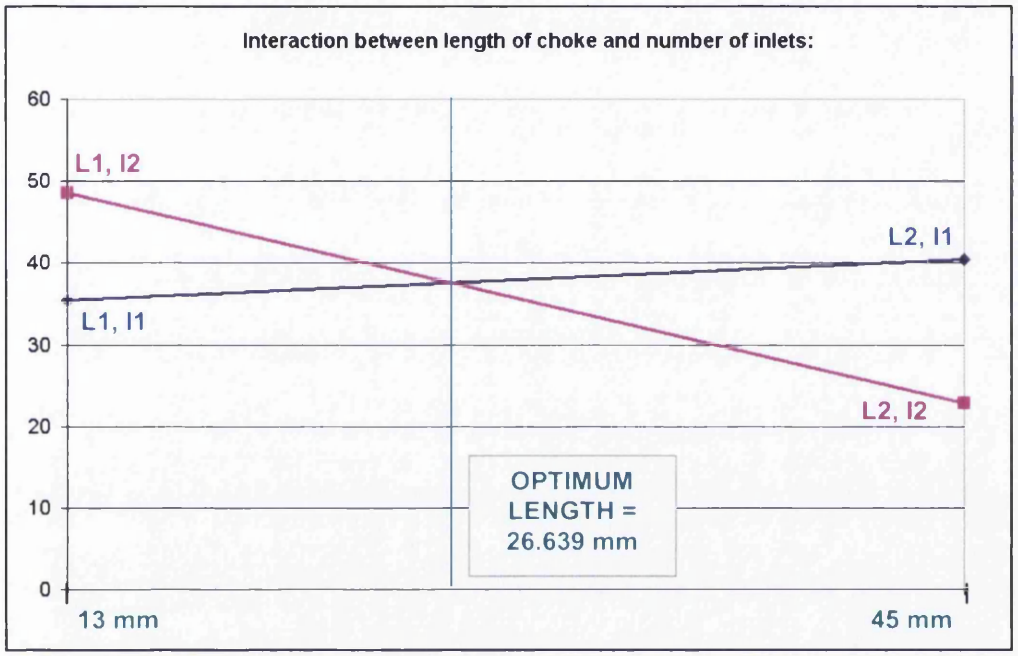

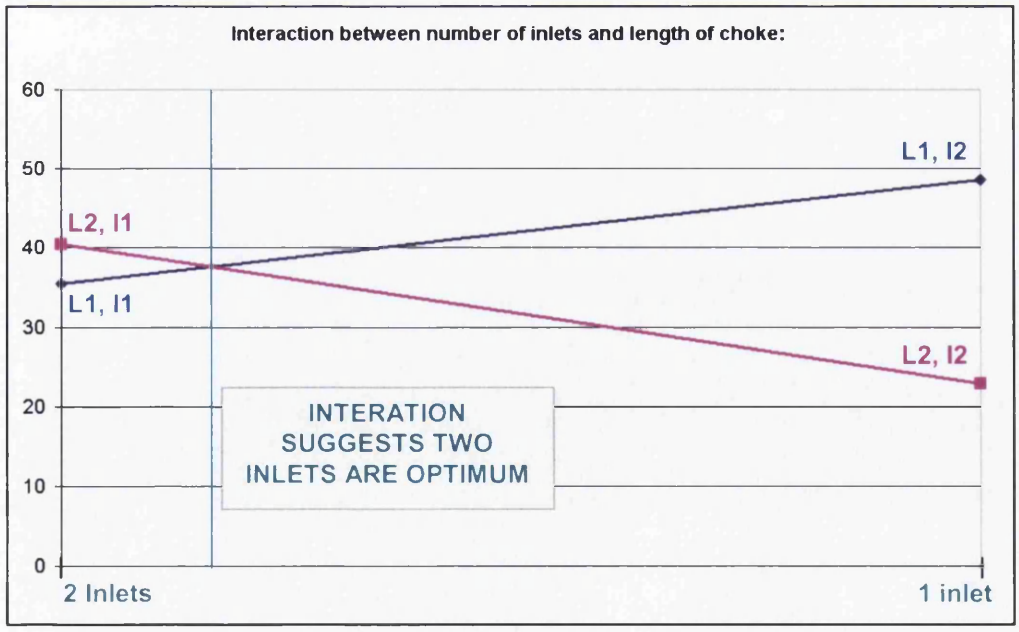

Figure 6.11: Interactions between length of choke and number of inlets.

	Diameter at level 1	Diameter at level 2
Volume at level 1	$Y_1 + Y_2/2 =$ **52.56**	$Y_5 + Y_6/2 =$ **48.67**
Volume at level 2	$Y_3 + Y_4/2 =$ **14.58**	$Y_7 + Y_8/2 =$ **31.50**

	Level 1	Level 2
Choke effective diameter (mm)	0.98	0.268
Chamber Volume (ml or cm³)	12.078 (tube)	20.55 (tube + chamber)

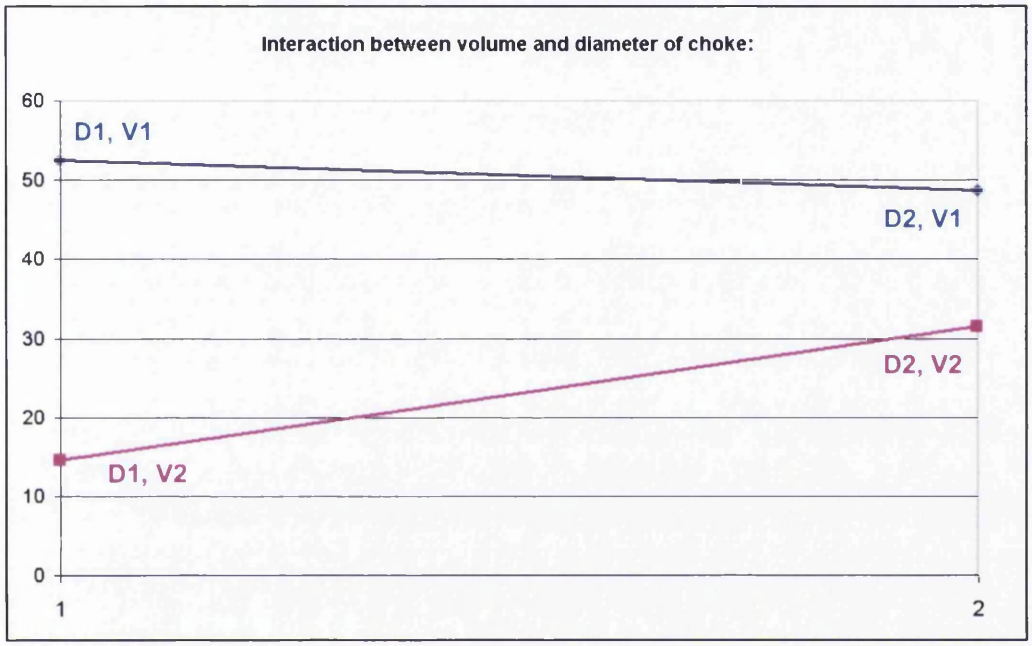

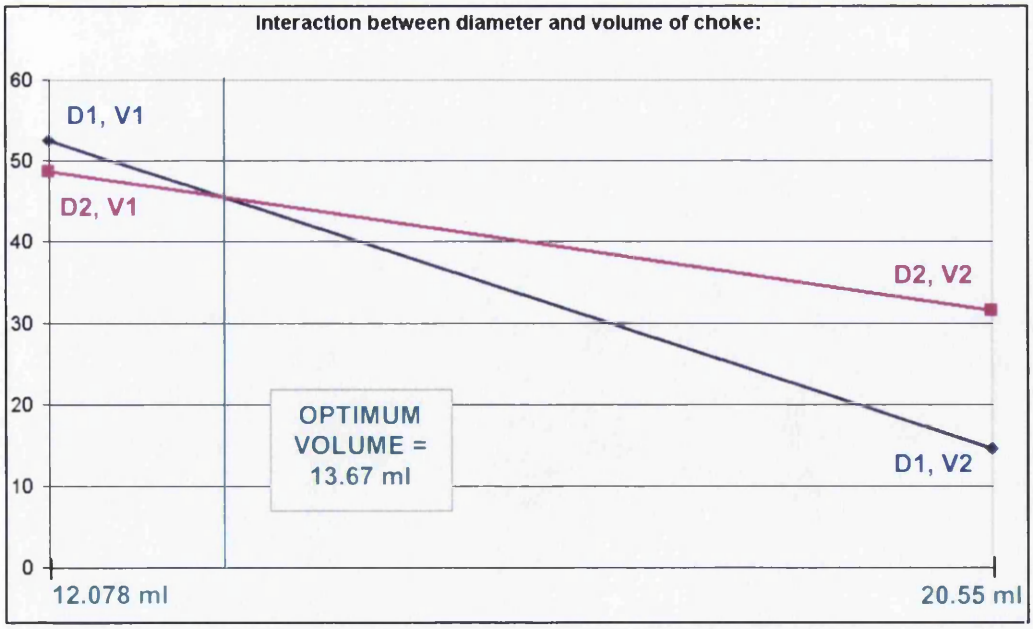

Figure 6.12: Interactions between volume and diameter.

	Inlets at level 1	Inlets at level 2
Volume at level 1	$Y_1 + Y_2/2 =$ 64.98	$Y_5 + Y_6/2 =$ 10.97
Volume at level 2	$Y_3 + Y_4/2 =$ 36.25	$Y_7 + Y_8/2 =$ 35.12

	Level 1	Level 2
Number of inlets	2	1
Chamber Volume (ml or cm^3)	12.078 (tube)	20.55 (tube + chamber)

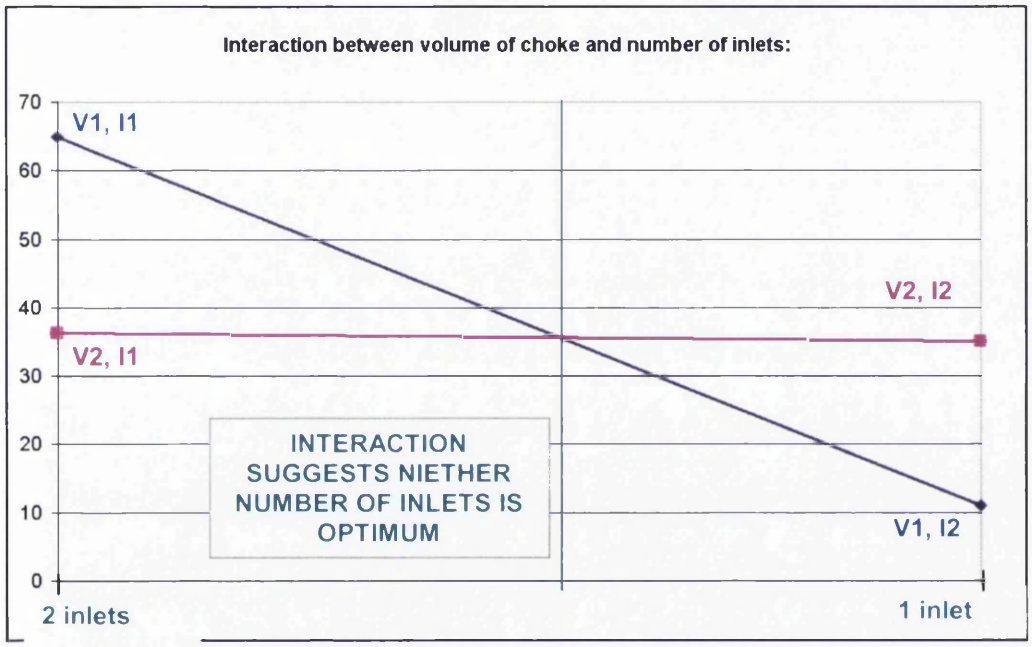

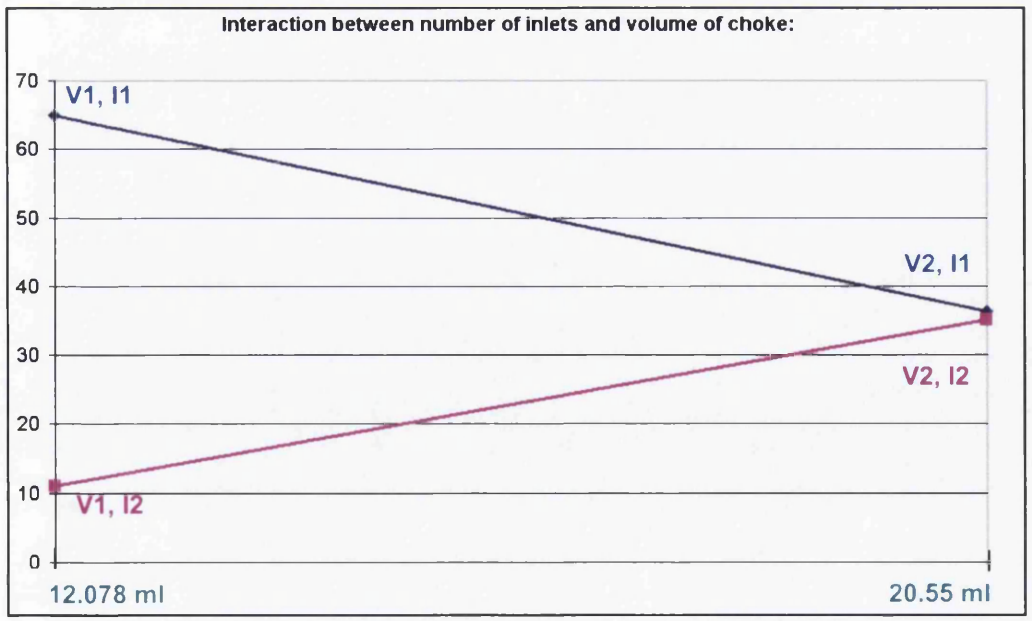

Figure 6.13: Interactions between volume and number of inlets.

	Inlets at level 1	Inlets at level 2
Diameter at level 1	$Y_1 + Y_2/2 =$ 37.02	$Y_5 + Y_6/2 =$ 30.13
Diameter at level 2	$Y_3 + Y_4/2 =$ 38.93	$Y_7 + Y_8/2 =$ 41.24

	Level 1	Level 2
Number of inlets	2	1
Choke effective diameter (mm)	0.98	0.268

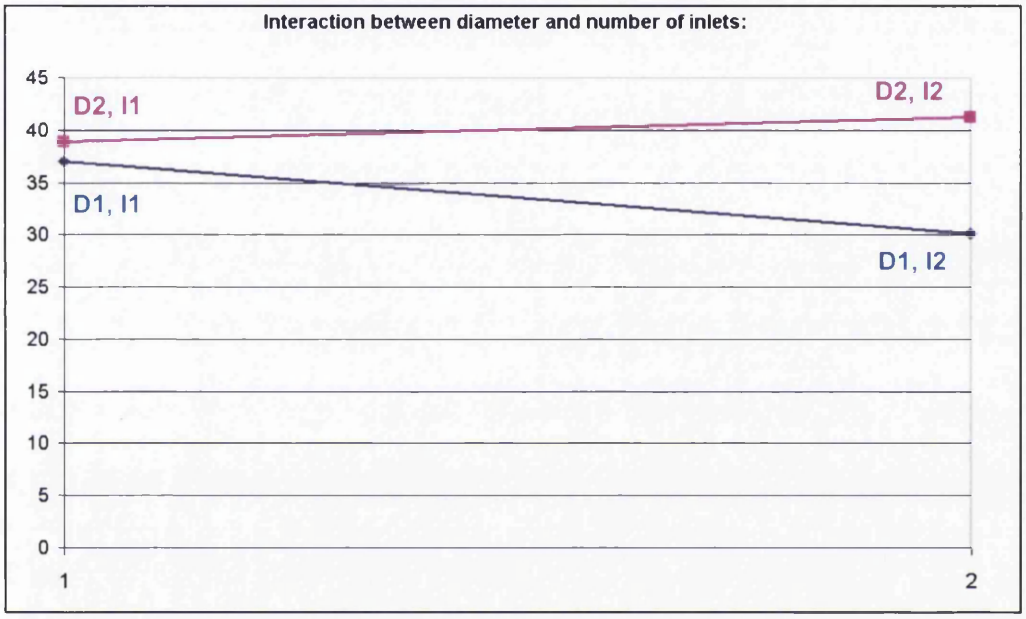

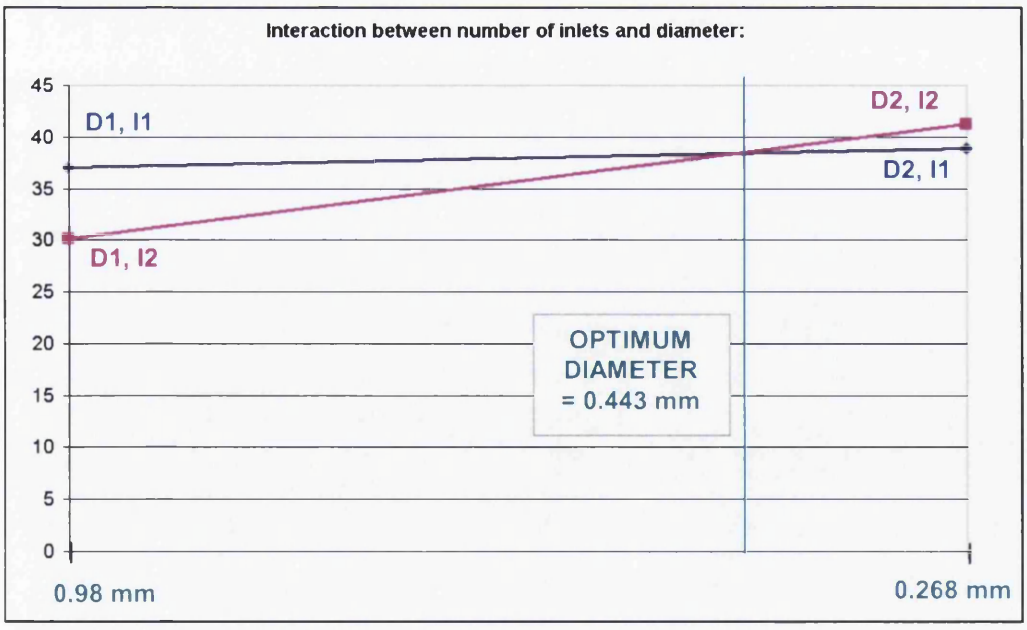

Figure 6.14: Interactions between diameter and number of inlets.

The optimum values obtained in Figures 6.9 to 6.14, calculated from the interactions between the factors are shown in Table 6.3.

Interaction	Parameter 1 Optimum	Parameter 2 Optimum
Diameter / Length	Diameter = 0.4494 mm	Length = 25.6 mm
Length / Volume	No interactions	No Interactions
Length / Number of inlets	Length = 26.639 mm	Two inlets
Volume / Diameter	No interactions	Volume = 13.67 ml
Volume / Number of inlets	Neither 1 or 2 inlets are optimum here	No interactions
Diameter / Number of inlets	No interactions	Diameter = 0.443 mm

Table 6.3: Table showing results of interactions study.

Where the interactions have produced more than one optimum value (diameter and length), it may be noted that the values are very close and therefore may be assumed to agree. An average is therefore taken and the optimum configuration is as follows:

- Choke effective diameter = 0.44 mm
- Choke length = 26 mm
- Chamber volume = 13.67 ml
- Number of inlets = 2

6.6 Conclusions

The orthogonal array technique used in this chapter was proven successful and has resulted in an optimum choke configuration. This configuration will be verified in a final wind tunnel experiment discussed in the following chapter.

Chapter 7 - Final System Verification

7.1 Introduction

The orthogonal array technique was used in the previous chapter to design an experiment to fully test every variable in the choke configuration. The results were then analysed for their interactions in order to obtain the optimum choke configuration:

- Choke effective diameter = 0.44 mm
- Choke length = 26 mm
- Chamber volume = 13.67 ml
- Number of inlets = 2

This configuration was then verified in a final wind tunnel test to confirm its function and attenuation of the pressure signal.

7.2 Method

The configuration to be verified was made up with a 0.84mm diameter needle, with 0.665mm diameter fishing line. This gave an effective diameter of 0.44mm. The needle was cut to length at 26mm and the volume in the static inlet porting tubes and chamber was set to 13.67ml. Two inlets were used.

The configuration was tested in the wind tunnel at the University of Wales Swansea using the same method as reported in Chapter 5. The choke configuration and a control sample were mounted onto a block and positioned midway through the tunnel. Different tests were carried out on the same sample including static and rotating tests, in clean, disturbed, direct and indirect airflow. A test was also carried out to determine any lag resulting from the choked inlet by varying the pressure inside the tunnel.

7.3 Results

The results from the wind tunnel tests were record by a PICO logger and transferred to an Excel spreadsheet for evaluation. The pressure traces were recorded in Volts and zeroed so that the control and test samples could be compared. The results are shown in Figures 7.1 - 7.7.

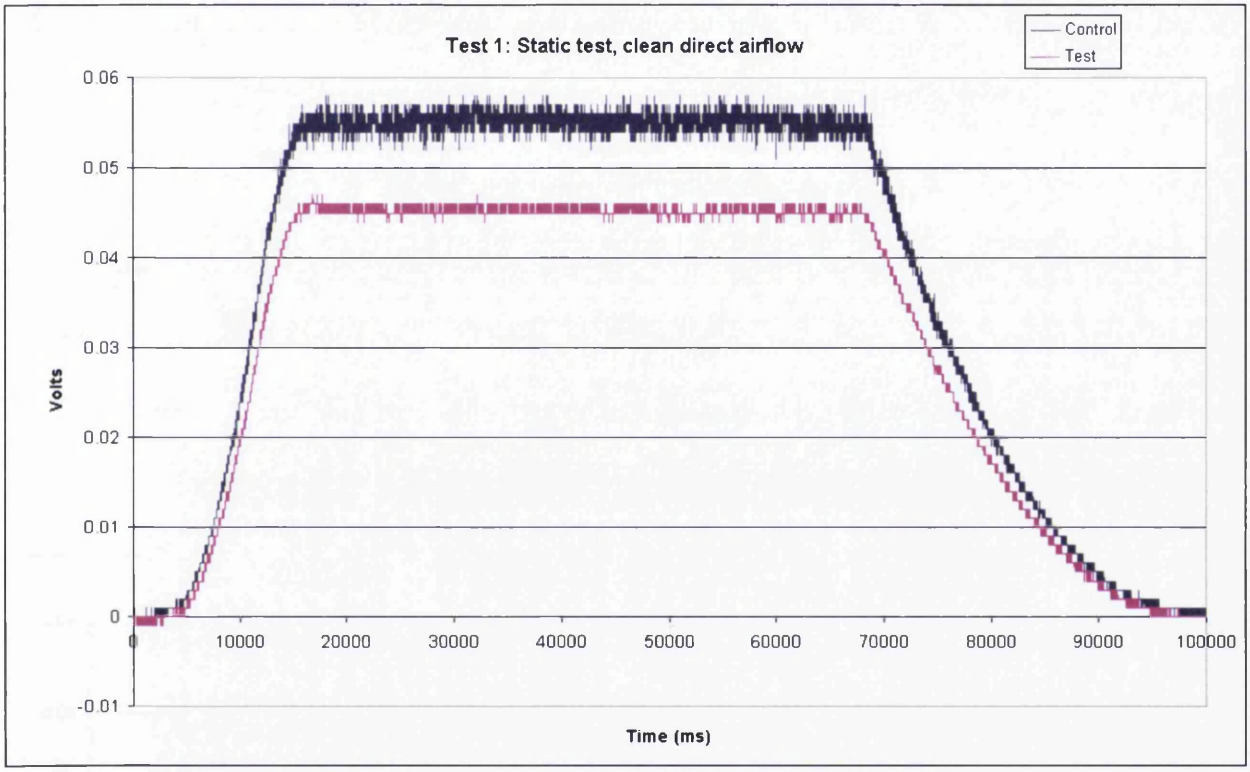

Figure 7.1: Static test with clean and direct airflow

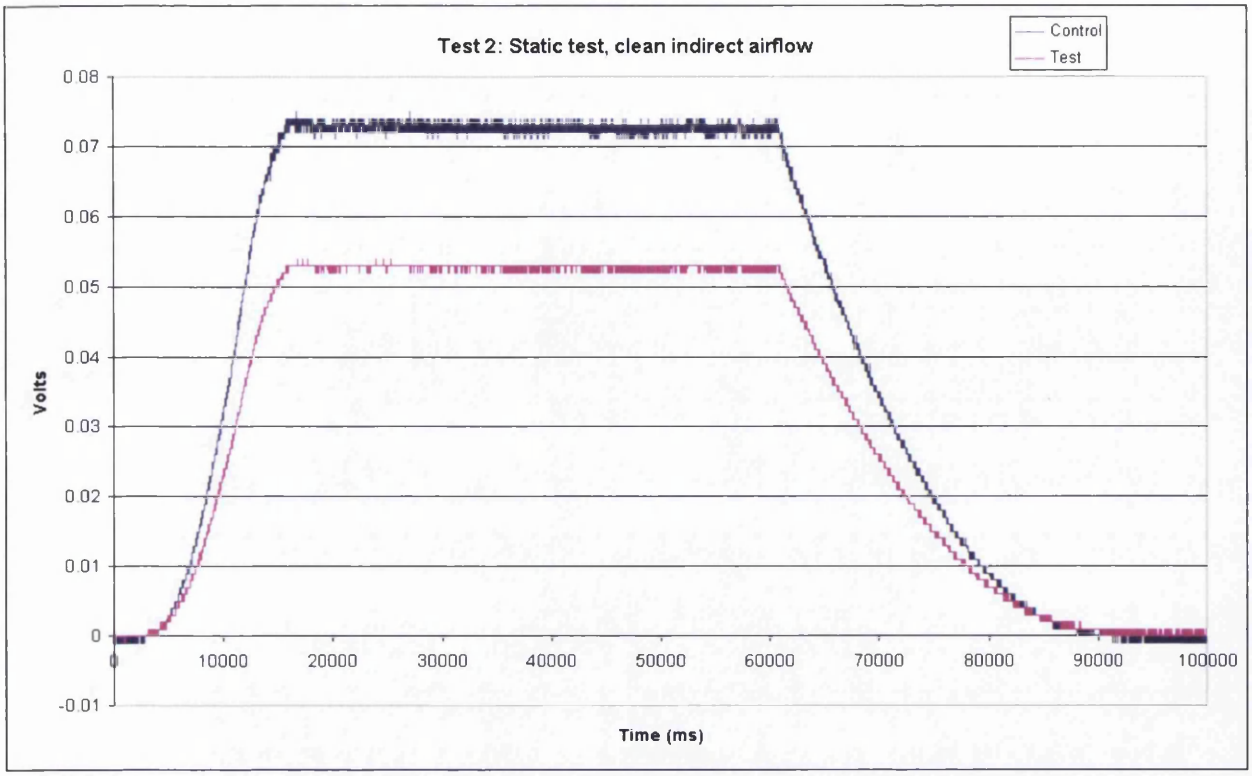

Figure 7.2: Static test with clean and indirect airflow

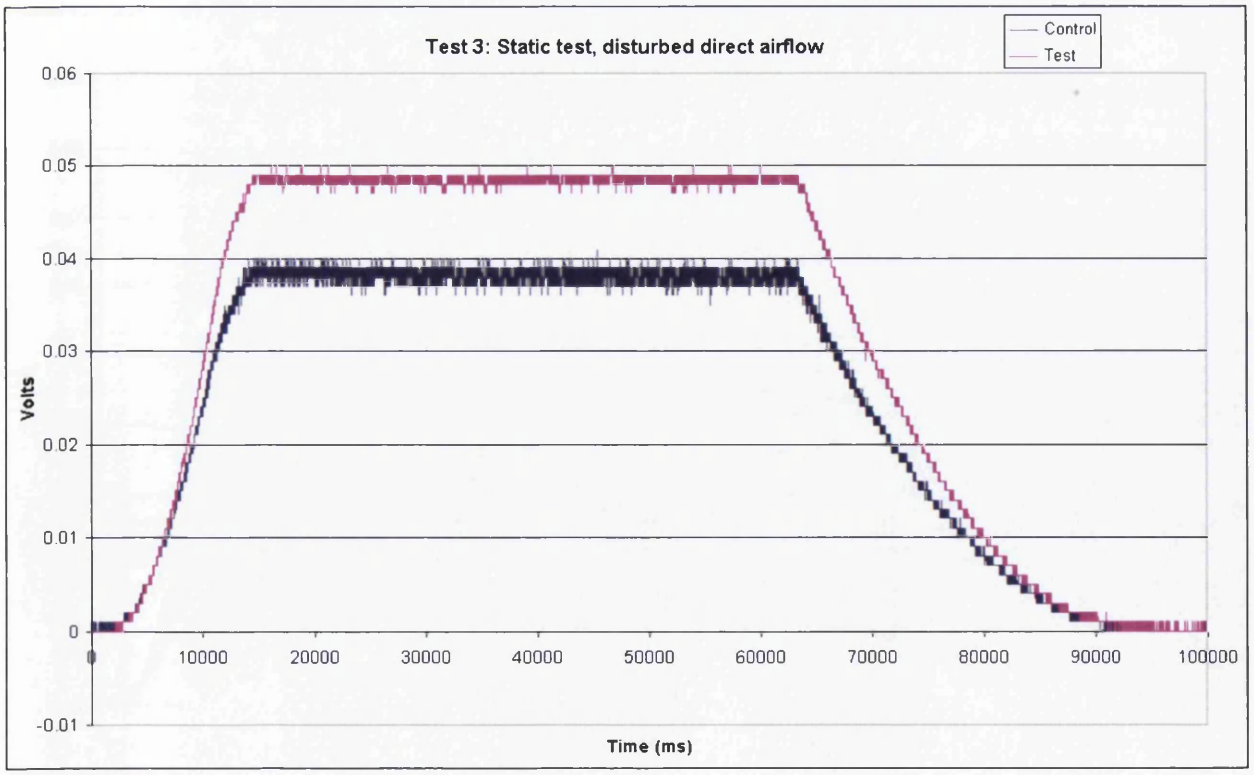

Figure 7.3: Static test with disturbed and direct airflow

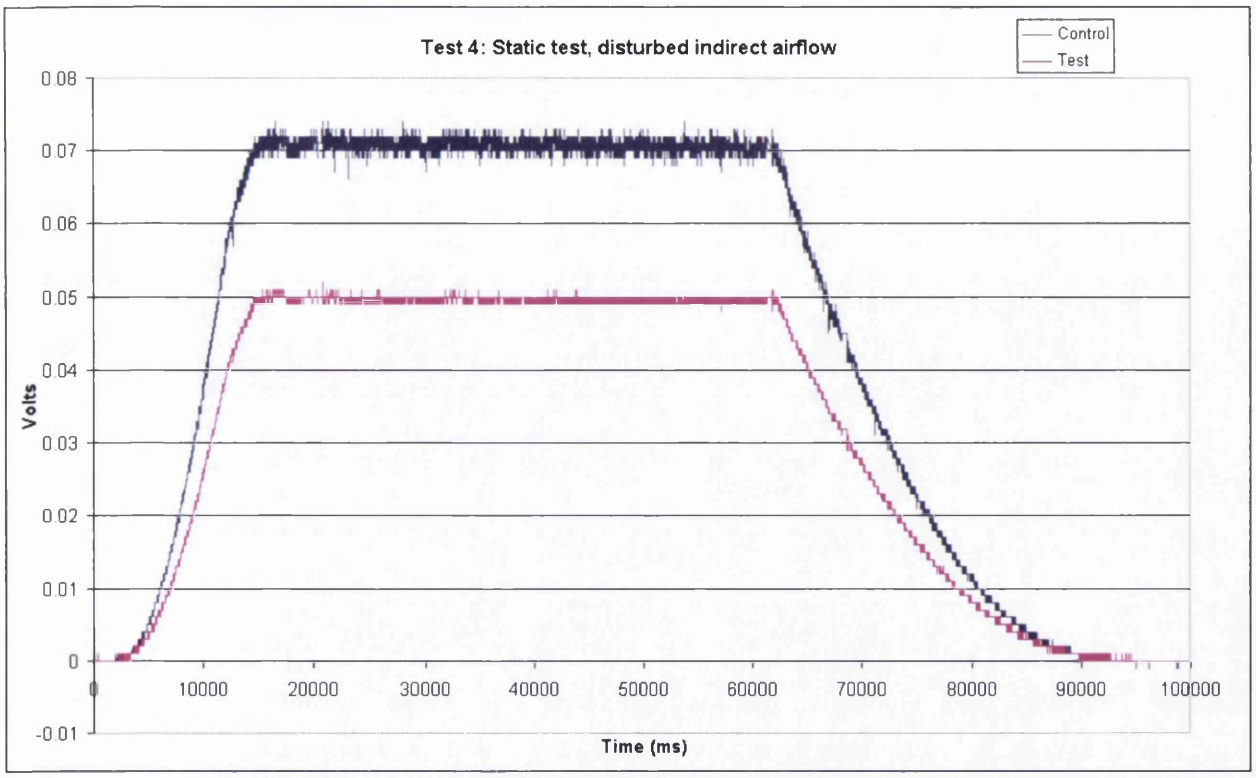

Figure 7.4: Static test with disturbed and indirect airflow

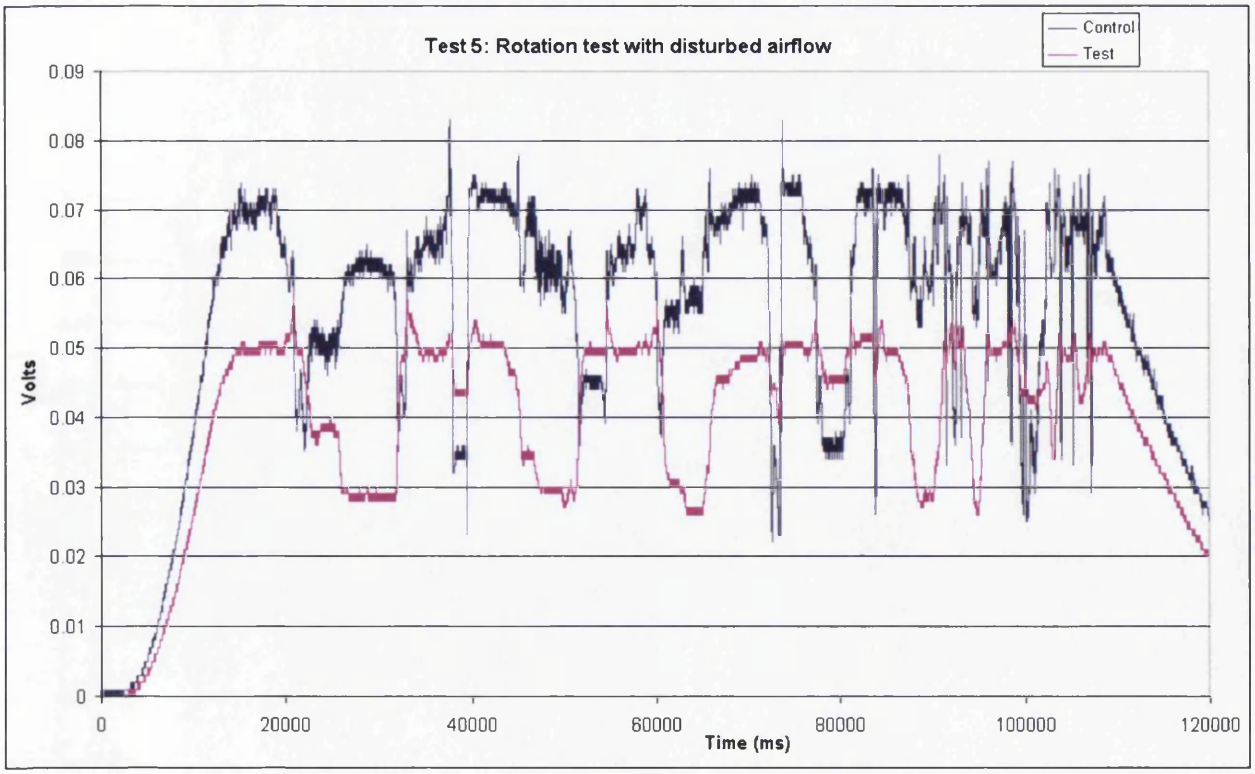

Figure 7.5: Rotation test with disturbed airflow

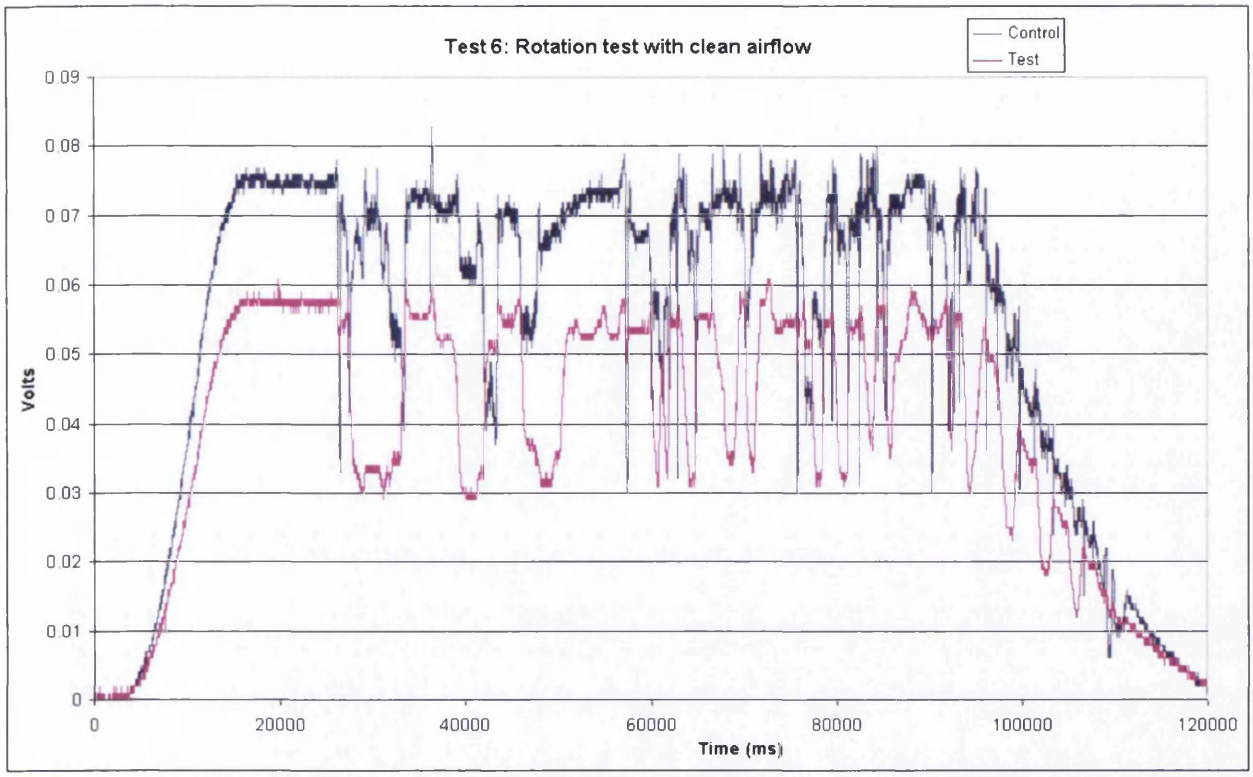

Figure 7.6: Rotation test with clean airflow

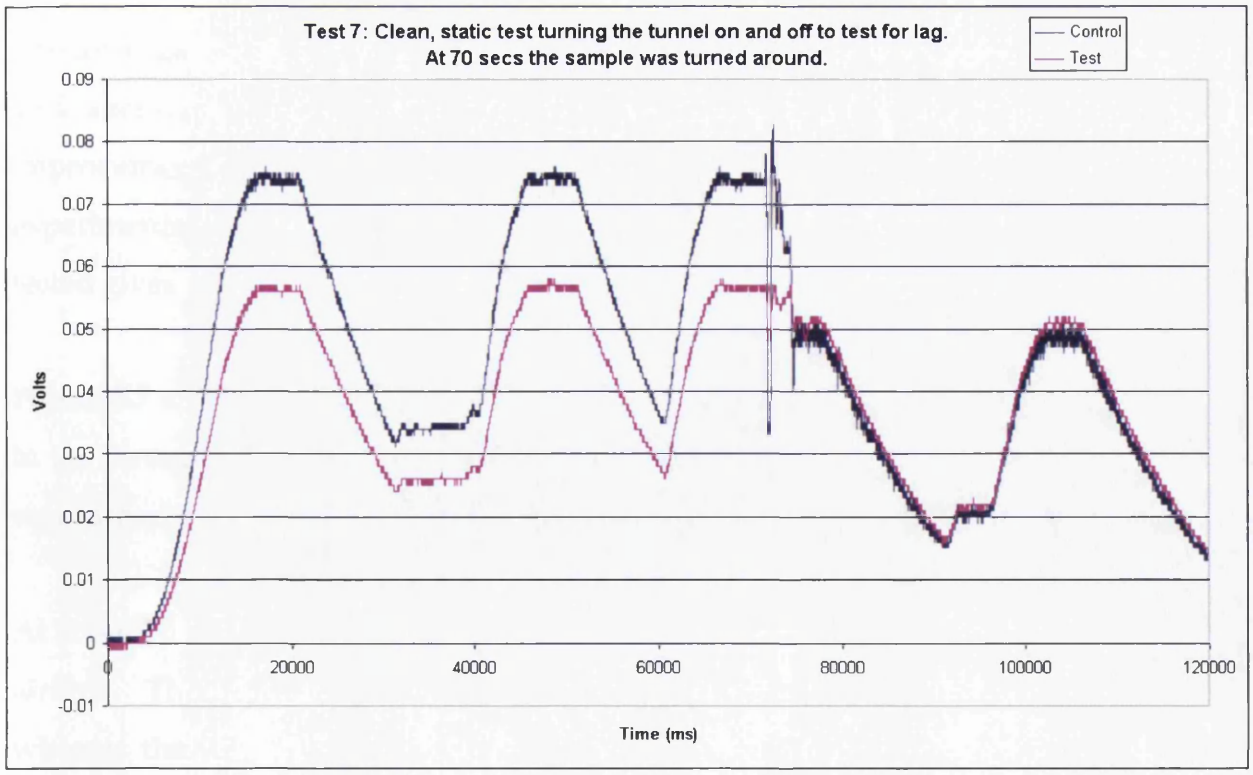

Figure 7.7: Static test with clean airflow, measuring lag on the sample in different wind tunnel pressure conditions

7.4 Analysis

The percentage attenuation was taken by calculating the difference between the maximum and minimum voltage values, avoiding any peak anomalies, from the test and control samples, and taking a percentage difference between the two values. The results from each test (1-6) are shown in Table 7.1.

	Control			Test			% Attenuation
	Min	Max	Difference	Min	Max	Difference	
Test 1	0.051	0.058	0.007	0.044	0.047	0.003	57%
Test 2	0.071	0.075	0.004	0.052	0.054	0.002	50%
Test 3	0.035	0.041	0.006	0.047	0.05	0.003	50%
Test 4	0.066	0.074	0.008	0.048	0.052	0.004	50%
Test 5	0.022	0.083	0.061	0.026	0.058	0.032	47.5%
Test 6	0.03	0.083	0.053	0.029	0.061	0.032	39.6%

Table 7.1: Percentage Attenuation of the pressure signal made by the pressure damping inlet

The average percentage attenuation taken from the results in Table 7.1, give a value of 49% attenuation. The predicted attenuation calculated in Chapter 4, gave a potential improvement of 54%. The actual attenuation is slightly less than expected but given experimental error and method of analysis, the pressure damping inlet configuration tested gives a good result.

Figure 7.7 shows the final test made on the configuration. The test piece was positioned in the centre of the tunnel section with the inlets facing indirect airflow, and the tunnel was turned on and off giving different pressure conditions.

At about 70 seconds the test piece was turned around so that the inlets were facing direct airflow. The control sample gave a very noisy reading as the block was repositioned, whereas the test sample damped this noise well. In the opposite orientation the test sample stuck much closer to the control sample readings. It is uncertain why the control sample changed so radically in the opposite orientation, but as it is the pressure damping

inlet that is of concern, it is not considered necessary to explore this further. The test sample did not display any noticeable lag due to damping that would be seen to be a problem.

7.5 Conclusions

Wind tunnel verification trials have been conducted on the final pressure damping inlet configuration. An analysis of the results show, that the configuration attenuates the pressure signal by an average of 49%. This will greatly improve the reliability of the Automatic Activation Device.

Chapter 8 - Conclusions

The Automatic Activation Device (AAD) calculates the height and derives the rate of descent of a parachutist by taking pressure readings throughout the descent. The pressure transducer reads an erratic inlet pressure, which is due to a combination of changing body position, flapping clothing and noise. This thesis has described a programme of work in which a pressure damping choke has been designed that will help to attenuate the pressure signal.

A theoretical model of the system was designed that could simulate different configurations and their damping characteristics. This resulted in a suitable choke configuration that was tested in a wind tunnel experiment to assess its attenuation of the pressure signal. Further studies included an orthogonal array experiment that produced an optimum design for the choke configuration. This was then verified in a final wind tunnel experiment.

The verification experiment was successful and the choke configuration was found to attenuate the pressure signal by 49%. This is a substantial improvement to the pressure signal that the AAD will use to calculate the height and derive the rate of descent of the parachutist. This will not only improve the reliability of the device but also the safety to the parachutist.

Further modifications to the choke configuration may include reducing the size of the choke inlets to reduce the bulkiness in the parachute pack. An investigation may also be carried out to see if the chamber volume could be utilised inside the AAD body to further reduce bulk to the parachute pack.

Further recommendations are to repeat the vertical wind tunnel trials described in Chapter 3, to compare the pressure damping inlet to the static port only configuration, and AAD only pressure readings. The benefit of the vertical wind tunnel as opposed to

carrying out real descents is that experiments can be repeated quickly, you have a longer period of time to gather data, and the whole experiment may be observed and filmed from the viewing platform.

It is then recommended that real drops from an aircraft will be carried out. This would confirm the data gathered in the vertical wind tunnel, and provide a full-system verification. This would also give a more reassuring verification to the user and would be used in the qualification of the system and airworthiness documentation.

References

[1]Massey BS, 1989, *Mechanics of Fluids*, 6th edition, London, Chapman & Hall

[2] Kempe, 2002, *Kempes Engineers Yearbook*, Kent, CMP Information Ltd

[3] Knacke. TW, 1992, *Parachute Recovery Systems Design Manual*, Santa Barbara, Para Publishing

[4] Williams. PM, 2001, *Test Results for Wind Tunnel Trials Conducted on the MOD AAD with Static Inlet Porting*, GQ TR 01001, Irving GQ Ltd

[5] Gethin DT and Claypole TC, 2002, *Process Optimisation Module Notes*, University of Wales Swansea

[6] Roy RK, 2001, *Design of Experiments Using the Taguchi Approach: 16 Steps to Product and Process Improvement*, New York, John Wiley & Sons

[7] Williams. PM, 2001, *AADSignal Injection Test Rig*, IGQ TR 005, Irving GQ Ltd

[8] Poynter. D, 1984, *The Parachute Manual: A treatise on Aerodynamic Decelerators*, 3rd edition, Santa Barbara, Para Publishing

[9] Williams.PM, 1999, *DRACAS report no. 213*, Irvin GQ Ltd.

[10] Ewing EG, Bixby HW and Knake TW, 1978, *Recovery Systems Design Guide*, Ohio, Air Force Flight Dynamics Laboratory

[11] Hoerner SF, 1965, *Fluid – Dynamic Drag*, Albuquerque, Hoerner Fluid Dynamics